

ABSTRACT

YAO, SHIYUE. Essays on Renewable Energy, Agrivoltaics, and Groundwater Sustainability. (Under the direction of Justin Baker and Zachary Brown).

With the escalating impacts of climate change, policymakers face the dual challenges of expanding renewable energy while ensuring sustainable resource management. Renewable energy policies such as Renewable Portfolio Standards (RPS) aim to accelerate the transition to cleaner energy sources, yet their effectiveness varies across technologies and regional contexts. At the same time, resource conservation policies, particularly in water-scarce agricultural regions, seek to regulate resources while maintaining economic viability. This dissertation explores the interactions between these policies and resource allocation decisions, focusing on bioenergy adoption under RPS, and agrovoltaics as a sustainable land-use solution in California's Central Valley (CV). Through econometric and optimization-based modeling approaches, this research offers novel insights into the trade-offs between renewable energy expansion, land uses, and groundwater sustainability.

Chapter 1 evaluates the effectiveness of RPS in driving biomass consumption in U.S. electricity generation both at the extensive margin and intensive margin. We conducted difference-in-differences and synthetic control analysis separately on 10 states with varying degrees of RPS stringency and bioenergy industries. Findings reveal that RPS did not significantly increase biomass use at the extensive margin in most states but encouraged the expansion of other renewables like solar and wind. At the intensive margin, co-firing biomass with coal increased only in New Hampshire. However, many states shifted toward landfill gas utilization, highlighting the importance of policy design and regional energy structures in shaping renewable adoption.

California's Central Valley (CV) is a vital agricultural region facing severe water shortages and long-term sustainability challenges. To address these issues and the increasing demand

for renewable energy, agrivoltaics (Ag-PV) — the integration of agriculture and solar energy production — presents a promising solution. Chapter 2 develops a regime-switching stochastic dynamic programming model to evaluate individual landowner decisions between traditional agriculture, solar farms, and agrivoltaics under uncertainty. By analyzing representative crops with varying irrigation needs and shade tolerance, the model identifies conditions under which Ag-PV adoption is optimal. Results show that agrivoltaics becomes favorable under high solar lease rates and elevated irrigation costs, particularly for high-value, water-intensive crops. Sensitivity analysis reveals that crop-specific shade tolerance and irrigation costs significantly influence adoption decisions. This research bridges the gap between energy and agricultural economics by providing a dynamic framework for understanding how landowners respond to economic and environmental incentives.

Building on the landowner-level insights from Chapter 2, Chapter 3 expands the analysis to a regional scale, incorporating hydrological and economic feedbacks that influence land- and water- use decisions in the Central Valley. This chapter develops a dynamic, spatially explicit hydroeconomic optimization model to assess how agrivoltaic adoption impacts land allocation, irrigation strategies, and groundwater sustainability under different policy and market scenarios, including SGMA-imposed groundwater restrictions and varying solar lease incentives. Results from this study highlight how AV can complement groundwater conservation goals, but only at high levels of land use change that may be incompatible with energy sector demands for regional solar production. Further, we highlight potential "water leakage" effects of solar and AV adoption, in which concentrated solar production in one region causes crop mix changes and irrigation intensification in other regions, potentially exacerbating groundwater management challenges.

© Copyright 2025 by Shiyue Yao

All Rights Reserved

Essays on Renewable Energy, Agrivoltaics, and Groundwater Sustainability

by
Shiyue Yao

A dissertation submitted to the Graduate Faculty of
North Carolina State University
in partial fulfillment of the
requirements for the Degree of
Doctor of Philosophy

Economics

Raleigh, North Carolina
2025

APPROVED BY:

Justin Baker
Co-chair of Advisory Committee

Zachary Brown
Co-chair of Advisory Committee

Junjie Wu

Harrison Fell

Jeremiah Johnson

DEDICATION

To my parents, whose love, sacrifices, and endless support have made this journey possible.

BIOGRAPHY

The author was born in Baoji, Shaanxi, China. She earned her Bachelor's degree in Energy Economics from Beihang University in 2019 and is currently completing her Ph.D. in Economics at North Carolina State University. Her research focuses on environmental and resource economics, particularly agrivoltaics, groundwater sustainability, and renewable energy policy.

ACKNOWLEDGEMENTS

Here, I would like to express my deepest gratitude to my advisor Dr. Justin Baker and Dr. Zachary Brown for their guidance and support throughout my Ph.D. journey. Dr. Baker has been an incredible mentor, providing both academic and personal support during my most challenging times. His encouragement and belief in my work have meant the world to me. Dr. Brown's sharp insights and expertise have been invaluable in helping me refine my modeling approach and navigate challenges in my research. I feel incredibly lucky to have had both of them as my advisors.

I also am sincerely grateful to my committee members, Dr. Junjie Wu, Dr. Harrison Fell, and Dr. Jeremiah Johnson for their thoughtful feedback and support. Their insights have strengthened this dissertation in countless ways.

I also acknowledge the support from U.S. Environmental Protection Agency (EPA) for Chapter 1 of this dissertation (Contract EP-BPA-16-H-002, Call Order #EP-B16H-00176). I extend my gratitude to my co-authors, Justin Larson, John Steller, Alison Bean de Hernandez, and Sara Ohrel, for their collaboration and contributions.

Chapters 2 and 3 were supported by the NSF INFEWS project (Grant #2025989). I am also grateful to the research team at China IWHR for their valuable feedback on an earlier presentation of this work.

Finally, to my family—thank you for your love, patience, and belief in me. I have not been able to return home for the past five and a half years, and I am truly sorry for the time we have lost. I hope to make it up to you soon. None of this would have been possible without you.

TABLE OF CONTENTS

List of Tables	viii
List of Figures	ix
Chapter 1 How Have Renewable Portfolio Standards Affected Bioelectricity Generation? Evidence from Diff-in-Diff Analysis	1
1.1 Introduction	2
1.2 Background	3
1.3 Literature Review	6
1.4 Data	9
1.5 Identification Strategy	10
1.5.1 Difference-in-Differences (DiD) for different renewable fuel use	10
1.6 Difference-in-differences for co-firing	11
1.6.1 Synthetic Control Method (SCM)	13
1.7 Results	14
1.7.1 Biomass Usage at dedicated bioenergy facilities	14
1.7.2 Other renewables (wind, solar, and geothermal) usage	15
1.7.3 Biomass feedstocks	16
1.7.4 Co-firing	18
1.7.5 Synthetic control results	19
1.8 Discussions	21
1.8.1 Maine	22
1.8.2 New Hampshire	23
1.8.3 Vermont	24
1.8.4 Landfill Gas	25
1.9 Conclusion	26
Chapter 2 Dynamic Decision Making and Agrivoltaics in California's Central Valley 30	
2.1 Introduction	30
2.2 Background and Literature Review	34
2.3 Theoretical Framework	37
2.3.1 Regime Switching Framework	38
2.3.2 Reward Functions	41
2.3.3 Bellman Equations	43
2.4 Computational Method	44
2.5 Data and Empirical Analysis	47
2.5.1 Data	48
2.5.2 Parameterization	51
2.5.3 Scenario Analysis	52
2.6 Results	53

2.6.1	Representative Crops	53
2.6.2	Scenario Analysis	55
2.6.3	Crop-specific Analysis	58
2.6.4	Sensitivity Analysis	58
2.7	Discussions	60
2.7.1	Key Findings	60
2.7.2	Policy Implications	62
2.7.3	Limitations and Future Work	63
2.8	Conclusions	64
2.9	Tables and Figures	66
Chapter 3	Optimizing Agrivoltaics Adoption to Support Groundwater Conservation in California's Central Valley	78
3.1	Introduction	79
3.2	Literature Review	80
3.2.1	Agrivoltaics and Regional Groundwater Management	81
3.2.2	Hydrologic and Hydroeconomic Models in the Central Valley	82
3.3	Methodology	84
3.3.1	Objective Function	85
3.3.2	Constraints	87
3.4	Data	90
3.4.1	Data sources	90
3.4.2	Linking Irrigation Demand to Yield Levels	92
3.5	Results	94
3.5.1	Baseline Land-Use scenarios	94
3.5.2	Sensitivity and Policy Analysis	104
3.5.3	SGMA Restrictions	105
3.5.4	Solar Lease Rate	107
3.5.5	Economic Impact	108
3.6	Discussion	109
3.6.1	Key Findings	109
3.6.2	Limitation	111
3.7	Conclusion	112
References		115
APPENDIX		124
Appendix A	Supplementary Materials	125
A.1	Synthetic Control Method: Placebo Test Results for Each RPS State	125
A.2	Parameter Values for Chapter 2	128
A.3	Supplementary Materials for Chapter 3	130
A.3.1	Initial Conditions	130
A.3.2	Total Water Use Across Land-use Scenarios	130

A.3.3	Impact of Solar and Agrivoltaics on Water Use	132
A.3.4	Land Use Allocation Across SGMA Scenarios	133
A.3.5	Impact of SGMA on Groundwater Level	135
A.3.6	Land Use Allocation Across Solar Lease Rate Scenarios	137
A.3.7	Impact of Varying Solar Lease Rates	138

LIST OF TABLES

Table 1.1	Diff-in-Diff Results for Biomass Usage at Dedicated Biopower Facilities	14
Table 1.2	Diff-in-Diff Results for Other Renewables	15
Table 1.3	Diff-in-Diff Results for Landfill Gas and Other Biogas Usage	16
Table 1.4	Diff-in-Diff Results for Wood Solid Waste Usage	17
Table 1.5	Diff-in-Diff Results for Other Biomass Energy Usage	18
Table 1.6	Diff-in-Diff Results for Biomass Co-Firing with Fossil Fuels	19
Table 1.7	Weights for States in Biomass Usage Analysis	20
Table 2.1	Sensitivity Analysis - Optimal Regime Under Steady State (α)	76
Table 2.2	Sensitivity Analysis - Optimal Regime Under Steady State (ρ)	77
Table 2.3	Sensitivity Analysis - Optimal Regime Under Steady State (γ)	77
Table 2.4	Sensitivity Analysis - Optimal Regime Under Steady State (K)	77
Table 3.1	Net Present Value (NPV) breakdown across land-use scenarios	104
Table 3.2	Percentage Change in Total NPV Relative to Status-quo	108
Table A.1	Parameters used for Representative Crops	128
Table A.2	Parameters used for All Crops (Part I)	129
Table A.3	Parameters used for All Crops (Part II)	129

LIST OF FIGURES

Figure 1.1	Total Generation in the United States (2020). Source: Energy Information Administration (EIA) form 923 (2020)	4
Figure 1.2	AEO annual report projections for biomass consumption	7
Figure 1.3	Treatment Effect of RPS Policies from Synthetic Control Method	21
Figure 2.1	Illustration of the Regime Switching Model	39
Figure 2.2	Historical Ag Revenue and Irrigation Cost in California	66
Figure 2.3	Simulated Ag Revenue and Irrigation Cost for All Crops	66
Figure 2.4	Simulated Ag Revenue and Irrigation Cost for Representative Crops	67
Figure 2.5	Policy Functions for Representative Crops (Baseline)	68
Figure 2.6	Policy Functions for Representative Crops (Low Shade Tolerance)	69
Figure 2.7	Optimal Land-Use Regime Distribution Over Time Under SGMA Scenarios	70
Figure 2.8	Optimal Land-Use Regime Distribution Over Time Under Solar Rent Scenarios	71
Figure 2.9	Optimal Land-Use Regime Distribution Over Time Under Risk Scenarios	72
Figure 2.10	Policy Functions Under Risk Scenarios	73
Figure 2.11	Policy Functions for All Crops	74
Figure 2.12	Policy Functions for All Crops (continued)	75
Figure 3.1	Modeled Crop Distribution in Central Valley	91
Figure 3.2	Crop-Specific Irrigation Requirements by Irrigation Intensity	94
Figure 3.3	Impact of Solar and Agrivoltaics on Agricultural Land Use Over Time	95
Figure 3.4	Crop-Specific Land Use Across Different Land-Use Scenarios	97
Figure 3.5	Regional allocation of land to solar-only (SO) and agrivoltaics (AV)	97
Figure 3.6	Water Use Over Time Under the Three Land-use Scenarios.	98
Figure 3.7	Agricultural Land By Irrigation Level.	99
Figure 3.8	Yearly Groundwater Pumping Distribution Under Each Scenario	100
Figure 3.9	Regional Impact of Solar-Only and Agrivoltaics on Groundwater Level	101
Figure 3.10	Yearly Surface Water Withdrawal Distribution Under Each Scenario	102
Figure A.1	Placebo Test Results for Each RPS State (I)	126
Figure A.1	Placebo Test Results for Each RPS State (II)	127
Figure A.2	Initial Condition of Surface and Groundwater by CVPM	130
Figure A.3	Total Water Use Across CVPM Regions	131
Figure A.4	Impact of Solar and Agrivoltaics on Groundwater Withdrawals	132
Figure A.5	Impact of Solar and Agrivoltaics on Surface Water Withdrawals	132
Figure A.6	Land Use Allocation Across SGMA Scenarios (S1)	133
Figure A.7	Land Use Allocation Across SGMA Scenarios (S2)	134

Figure A.8	Land Use Allocation Across SGMA Scenarios (S3)	134
Figure A.9	Impact of SGMA on Groundwater Level (S1)	135
Figure A.10	Impact of SGMA on Groundwater Level (S2)	135
Figure A.11	Impact of SGMA on Groundwater Level (S3)	136
Figure A.12	Land Use Allocation Across Solar Lease Rate Scenarios (S2)	137
Figure A.13	Land Use Allocation Across Solar Lease Rate Scenarios (S3)	137
Figure A.14	Impact of Varying Solar Lease Rate on Groundwater Level (S2)	138
Figure A.15	Impact of Varying Solar Lease Rate on Groundwater Level (S3)	138

CHAPTER

1

HOW HAVE RENEWABLE PORTFOLIO
STANDARDS AFFECTED BIOELECTRICITY
GENERATION? EVIDENCE FROM
DIFF-IN-DIFF ANALYSIS

1.1 Introduction

Renewable electricity generation in the United States has grown significantly over the last two decades, driven by a combination of national and state policy incentives and technological advancements that have decreased the relative costs of wind and solar. Renewable Portfolio Standards (RPS) are a popular incentive structure in U.S. states that impose mandatory or voluntary targets for renewable electricity generation. By requiring a minimum percentage of electricity generated from renewable energy with a specific timeline, RPS policies can both promote renewable electricity generation expansion as well as a reduction in fossil fuel consumption as a total proportion of fuel input for electricity generation. Currently, there are 32 states that have active RPS policies with different levels of stringency and emphasis on different sources of renewables (DSIRE 2022).

Though the RPS policies aim at increasing total renewable energy use, different renewable sources vary in availability, stability, and cost-effectiveness. For example, wind and solar are two primary sources of renewable electricity as they do not directly emit greenhouse gas (GHG) emissions to generate power; however, the generation output from these sources is variable, depending on factors such as the weather or time of the day.

In contrast, bioenergy (energy derived from biogenic resources such as wood, agricultural materials, and landfill gas) can provide a steady and reliable baseload output and thus could offer a near-term renewable energy investment option for baseload supply. However, bioenergy emits GHG emissions at the point of energy production, and the costs associated with procuring a constant supply vary and may be significant. Biomass is also unique in that it can allow electricity providers the flexibility to invest in both extensive margin (e.g., new biomass facilities) and/or intensive margin (by introducing or increasing co-firing in existing coal-fired facilities) of the power industry. Despite this flexibility and growing stringency of state-level RPS policies, it is unclear whether U.S. biomass electricity

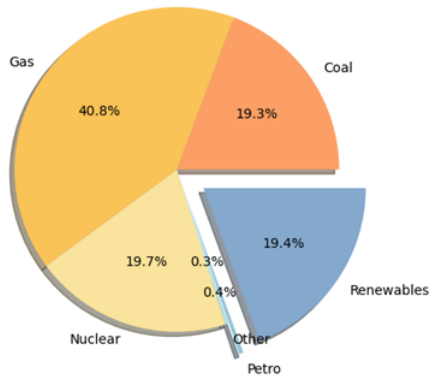
will expand or contract in the future and whether existing state policies have incentivized changes in biomass consumption in energy systems. This paper investigates to what extent bioenergy usage, including different sources of biomass, in-state electricity generation portfolios is impacted by the RPS policies.

1.2 Background

Of the 4,003.3 terawatt hours (TWh) of total U.S. net electricity generated in 2020, renewable resources made up approximately 19.4%, as shown in Figure 1.1. Hydroelectric, solar and wind generation accounted for 17.6% of net electric generation while total biomass accounted for only 1.5%. Of the electric power generated by biomass, wood and wood-derived fuels¹ are the most prevalent as fuel used for electricity generation. From 2009 to 2020, U.S. net electricity generation from biomass increased, with most of the additional generation coming from landfill gas, and wood and wood fuels. For states with RPS policies, biomass is often generally referred to as an eligible renewable energy technology or fuel input as opposed to specific types of biomass individually identified within the policy. However, specific definitions of biomass and how it can be used toward an RPS' goals can vary state by state. Some states limit the use of biomass for achieving RPS targets by stipulating the types of biomass eligible under the program. Some states, such as Massachusetts, require that biomass materials used for energy can be considered eligible after elements such as greenhouse gas emissions, old-growth forests, sustainable forestry, and best management practices are taken into account, among other environmental requirements (Barnes 2012). Another example is Connecticut, which excludes biomass materials such as, "construction and demolition waste, finished biomass products from sawmills, paper mills or stud mills,

¹This analysis adopts the Form EIA-923 classification of fuel inputs for wood and wood-derived fuels (EIA 923 2022)

Net Electric Generation in the U.S. in 2020: 4003.3 TWh



Renewable Generation in the U.S. in 2020: 777.2 TWh

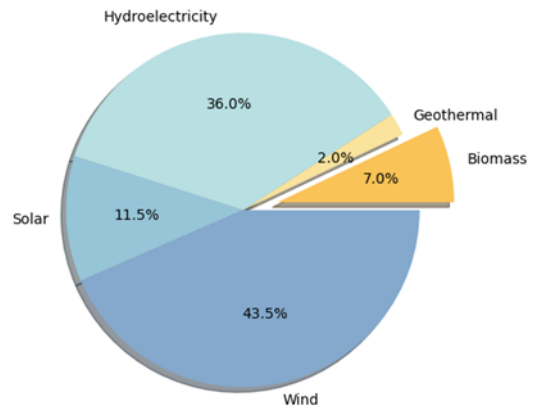


Figure 1.1: Total Generation in the United States (2020). Source: Energy Information Administration (EIA) form 923 (2020)

organic refuse fuel derived separately from municipal solid waste, or biomass from old growth timber stands." In the North Carolina RPS policy, biomass is defined as, "agricultural waste, animal waste, wood waste, spent pulping liquors, combustible residues, combustible liquids, combustible gases, energy crops, or landfill methane." The policy specifies that in 2018, and each year after, at least 0.2% of total electricity sold must be supplied from swine waste. Similarly, by 2014 and after, 900,000 MWh of electricity sold must come from poultry waste resources (DSIRE 2022).

Given the heterogeneity in biomass types, biomass availability, and how state RPS policies approach bioenergy, we estimate state-specific RPS policy effects for a subset of U.S. states – Maine, Vermont, New Hampshire, Connecticut, Massachusetts, Oregon, Washington, North Carolina, Virginia, and New York. These states are chosen for the representation of differing policies, geographic regions and respective electricity markets, and availability of biomass materials. First, the state policies differ depending on factors such as if the state implements solar or wind targets, whether the state includes alternative compliance

payments (ACP) or cost caps, whether it allows for outside state RECs, and each state's definition of renewable resources and technologies (Barnes 2014; EPA 2015). Second, the electricity markets differ by geographic regions and regulatory openness. For example, markets in Maine, New Hampshire, and Oregon have competitive markets, while Vermont, North Carolina, and Washington have traditionally regulated markets (EPA 2017). Last, the availability of biomass varies widely across the states in our sample, and generally varies considerably over time in, for example, states with active forest industries as markets and related harvests may fluctuate over time (Baker et al. 2018).

Our results confirm that RPS policies have had only a modest impact on biomass electricity investments at the extensive margins, while investments in wind and solar have been positively impacted by the policies. Somewhat surprisingly, we find limited or no impact of RPS policies at the intensive margin outside of New Hampshire, i.e., no additional biomass co-firing in response to the renewable energy policy. This null result suggests that electricity providers are bypassing intermediate investments at the intensive margin that could extend the lifetime of existing energy infrastructure and are focusing investments in increasing capacity at the extensive margin in other renewables that receive complementary incentives (namely wind and solar). Uncertainty regarding financial (e.g, the availability and cost of biomass inputs (Baker et al. 2018), social (e.g., varying degrees of acceptance of biomass energy (Fytili and Zabaniotou 2017) and policy (e.g., debates about potential environmental outcomes associated with biomass use for energy (Khanna and Zilberman 2017) conditions surrounding biomass energy could also be contributing to this under-investment, but the role of those potential drivers are beyond the scope of this analysis (White et al. 2013b).

1.3 Literature Review

There is a growing literature around the potential role of biomass in renewable energy policy futures. This literature includes integrated assessment modeling studies that have investigated bioenergy in the context of climate stabilization scenarios that do not define specific policies but model general decarbonization pathways in the global energy and industrial systems to achieve some atmospheric CO₂ concentration level under different socioeconomic development assumptions (Popp et al. 2017; Riahi et al. 2017). Under these ambitious stabilization pathways, biomass energy in conjunction with carbon capture and storage (CCS) plays an important role in reducing net emissions (Kikstra et al. 2022; Roe et al. 2019), despite the industry being relatively nascent and facing a number of logistical and institutional challenges (Galik 2020).

Other recent studies have taken a policy agnostic view to evaluate the technical and economic potential of bioenergy, including the U.S. Billion Ton Report (Langholtz et al. 2016). Further, some studies have assumed RPS policies are a primary driver of forest and agricultural biomass demand and have conducted scenario analysis around specific feedstocks (Baker et al. 2018) and portfolio of feedstocks under different policy and market assumptions (Latta et al. 2013; White et al. 2013b). Another portion of the literature has examined bioenergy in conjunction with other climate mitigation levers, including incentives to expand forest carbon storage (Baker et al. 2019; Favero et al. 2017).

Regardless of the analytical approach, the focus on biomass energy in the modeling literature is predicated on the assumption that biomass will play a critical role in renewable energy policy futures. While potentially true, it is worth noting that the anticipated role of bioenergy as a renewable energy source has declined in recent Annual Energy Outlook (AEO) reports, which assume competition between alternative energy sources. Figure 1.2 shows an example of this, with biomass projections varying significantly across AEO reports,

with differences driven by scenario assumptions and policies reflected in the reference case scenario and relative costs of different renewable energy sources.²

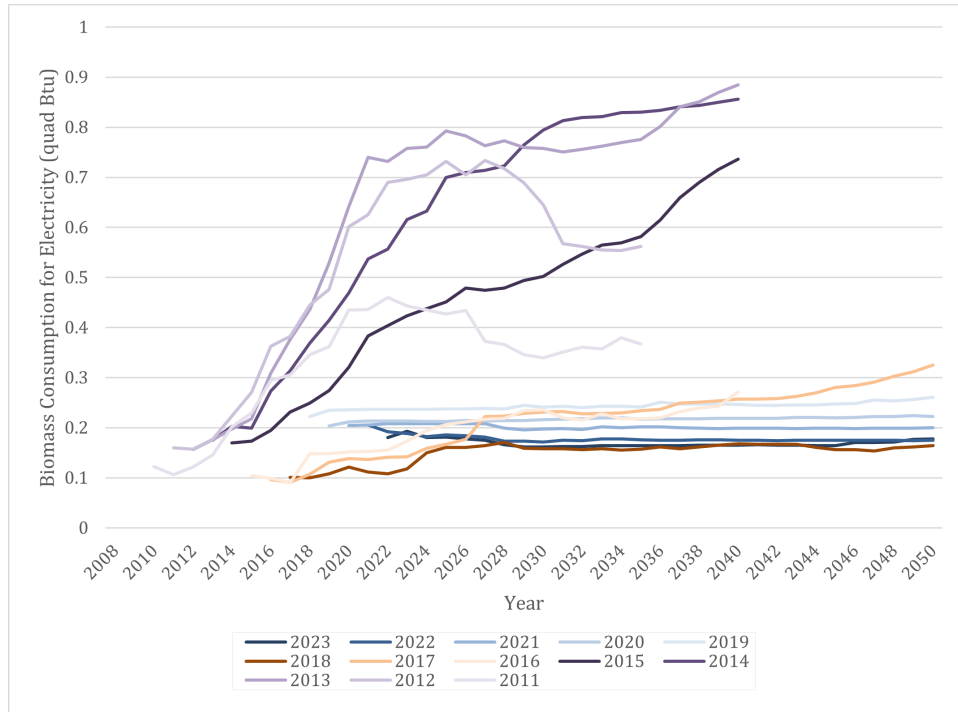


Figure 1.2: AEO annual report projections for biomass consumption

Given the focus of bioenergy as a renewable energy source in the modeling literature, there are few studies that have empirically assessed how biomass energy has responded to different policy drivers, especially in the U.S. This is a specific gap in the literature we attempt to start to fill with this analysis, specifically within the context of RPS policies.

With heterogeneity across state RPS policies, the literature has focused on the policy design, studying the effectiveness of one or more specific RPS attributes (Barbose et al. 2015; Carley et al. 2018; Fischlein and Smith 2013; Shayegh and Sanchez 2021; Wisner et al. 2017; Yin

²Recent updates to the AEO have lowered the levelized costs of wind and solar energy, making these energy alternatives more competitive with biomass and fossil fuels (AEO, 2017).

and Powers 2010). Yin and Powers (2010) is one of the earliest studies to address the different impact of RPS policies in different states, and incorporate analysis of heterogeneity in the coverage of facilities, whether existing capacity can fulfill the requirement, RECs trading, and alternative compliance payment (ACP). But after the publication of that paper, there are more states that established new RPSs that also vary in many aspects. Recent papers include more policy attributes into the evaluation, for example, carve-outs (Buckman 2011) credit multipliers (Carley et al. 2018), lifetime of RECs (Joshi 2021), electricity market structure (Shayegh and Sanchez 2021), and number of interviews per year (Carley et al. 2018).

Not only does the specification of policy design differ in the literature, recent studies also start to acknowledge the importance of outcome variable selection in RPS effectiveness evaluations (Fischlein and Smith 2013). Carley (2009) investigates renewable generation from 1998 to 2008 and finds that although the total generation from renewables has increased, the percentage of electricity from renewable sources, which is the target for most RPSs, has not been significantly impacted by the policy. Joshi (2021) and Yin and Powers (2010) focus on the share of capacity generated by renewable sources as the outcome of interest, studying whether RPSs has incentivized new renewables to be installed. In this paper, we focus on the fuel usage associated with each renewable source, which is not only generated by new capacity (or the extensive margin), but also the increase of usage in the intensive margin (co-firing at existing facilities).

Though there has been wide literature in empirical evaluations of the RPS policy that studies whether RPS increases renewable electricity in general (Joshi 2021; Yin and Powers 2010), several studies focused on wind (Adelaja et al. 2010) or solar specifically, little empirical work to date has assessed how biomass energy has responded to different policy drivers such as the RPS, despite the large and varied modeling literature that has projected future market and resource implications of assumed biomass policy shocks. This paper builds on the working paper by Larson et al. (2019) by developing a new identification strategy

and further investigating the role that different biomass feedstock sources have played in electricity generation for states with existing RPS policies and adequate biomass feedstock supplies (e.g., high proportion of forest cover or agricultural and forest sector production potential).

1.4 Data

The main outcome of interest for this analysis is how/to what degree/whether biomass fuel consumption levels for electricity generation have been influenced by existing RPS policies. We analyzed observed fuel consumption from the EIA Form 923 for the years 2001 to 2020. We limit the analysis to this time frame to avoid potential lag effects of the COVID-19 pandemic on fuel prices, consumption patterns, and electricity mixes beyond 2020.

Form 923 asks power plants to report information on net generation and fuel consumption (broken into distinct fossil and renewable fuel categories) at monthly and annual levels. The published data also includes plant characteristics such as operator, census region, NERC region, and primary fuel used for electricity generation. The generation and fuel consumption data are downloaded as annual cross-sections directly from the EIA website and compiled as panel data. For all EGU facilities included in this analysis, we filtered biomass and non-biomass renewable energy sources according to EIA classifications. Further, we use plant-level data on biomass fuel consumption to analyze the RPS's effect on the use of bioenergy in co-firing plants.

1.5 Identification Strategy

In this paper, we adopt both a difference-in-differences framework and the synthetic control method following Abadie et al. (2010) to evaluate the potential causal relationship between RPS policy and renewable energy use in electricity generation. The identification assumption for the synthetic control method is similar to a typical difference-in-differences method: the common trend assumption, which assumes that the treated and control groups would have trended the same way if there were no treatment.

1.5.1 Difference-in-Differences (DiD) for different renewable fuel use

The following equation represents our based difference-in-differences specification, where we examine facility-scale fuel consumption patterns:

$$Y_{i,t}^k = \beta_0^k + \beta_1^k \text{RPS}_i \text{Post}_t + \delta_i^k + \gamma_t^k + \epsilon_{it}^k \quad (1.1)$$

where i is the facility identifier, k is the fuel type indicator, and t is the year indicator from 2000 to 2020. $Y_{i,t}^k$, the key outcome variable of interest is the consumption of fuel in millions of Btus for the purpose of generating electricity³. β_0^k is the intercept coefficient that varies with fuel type. In our analysis, we assume that the RPS policies can only have an impact when it is effective, not when the policy is enacted. Additionally, if the policy's effective date is in November or December of the year, then the impact will not be detected until the next year. δ_i^k and γ_t^k are individual fixed effects and year fixed effects that vary with fuel type. ϵ_{it}^k is the error term.

To account for the heterogeneity of RPS attributes, including specific renewable targets

³In combined heated and electricity plants, the fuel consumption is only for electricity.

⁴Total fuel consumption, net generation, share of generation are also used as outcome variables, results presented as robustness checks.

and tradable RECs as discussed in section 1.2, we run the regression for each RPS state with the same set of control states. The coefficients of interest in this model are the set of β_1^k s that reflects the impacts of RPS policies on each state’s consumption of renewable fuels in electricity generation. We first separate the non-hydro renewables into biomass ($k = 1$) and other renewables ($k = 2$ for solar, wind, and geothermal combined), according to the reported fuel type in EIA 923.

Furthermore, we separate biomass into different categories 1) landfill gas and other biogas, ($k = 11$); 2) wood solid waste ($k = 12$), and 3) other biomass ($k = 13$) including agricultural by-products, municipal waste, wood liquid waste, sludge waste and other bio liquid and solid. For the remainder of this analysis, we adopt the term “biomass” to represent all biomass-derived fuel inputs, including solid, liquid, or gaseous forms as categorized by EIA.

1.6 Difference-in-differences for co-firing

In most states, one possible option for a utility to meet RPS requirements is to co-fire biomass with fossil fuels, for example, burning wood chips in conjugation with the primary fossil fuel input such as coal. To examine the effects of RPS on co-firing, we adopt the same DiD framework, but at the plant level where we consider the coal-fired power plants that have engaged in co-firing for at least one year within our observation window. We use a different outcome variable, which is calculated as the share of generation from the facility that is due to co-firing biomass. The regression can be further written as:

$$\text{pct}_{jt} = \alpha_0 + \alpha_1 \text{RPS}_j \text{Post}_t + \phi_j + \zeta_t + u_{jt} \quad (1.2)$$

where the outcome variable $\text{pct}_{j,t}$ is the percentage of co-firing in plant j , year t . Here, the RPS_j indicator equals 1 if plant j is in an RPS state. ϕ_j is the plant fixed effect and ζ_t is the year fixed effect. Still, we want to incorporate heterogeneity between different RPS attributes, so the regression is run for each of the 10 RPS states in the analysis. The coefficient of interest will be α_1 , reflecting the impact of each state's RPS policy on the usage of co-firing in coal facilities. This methodology extends our analysis by investigating the effectiveness of RPS policies on the intensive margin at a facility level.

From section 1.5.1 and 1.6, we utilize a similar two-way fixed effect difference-in-differences framework to examine the impact of RPS policies on both the extensive margin and the intensive margin. The advantage of the DiD approach is its simplicity. Estimates can be interpreted easily, estimation is not computationally intense, and DiD uses a well-established framework (linear regression) that is familiar to researchers and policymakers. However, DiD has its disadvantages. First, the parallel trend assumption implies that the control group is not impacted at all by the treatment (Meyer 1995). Another drawback is the sensitivity of results to control group selection. Since DiD requires that the researcher make judgments on picking the control group, these selections have direct implications for results. Ancillary policies (tax incentives), differing economic environments (regional biomass availability and supporting industrial activity), and spillovers (related energy policies in bordering states) all pose challenges to the researcher in producing an adequate representation of what the treatment group would have been in the absence of the treatment. Due to these two disadvantages, DiD on its own may not be adequate for estimating the treatment effect of policies at a state or regional level (Abadie et al. 2010).

1.6.1 Synthetic Control Method (SCM)

Given that the selection of counterfactual is essential to estimating the treatment effect, we test the robustness of our findings by implementing the synthetic control method, following Abadie, Diamond and Hainmueller (Abadie et al. 2010, 2015). We include all the potential control units (namely, all the 13 states without any RPS) in the donor pool, and instead of using a flat average as in DiD, SCM then weighs each unit based on its similarity to the treated group during the pre-treated period. By finding out the optimal weight, SCM can construct a better counterfactual than the DiD framework.

Following Abadie et al. (2010), the outcome variable can be modeled as $Y_{it} = Y_{it}^N + \alpha_{it} D_{it}$, where treated unit is labeled $i = 1$, and the J units in the donor pool are labeled $i = 2, 3 \dots J+1$; $D_{it} = 1$ if unit i is treated at period t ; and the outcome for the untreated can be modeled as $Y_{it}^N = \delta_t + \theta_t \mathbf{Z}_i + \lambda_t \mu_i + \epsilon_{it}$, where \mathbf{Z}_i is a vector of observable covairates that are not affected by the intervention, and λ_t consists of unobserved common factors that are state-invariant.

The objective of SCM is to find the optimal weighting vector $W^* = (w_2^*, w_3^*, \dots w_{J+1}^*)'$ that minimizes the distance between the treated and the synthetic control before the intervention. The distance we consider here includes the pretrend outcome variable and the vector of observables \mathbf{Z}_i including share of generation, number of plants and facilities, state total generation, and total electricity sales. Let $\mathbf{X}_i = [\{Y_{it}\}_{t=0}^T, \mathbf{Z}_i]'$ the optimization problem can be written as:

$$\begin{aligned} (w_2^*, \dots w_{J+1}^*) &= \arg \min_{w_2, \dots, w_{J+1}} \|X_1 - \sum_{i=2}^{J+1} w_i \mathbf{X}_i\| \\ \text{s.t. } w_i &\geq 0, \text{ and } \sum_{i=2}^{J+1} w_i = 1 \end{aligned} \tag{1.3}$$

The counterfactual, or the synthetic control, is then composed as $Y_{it}^N = \sum_{i=2}^{J+1} w_i^* Y_{it}$. We then compare each RPS state with their synthetic control counterfactual.

1.7 Results

In our analysis, we break down the question of RPS effectiveness into three parts. First, for each state, we assess the impact of RPS on biomass consumption for electricity generation at dedicated bioenergy facilities and compare the results with the RPS effect on other renewables. Further, we classify bioenergy into different feedstocks, investigating what kind of biomass is driving the change in biomass consumption for electricity generation. Finally, we evaluate whether RPS policies affect intensive margin biomass co-firing at coal-fired power plants.

1.7.1 Biomass Usage at dedicated bioenergy facilities

Table 1.1: Diff-in-Diff Results for Biomass Usage at Dedicated Biopower Facilities

VARIABLES	(1)	(2)	(3)	(4)	(5)	(6)	(7)	(8)	(9)	(10)
	ME	VT	NH	CT	MA	OR	WA	NC	VA	NY
rps_effect	-12.23*** (2.549)	-2.894 (3.352)	5.604* (3.051)	2.685 (3.707)	2.792 (3.736)	2.340 (3.051)	-0.929 (3.485)	2.471 (2.752)	4.168 (4.367)	3.426 (3.972)
Observations	253	253	253	253	253	253	253	253	253	253
R-squared	0.847	0.826	0.832	0.819	0.819	0.826	0.826	0.830	0.805	0.821
Year FE	Yes	Yes	Yes	Yes	Yes	Yes	Yes	Yes	Yes	Yes
State FE	Yes	Yes	Yes	Yes	Yes	Yes	Yes	Yes	Yes	Yes

Robust standard errors in parentheses.

*** p<0.01, ** p<0.05, * p<0.1

Table 1.1 contains the two-way fixed effect Diff in Diff results for biomass use for electricity generation at dedicated biopower facilities. The row rps_effect represents the treatment effect of the RPS policy on biomass consumption in each state compared with the control states. Surprisingly, we find that for most states, RPS did not have a significant impact on biomass consumption. New Hampshire is the only state we find that significantly increased their biomass usage. On average, compared with control states, biomass consumption in

New Hampshire increased by 5.6 mmBTU after the state’s RPS policy. However, in Maine, Vermont, and Washington, RPS even had a negative impact on their biomass use. In section 1.7.2 we will further decompose the analysis to different biomass types and investigate which biomass source is driving this change.

1.7.2 Other renewables (wind, solar, and geothermal) usage

Table 1.2: Diff-in-Diff Results for Other Renewables

VARIABLES	(1)	(2)	(3)	(4)	(5)	(6)	(7)	(8)	(9)	(10)
	ME	VT	NH	CT	MA	OR	WA	NC	VA	NY
rps_effect	-3.117 (5.741)	-13.33** (5.701)	-1.595 (1.466)	33.91** (12.73)	33.95** (12.40)	34.81*** (5.972)	36.14*** (5.996)	19.90*** (1.466)	29.82** (11.84)	37.66*** (10.90)
Observations	169	175	168	163	169	175	174	168	162	175
R-squared	0.686	0.672	0.673	0.682	0.679	0.799	0.802	0.656	0.670	0.718
Year FE	Yes	Yes	Yes	Yes	Yes	Yes	Yes	Yes	Yes	Yes
State FE	Yes	Yes	Yes	Yes	Yes	Yes	Yes	Yes	Yes	Yes

Robust standard errors in parentheses.

*** p<0.01, ** p<0.05, * p<0.1

Table 1.2 shows the RPS treatment effect in other renewable consumptions for electricity generation. In large part, results suggest that post-treatment renewable electricity generation increased for our treatment states. Specifically, we find that in Connecticut, Massachusetts, Washington, North Carolina, Virginia, New York State, and Oregon, RPS had a significant positive impact on other renewable electricity generations in varying degrees, suggesting a positive impact of the policies on the adoption of non-biomass renewable energy generation technologies. Nevertheless, compared with the non-RPS control states, Vermont significantly decreased the other renewable electricity by 13.33 MMBtu on average. Other than that, Maine and New Hampshire have seen a non-significant decrease.

1.7.3 Biomass feedstocks

Despite the null results in biomass consumption in most RPS states (except for negative ones in Maine and Vermont) we gain from table 1.3, we further break down the biomass usage into different types of biomass feedstocks, to determine whether the RPS policies support the increase in specific feedstocks instead of biomass consumption in aggregate. We disaggregate biomass fuel consumption into specific categories, including 1) Landfill gas and other biogas, (about 21% of the bio-source electricity on average); 2) Wood solid waste, which is on average 50.3% of the biomass generation; and the rest are 3) other biomass sources including agricultural byproducts, municipal waste, and sludge waste.

Table 1.3: Diff-in-Diff Results for Landfill Gas and Other Biogas Usage

VARIABLES	(1)	(2)	(3)	(4)	(5)	(6)	(7)	(8)	(9)	(10)
	ME	VT	NH	CT	MA	OR	WA	NC	VA	NY
rps_effect	0.0838 (0.0829)	0.0919 (0.104)	-1.148*** (0.296)	0.951* (0.448)	0.934* (0.460)	1.282*** (0.300)	-0.180 (0.281)	2.475*** (0.327)	1.915** (0.861)	1.846** (0.792)
Observations	176	177	184	184	184	183	184	184	184	184
R-squared	0.795	0.794	0.783	0.779	0.782	0.802	0.785	0.809	0.753	0.855
Year FE	Yes	Yes	Yes	Yes	Yes	Yes	Yes	Yes	Yes	Yes
State FE	Yes	Yes	Yes	Yes	Yes	Yes	Yes	Yes	Yes	Yes

Robust standard errors in parentheses.

*** p<0.01, ** p<0.05, * p<0.1

Landfill gas and other biogas Municipal waste is one of the largest human-generated sources of methane emissions. Without proper treatment, landfill gases contain 50%-55% methane by volume, which has a global warming potential that is more than 28 times greater than carbon dioxide (IPCC 2014). As a result, burning landfill gas for electricity not only generates direct economic benefits but also reduces methane emissions and contributes to the economy in the long run. Table 1.3 shows the treatment effect of RPS policies on landfill gas and other gas sources in dedicated biopower facilities. Except for New Hampshire and

Washington, most states increased their landfill gas consumption as a source of electricity generation compared to the non-RPS control states, and this effect is significant in the majority of states analyzed. Thus, while aggregate biomass consumption for electricity generation was not significantly impacted by RPS implementation for most states in our analysis, landfill and other biogas consumption are positively impacted by the policy in most states.

Table 1.4: Diff-in-Diff Results for Wood Solid Waste Usage

VARIABLES	(1)	(2)	(3)	(4)	(5)	(6)	(7)	(8)	(9)	(10)
	ME	VT	NH	CT	MA	OR	WA	NC	VA	NY
rps_effect	-10.74*** (1.191)	-0.0293 (1.196)	7.811*** (1.134)	-1.530 (2.476)	-1.527 (2.382)	2.466* (1.133)	0.784 (1.113)	0.988 (1.175)	-0.0783 (2.950)	-1.488 (2.387)
Observations	235	235	235	233	235	235	235	235	235	235
R-squared	0.861	0.728	0.790	0.734	0.730	0.727	0.734	0.756	0.678	0.722
Year FE	Yes	Yes	Yes	Yes	Yes	Yes	Yes	Yes	Yes	Yes
State FE	Yes	Yes	Yes	Yes	Yes	Yes	Yes	Yes	Yes	Yes

Robust standard errors in parentheses.

*** p<0.01, ** p<0.05, * p<0.1

Wood Solid Waste In the U.S., more than half of the biomass electricity comes from wood and wood waste (which includes solid sources in municipal solid waste streams, e.g., wasted construction materials, wood pallets, and furniture). Bark, sawdust, wood chips, wood scrap, and paper mill residues are the main sources of wood solid waste, as determined by EIA923. Table 1.4 shows the DiD results for wood solid waste usage in electricity generation facilities. We see that compared with the control states, after RPS Oregon and New Hampshire had a significant increase in their wood and solid wood waste consumption post-RPS, with effects ranging from 2.47 to 7.81 MMBtu, respectively. Maine decreased their wood solid waste usage by 10.74 mmBTU.

Other biomass energy All other biomass forms are categorized in Table 1.5, including agricultural byproducts and sludge waste, which is only a small percentage of all the biomass used in the power facilities. These materials are mostly by-products that come with agricultural production activities, which are fundamentally tied to the agricultural production and commodity demand rather than renewable energy policies, therefore, are less likely to be directly incentivized by the RPS policy. The null results in other biomass are consistent with our initial expectations. Vermont dropped out from the analysis because none of the biomass in this category is being used in Vermont for electricity generation.

Table 1.5: Diff-in-Diff Results for Other Biomass Energy Usage

VARIABLES	(1)	(2)	(3)	(4)	(5)	(6)	(7)	(8)	(9)	(10)
	ME	VT	NH	CT	MA	OR	WA	NC	VA	NY
rps_effect	-2.080 (1.660)	1.041 (2.171)	-4.483 (3.052)	-4.781 (3.217)	1.631 (2.171)	0.977 (2.585)	1.947 (1.887)	-3.092 (2.667)	-4.660 (3.146)	-3.836 (2.793)
Observations	212	192	212	212	212	212	212	212	212	212
R-squared	0.944	0.944	0.944	0.938	0.939	0.944	0.944	0.944	0.942	0.939
Year FE	Yes	Yes	Yes	Yes	Yes	Yes	Yes	Yes	Yes	Yes
State FE	Yes	Yes	Yes	Yes	Yes	Yes	Yes	Yes	Yes	Yes

Robust standard errors in parentheses.

*** p<0.01, ** p<0.05, * p<0.1

1.7.4 Co-firing

Co-firing⁵ of biomass and fossil fuels in coal-fired plants is one potential option for the utility to meet RPS requirements. In some facilities, burning wood chips with coal can be used to reduce sulfur dioxide emissions. For this part of our analysis, we focus on estimating the potential effects of RPS policies on levels of biomass co-firing at coal-fired power plants for the same focus states. Utilizing the DiD framework, we reduced the sample down to

⁵Co-firing is defined as a power plant burning a secondary fuel (e.g., wood waste) in conjunction with its primary fuel (e.g., coal).

Table 1.6: Diff-in-Diff Results for Biomass Co-Firing with Fossil Fuels

VARIABLES	(1)	(2)	(3)	(4)	(5)	(6)	(7)	(8)	(9)	(10)
	ME	VT	NH	CT	MA	OR	WA	NC	VA	NY
rps_effect	0.0113 (0.0222)		0.563*** (0.0298)	0.00330 (0.0243)	0.00330 (0.0243)		-0.0274 (0.0236)	0.0429 (0.0270)	0.0405 (0.0540)	0.0463 (0.0492)
Observations	518	468	483	468	468	468	493	609	594	498
R-squared	0.018	0.016	0.086	0.016	0.016	0.016	0.016	0.030	0.043	
Number of sid	38	35	36	35	35	35	37	45	46	38
Year FE	Yes	Yes	Yes	Yes	Yes	Yes	Yes	Yes	Yes	Yes
State FE	Yes	Yes	Yes	Yes	Yes	Yes	Yes	Yes	Yes	Yes

Robust standard errors in parentheses.

*** p<0.01, ** p<0.05, * p<0.1

coal-fired power plants that exhibited co-firing for at least one year within the observation window. We then created an outcome variable, which is the share of total generation from the facility from co-firing biomass. If RPS policies impact the usage of biomass co-firing, then we should see a significant change in the share of the total generation that is from co-firing. From Table 1.6, we found that New Hampshire is the only state where co-firing has been positively impacted significantly, though on average, the RPS only increased the percentage of co-firing by 0.56% in New Hampshire.

1.7.5 Synthetic control results

Table 1.7 shows the composition of each synthetic control counterfactual for each of the RPS state; for example, the counterfactual Massachusetts is composed of 0.11 Alaska, 0.31 Florida, and 0.58 Idaho. From Table 1.7, we find that Florida is included in the synthetic control group in seven out of the ten states, which is not surprising given the similarity in biomass availability between Florida and the RPS states. After generating the synthetic control weights that compose the counterfactual, we compare each state's total biomass consumption for electricity with its optimal synthetic control (including both co-firing and biopower facilities). By plotting the treatment effect over time, we are able to track how the impact of RPS policies evolved. Figure 1.3 displays the trend in the effect of RPS policies

Table 1.7: Weights for States in Biomass Usage Analysis

Weights	CT	MA	ME	NC	NH	NY	OR	VA	VT	WA
AK	0.941	0.108	0	0.093	0	0	0.273	0	0	0.123
AL	0	0	0	0.171	0.192	0	0.056	0	0.23	0.226
AR	0	0	0	0	0	0	0.13	0	0	0
FL	0	0.308	0.804	0.164	0.233	0.197	0	0.323	0	0.451
GA	0	0	0	0.343	0	0	0	0	0	0
ID	0.02	0.584	0	0	0.576	0	0.163	0.677	0.77	0.2
KY	0	0	0	0	0	0	0	0	0	0
LA	0.04	0	0.196	0.228	0	0.275	0.379	0	0	0
MS	0	0	0	0	0	0	0	0	0	0
NE	0	0	0	0	0	0.528	0	0	0	0
TN	0	0	0	0	0	0	0	0	0	0

over time, and Appendix A.1 displays the results of the placebo test, from which we can conclude the effectiveness of RPS policies in each state. The placebo test results indicate that while RPS had no significant impact on biomass consumption in Vermont, Massachusetts, Washington, Oregon, and North Carolina, New Hampshire, Connecticut, Virginia, and New York experienced an increase in biomass consumption for electricity following the implementation of RPS. However, in line with our DID results, Maine significantly decreased its biomass consumption compared to the synthetic control and all the placebo outcomes.

In addition to the overall treatment effect, it is also helpful to examine the trends in the impact of RPS policies in each state. From Figure 1.3 we can identify several noteworthy trends. For example, the treatment effect in New Hampshire peaked around 2016 and then started to fall back. In New York and Connecticut, the RPS started to increase biomass usage within the first several years of their RPSs. However, in Virginia, for the first several years after RPS in effective, it did not increase biomass consumption until around 2013. These trends highlight the varying impacts of RPS policies in different states and the need for a closer look at the state-specific policy analyses. In the following section, we dig deeper into each state's RPS policy trying to understand what is behind the heterogeneities, and

to identify the specific policy features that may have contributed to the observed trends in biomass consumption. By examining the details of each state's RPS policy, we can gain a better understanding of the factors that determine the effectiveness of RPS policies in promoting the adoption of biomass to support state-specific renewable energy goals.

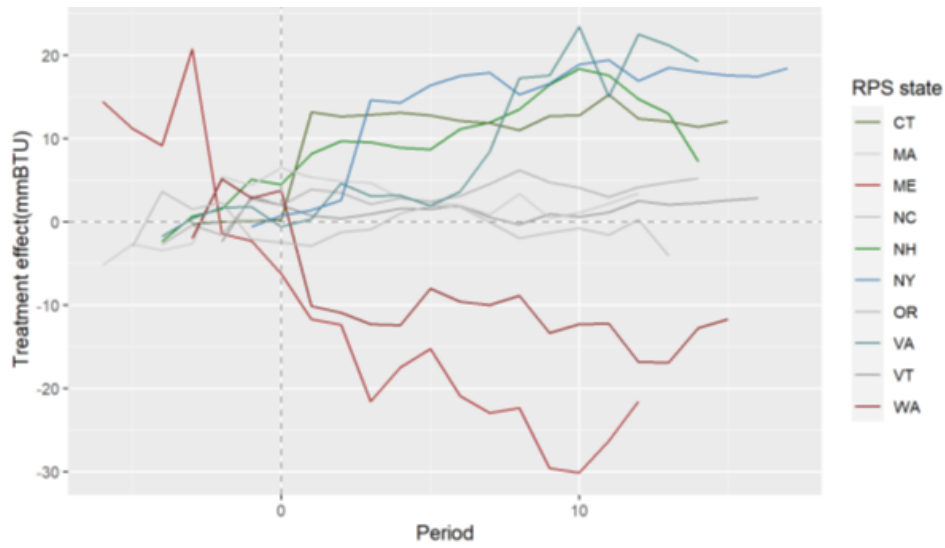


Figure 1.3: Treatment Effect of RPS Policies from Synthetic Control Method

1.8 Discussions

Based on the empirical results we have identified several general findings regarding the effectiveness of RPS policies:

1. RPSs have null impacts on many states, in more than half of the states we study, meaning that the results show no evidence of an effect (positive or negative) of RPS policies on biomass consumption for electricity generation at dedicated facilities. This finding suggests that RPS policies alone may not be sufficient to drive substantial changes in biomass usage within certain contexts.

2. RPS had a more significant positive impact on other renewables, including solar, wind and geothermal than on biomass (excluding biogas).

These findings highlight the need for a nuanced understanding of the impacts of RPS policies based on each state's resource availability, specific target, Renewable Energy Credits (RECs) tradability, and also the market dynamics within each state. Further, given interstate RECs and energy trading, facilitated by regional networks like the Regional Greenhouse Gas Initiative (RGGI), isolating the effect of the RPS policies for an individual state remains an empirical challenge. However, by comparing the varying results in different states, we identify a few notable observations, as outlined in the following sections.

1.8.1 Maine

In Maine, while all the other states are increasing or have stable biomass use, Maine decreased biomass consumption significantly. By breaking the analysis down to different feedstocks, we find that it is mostly due to the decrease in the usage of wood solid waste. To understand the context of this finding, it is important to consider the background of Maine as a state with a significant forested area, covering approximately 89% of the land. The abundance of forest resources has facilitated the establishment of numerous wood production industries in the state. Each year, over 500,000 acres of forest are harvested, and then woody materials are made into wood products or into paper manufacturing. Along with wood products, there are byproducts and other materials generated, such as bark, sawdust, wood chips, wood scrap, and paper mill residues, that have been used to produce steam and electricity. As a result, the traditional supply of biomass was highly dependent on the wood product and paper industry.

However, since the 2000s, the paper industry in Maine has seen significant contraction (Hillard 2021), leading to the closure of more than half of the paper mills in the state. As

of the end of 2013, there were 12 mills in operation, but by the end of 2021, there were only 6 left, with further closures announced for the near future. This decline in the paper manufacturing sector has had a direct negative impact on biomass consumption in Maine, as it significantly reduced the availability of wood solid waste, a primary feedstock for biomass energy generation.

Although the change in paper manufacturing markets partially explains why RPS policies did not positively impact biomass consumption for electricity, we also did not find a positive impact of RPS on other renewables in Maine. This result was surprising given specific policy targets for wind energy and large wind potential in coastal waters and offshore locations (DSIRE). After reviewing the annual reports on renewable resource portfolio requirements from 2008 -2020 (Maine Public Utilities Commission 2020), we found that most of the compliance occurred through purchasing RECs from the New England Power Pool (NEPOOL) regardless of where the facility is located at. The tradability of RECs is one possible explanation why there's no significant impact shown on other renewables including wind, solar, and thermal.

1.8.2 New Hampshire

As the second most forested state in the U.S. only after Maine, New Hampshire is also rich in forest resources, which provides a reliable supply of wood solid waste. However, in contrast to Maine, the RPS in New Hampshire has significantly increased biomass usage in dedicated biomass facilities and through co-firing in coal fired facilities.

The positive impact of RPS policies in New Hampshire can be attributed to several key policy features. Firstly, the state's RPS target places a strong emphasis on bioenergy, addressing both the extensive and intensive margins of biomass utilization. With a specific goal of achieving 8% of existing capacity from biomass by 2017, New Hampshire's

policy framework provides a clear directive and creates a favorable environment for the development and utilization of biomass.

Secondly, New Hampshire stands out as the only state that explicitly classifies the co-firing of biomass with fossil fuels as a Class I renewable energy source. This recognition and classification of co-firing as a renewable energy practice explains why New Hampshire is the sole state where a significant positive impact on co-firing has been observed. By including co-firing in its RPS policy, New Hampshire effectively incentivizes utilities to adopt this practice, driving the increased consumption of biomass in coal-fired power plants.

1.8.3 Vermont

Vermont, despite having abundant forest resources like other states in the New England area, surprisingly showed a negative impact on other renewables and a non-significant impact on biomass consumption. This can be primarily attributed to the unique energy structure of the state. First, Vermont relies heavily on electricity imports, with more than half of its electricity coming from neighboring states, primarily from hydroelectric plants located at dams in the surrounding regions. This dependence on imported electricity, which already incorporates a significant renewable energy component, diminishes the direct impact of RPS policies on increasing renewable energy usage within Vermont.

Second, in terms of in-state electricity generation, Vermont had already achieved an impressive milestone by reaching nearly 100% renewable electricity in 2020 and 2021 (EIA, 2023). This high level of renewable energy penetration surpasses the RPS targets set for the state, which aimed for 55% renewable capacity by 2017 and 75% by 2032. Consequently, the RPS policies in Vermont have less room for driving significant additional renewable energy development within the state.

Third, the RPS policy in Vermont allows for the trading of Renewable Energy Certificates

(RECs) with other New England states. This fact means that Vermont can satisfy its RPS requirements by purchasing RECs from neighboring states rather than solely relying on in-state renewable energy generation. This flexibility in REC trading further mitigates the direct impact of RPS policies on promoting renewable energy deployment within Vermont. The unique combination of these factors, including reliance on imported hydroelectricity, already high levels of in-state renewable energy generation, and the ability to fulfill RPS requirements through REC trading, has resulted in null or even negative impacts of RPS policies in Vermont.

1.8.4 Landfill Gas

Using landfill gas for electricity is beneficial in terms of being a renewable energy resource, and its use can also reduce greenhouse gas emissions and air pollution and possibly create health and safety benefits.

Landfill gas is a natural byproduct of the decomposition of organic material in landfills, which contains 50-55% methane by volume if directly released into the atmosphere, and the rest is predominantly CO₂. However, landfill gas can be captured and converted into renewable energy to be used onsite or in power plants, for industrial uses, as vehicle fuel, or as pipeline gas. From 2000 to 2020, there are more than 1,060 landfills operating across the U.S., generating approximately 2.8 billion standard cubic feet of landfill gas per day⁶ (as reported by the LMOP), which creates an enormous renewable energy potential.

Unlike other biomass feedstocks like woody materials and agricultural byproducts that highly depend on the geographic region, availability, and transportation infrastructures, landfill gas from municipal wastes has less variability and is more consistently available across the country. Further, there are existing federal and state-level incentives supporting

⁶Data from EPA- Landfill methane outreach program (LMOP) <https://www.epa.gov/lmop/landfill-gas-energy-project-data>

landfill and biogas electricity investments, including investment tax credits (ITC) and production tax credits (PTC) incentivizing the development of landfill gas to energy (LFGE) projects. Recognizing the potential advantages of utilizing landfill gas for energy production or other uses, most of the RPS policies define landfill gas as an eligible renewable source, either as part of biomass or separately in Class I renewables, which effectively incentivized landfill gas usage in the electricity sector.

1.9 Conclusion

Using the EIA form 923 data set in concert with DiD and the SCM, there are three preliminary conclusions we can generally draw about the relationship between RPS policies in the states analyzed and levels of bioelectricity production.

Our results suggest that even in states with both large forest biomass resources and an active forest products industry, the impact of RPS can be drastically different depending on the state's energy structure, the RPS policy specifics, and other external factors like market changes for other commodities. States were chosen for this analysis due to their existing energy policies and potential to support and expand bioenergy due to resource availability and current industrial transportation infrastructure to support a transition to increased biomass electricity generation. For example, Maine and Vermont have seen a significant negative effect on biomass consumption for electricity generation at dedicated biopower facilities, indicating a net reduction in biomass utilization after the RPS was enacted. Other states (including Connecticut, Massachusetts, Oregon, Washington, North Carolina, Virginia, and New York) showed no significant results in both biomass dedicated plants and coal-fired plants, although these states all have substantial forest resources. New Hampshire is an example that stands out in this analysis as its RPS, along with other policies, successfully and significantly incentivized biomass usage. With an emphasis on

biomass and explicit recognition of co-firing as an eligible source for RPS, this state has seen a positive and significant impact of RPS on bioelectricity generation on both the extensive margin and intensive margin. This finding suggests that the flexibility and adaptability of RPS policies can help states effectively target biomass usage as part of their renewable energy strategies.

Second, we find that reliance on other renewables (primarily wind and solar) is positively and significantly impacted by the RPS policies. This result suggests that RPS policies may affect alternative forms of renewable energy differently, and there are several potential reasons that could explain this. The U.S. has seen a paradigm shift over the last decade where coal-fired energy has lost a significant share of the base load market to natural gas-derived electricity, largely due to the lower prices of natural gas relative to coal. As the economics of the electricity sector have therefore shifted, investments in infrastructure that require labor-intensive procurement chains for reliable supplies of fuel inputs (e.g., coal and biomass) may be deemed less cost-effective overall (in the longer term) than capital-intensive investments (e.g., natural gas and renewables). Furthermore, while the U.S. has substantial biomass resources, meeting overseas demand for U.S.-sourced wood pellets has increased consumption of lower-cost residual biomass in the U.S. for pellet production (Baker et al. 2019) and could raise the costs of domestically sourced wood-based biomass electricity in the coming decades. Thus, wind and solar could be viewed as lower variable cost solutions to meet renewable energy requirements relative to bioenergy, which requires consistently managed supply chains to procure requisite fuel inputs. Declining costs for these energy sources (Jones-Albertus et al. 2018; White et al. 2013a) are likely also contributing to wind and solar adoption relative to biomass energy. Scientific and policy uncertainty could also be impacting demand for biomass energy. Ambiguity about the GHG benefits of using different types of biomass for energy exists due in part to different approaches for evaluating impacts associated with biomass use for energy (Khanna and

Zilberman 2017) as well as different policy objectives and designs at different levels of decision-making (ranging from international to local levels of government).

Third, our preliminary analysis of different biomass feedstock shows that among all the feedstocks, landfill gas has been positively impacted by RPSs in a majority of the studied states. Unlike other biomass sources such as wood solid waste and agricultural byproducts, landfill gas and biogas have the unique advantage that it is very flexible as they can be transported through pipelines and are easier to be used for electricity production, making them an attractive option for meeting renewable energy targets. Moreover, the combustion of landfill gas for electricity generation actively uses emissions that would have been generated anyway and thus benefits efforts to reduce overall GHG emissions as well as the economy in the long run, which could be why it has generated more policy and investment interest. These elements are likely to have contributed to landfill gas experiencing greater support and expansion through RPS policies compared to other bio-based fuels.

In summary, our analysis adds to the current literature by focusing on specific renewable energy sources and biomass feedstocks and how their use for energy responds to different states' RPS policies. Previous literature focused on assessing the effects of RPS policies in on total renewable energy without recognizing the differences in each renewable source and the underlying differences in the state's varying resource availability and policy attributes. Furthermore, we employed the synthetic control method to better quantify the responses for different states, and we evaluate both intensive and extensive margin changes in biomass consumption for electricity production.

Our analysis has important lessons and possible implications for public policy and research communities. First, policies such as renewable portfolio standards that are generally agnostic in defining which renewable energy sources should be used to fulfill portfolio requirements will result in market-oriented outcomes, meaning that energy firms may opt for potential higher fixed cost capital investments in renewable energy sources that

potentially offer lower variable costs (i.e., may choose wind or solar over biomass). Secondly, potential benefits of biomass energy expansion (Langholtz et al. 2016), including boosting rural incomes and supporting local forest product industries, are not directly captured by RPS policies. If policymakers seek to realize these benefits through renewable energy policies, then complementary incentives may be needed to ensure such benefits from bioenergy consumption in the context of the RPS.

Finally, while there is a growing literature around the potential implications of biomass energy expansion on resource utilization in the land use sectors, our results suggest that the premise of using RPS policies as a demand driver for increases in biomass consumption in sectoral analyses of bioenergy should better qualify this assumption. Further, new integrated analysis of electricity and biomass energy production systems is needed to compare the relative competitiveness of biomass with other renewables under alternative cost, policy, and socioeconomic assumptions, and such analyses can benefit from empirical investigations of technology adoption such as this study that highlights how interactions between policies may benefit certain renewable energy sources over biomass.

CHAPTER

2

DYNAMIC DECISION MAKING AND AGRIVOLTAICS IN CALIFORNIA'S CENTRAL VALLEY

2.1 Introduction

California's Central Valley (CV) is a key agricultural hub, producing approximately 8% of the United States' total agricultural output and 40% of the nation's fruits, nuts, and other table foods. Agricultural productivity in the CV is supported by extensive irrigation, with

the region containing nearly three-quarters of California's and 17% of the nation's irrigated cropland. Groundwater is the primary source of irrigation water in the CV, accounting for approximately two-thirds of the total water used. However, chronic droughts and historically intensive pumping have led to significant groundwater depletion, raising concerns about the long-term sustainability of agricultural production and water resources in the region (Liu et al. 2022).

To address groundwater overdraft, California enacted the Sustainable Groundwater Management Act (SGMA) in 2014. SGMA mandates the formation of groundwater sustainability agencies (GSAs) to develop and implement groundwater sustainability plans (GSPs) aiming at achieving sustainable groundwater conditions by the early 2040s. These GSPs have significant implications for agricultural production in the Central Valley, as they reduce water availability for irrigation, thereby impacting farmers' irrigation practices and agricultural planning (California Department of Water Resources, 2022). From earlier studies, SGMA is estimated to cause 86,000 ha to 200,000 ha of irrigated cropland to retire (Bryant et al. 2020; Hanak et al. 2019).

Simultaneously, California has demonstrated a strong commitment to clean energy production through state policies such as Renewable Portfolio Standards (RPS) and SB100, which aim to achieve 100% zero-carbon energy by 2045. These initiatives have significantly influenced land-use patterns across the state. Rich in solar resources, certain areas in California, including Central Valley, are potentially ideal for solar energy production from a physical perspective. This resource advantage, combined with increasing irrigation costs and stretched water resource supplies, has led some landowners to consider shifting from traditional farming to establishing utility-scale solar farms (Buckley Biggs et al. 2022).

While transitioning to solar farming could offer a more stable income and reduce reliance on increasingly scarce water resources, it also poses potential challenges. One of the primary concerns is the direct competition between solar energy development and food

production (Turnley et al. 2024). Given the CV's critical role in supplying a substantial portion of the US's food, reducing arable land for agriculture could have broader implications for both local and national food security (Li et al. 2023).

Additionally, many communities in the Central Valley are economically dependent on agriculture, therefore, large-scale conversion of farmland to solar farms could disrupt local economies, potentially leading to job losses in traditional farming sectors. While the solar industry provides some employment opportunities, these may not fully offset the economic impacts of reduced agricultural activity. The Central Valley also serves as a habitat for a variety of plant and animal species, and utility-scale solar farms can potentially disrupt existing wildlife habitats (Hays and Baker 2023). Therefore, planning for solar infrastructure must integrate detailed spatial analysis to minimize ecological and social impacts (Wu et al. 2023, 2019).

Given the increasing water stress and the potential impact of large-scale land conversion to solar in the Central Valley, innovative solutions are needed to balance renewable energy development with agricultural and water sustainability. One emerging technological intervention that could help minimize tradeoffs between solar development and food production on agricultural lands is agrivoltaics (Ag-PV, also referred as agrisolar, or agriphotovoltaics, APV) ¹

Agrivoltaics has been identified as a potential method to increase land-use efficiency and, in many cases, improve water-use efficiency (WUE) of agricultural production systems. Water savings from agrivoltaics production is enabled due to partial shading of crops in areas with high solar radiation and evaporative water losses. Increased WUE can save farm production costs and complement water conservation efforts. In addition to its water

¹There are four types of agrivoltaics applications, 1) crop and food production, 2) livestock grazing, 3) ecosystem services, and 4) solar greenhouses. In this manuscript, we consider agrivoltaics systems as partial solar generation combined with crop production, a joint land-use that integrates agricultural activities and solar energy generation on the same unit of land.

savings potential, agrivoltaics can offer diversified income streams to farmers through joint production. Its implementation in the Central Valley has gained significant interest due to these benefits. However, the high installation cost, technical complexity in optimizing energy and crop yields simultaneously, and uncertainty regarding long-term economic and ecological impacts remain considerations in its broader adoption.

This study aims to identify the conditions under which the adoption of intensive solar and/or crop production would be strictly preferred to agrivoltaics. By doing so, we assess the feasibility and implications of agrivoltaic adoption in California's Central Valley, addressing the dual challenges of water scarcity and the increasing demand for renewable energy. Using a regime-switching stochastic dynamic programming model, we analyze optimal land-use decisions between traditional agriculture, solar farming, and agrivoltaics under uncertainty. Our primary objective is to evaluate how factors such as crop type, irrigation costs, solar lease rates, and environmental volatility influence land-use decisions and to determine the economic and environmental conditions under which agrivoltaics becomes a viable option.

Our findings suggest that agrivoltaics is particularly beneficial for high-value crops with high water demand, as the water-saving benefits and diversified income streams can offset the costs of installation and potential yield reductions. However, traditional crop production remains preferable under lower irrigation costs and solar lease rates. Additionally, we find that increased market and weather volatility can delay transitions to agrivoltaics, as landowners may prefer to wait for more favorable conditions before committing to irreversible investments. These insights provide valuable guidance for policymakers and stakeholders seeking to balance agricultural productivity with renewable energy generation in the Central Valley.

In the next section, we will provide a more detailed overview of agrivoltaics, including the types of configurations, potential benefits, associated costs, and its relevance to the

Central Valley.

2.2 Background and Literature Review

The concept of agrivoltaics combined with crop production involves the strategic installation of solar panels above farmlands. There are broadly two types of configurations: elevated systems and inter-row systems. These configurations are tailored to accommodate various agricultural practices, soil types, and crop requirements while maximizing the productivity of land (Macknick et al. 2022).

For elevated systems, solar panels can be elevated to 6 to 8 feet above the ground to allow for routine farmwork underneath (including animal grazing in some cases). The configuration of panels must be designed to ensure that crops receive sufficient sunlight while benefiting from the partial shading provided by the panels. Panel configuration can also offer protection from inclement weather and heat stress (while reducing water demands), making this configuration particularly suitable for high-value crops such as berries, vineyards, and delicate vegetables. However, the shading from the panels may reduce sunlight exposure, potentially leading to lower yields for certain crops that are shade intolerant.

In contrast, inter-row systems space traditional ground-mounted PV arrays more widely apart to accommodate large farm machinery. While these systems provide less shade and less protection, they allow for more sunlight to reach the crops, which may be advantageous for vegetation requiring more direct sunlight. In addition, water collected from precipitation runoff or solar panel cleaning can still be utilized to supplement irrigation needs. Such inter-row systems are often employed for lower-value crops such as alfalfa and grains, where de-intensification of crop production does not carry a steep revenue penalty.

These designs have been tested in various settings to assess their impact on agricultural

productivity and water usage. Field experiments conducted in Montpellier, France were among the first to explore the feasibility of agrivoltaics. Studies by Dupraz et al. (2011) and Dinesh and Pearce (2016) have studied the effects of solar panel shading on crops' yield. Elamri et al. (2018) and Marrou et al. (2013) have investigated the microclimate change under the panels, finding that the shading from solar panels can lead to significant reductions in water usage. Notably, Elamri et al. (2018) implemented simulation methods to show that agrivoltaics can reduce irrigation needs by up to 20% while tolerating a 10% reduction in crop yield, highlighting the potential of agrivoltaics to address both agricultural and environmental challenges.

There have also been field experiments conducted in Germany (Trommsdorff et al. 2021), Asia (Ali Abaker Omer et al. 2022; Irie et al. 2019), and the U.S. exploring various configurations for the agrivoltaics systems. In the United States, the InSPIRE (Innovative Solar Practices Integrated with Rural Economies and Ecosystems) project has collaborated with universities, local governments and industry partners to develop strategies for low-impact solar development. For agrivoltaics systems combined with crop production, InSPIRE is leading field experiments on vegetables in Ohio (Quarshie 2023), tomatoes in Oregon (Al-Agele et al. 2021; Tahir and Butt 2022), and berries in Massachusetts (Mupambi et al. 2021). Macknick et al. (2022) summarizes lessons learned from research across various field experiments and supporting evidence on how agrivoltaic systems can reduce environmental impacts relative to traditional production systems while maximizing agricultural and energy production efficiency.

From an investment perspective, the conversion to agrivoltaic systems often presents an irreversible commitment for 20-30 years, which also limits operational flexibility for landowners. The irreversible nature of adopting agrivoltaic systems also raises concerns among landowners regarding future uncertainties, including farming income, the impact of climate change, and changes in agricultural and renewable energy policies. For a risk-averse

landowner, this uncertainty could work in multiple directions – first, uncertainty regarding future returns or water availability could hasten the decision to adopt an income-diversifying practice, while uncertainty in future energy prices or rents paid by solar companies could delay adoption until more evidence is available (Macknick et al. 2022).

There is a growing literature focused on the potential design of agrivoltaic systems and the benefits and costs of these systems within the coupled food-energy-water nexus (Barron-Gafford et al. 2019; Mamun et al. 2022). There are also qualitative studies about land-owner decisions on solar adoption. For example, Buckley Biggs et al. (2022) conducted interviews with farmers, ranchers, solar developers, and government organizations in California and identified the key factors affecting landowner decisions, including profit maximization, water availability, visual and ecological landscape values, and agricultural land preservation ethics. Besides, Ketzer et al. (2020) uses Causal Loop Diagrams (CLDs) to analyze the driving and restraining forces for the adoption of agrivoltaics based on data from citizen workshops, literature reviews, and expert discussions.

More recent research has used quantitative modeling to explore optimal agrivoltaic system design and harvesting cycles. Sarr et al. (2024) develops a model that determines the configuration of agrivoltaic systems that optimizes energy production efficiency and crop yield. Yajima et al. (2023) establishes a model incorporating the amount of electricity generated by solar irradiation to estimate the correct start date to remediate the potential loss of late harvest due to shading.

While qualitative analyses provide insights into the social and economic factors influencing landowner decisions and recent quantitative models address specific design and operational efficiencies, there remains a significant gap in comprehensive dynamic modeling that accounts for the uncertainties inherent in long-term land use decisions at the intensive and extensive production margins. This gap is particularly critical in light of the complex interdependencies within the Food-Energy-Water nexus and the unpredictable

nature of climate conditions, markets, and policy developments.

To address these key knowledge gaps, we adopt a real options framework, building on Insley (2002); Dixit and Pindyck (1994) as well as more recent applications in agricultural economics such as Bangjun et al. (2022). Our contribution extends this literature by focusing on both intensive land management and extensive land management options. We develop a regime-switching model to assess the land use decisions among purely crop production, solar production, and agrivoltaics under uncertainty. We also develop scenarios that account for potential external conditions that affect the uncertainty of long-term economic returns to different land management options, including market volatility, climatic changes, and policy shifts, to identify the conditions under which the adoption of intensive solar and/or production would be strictly preferred to agrivoltaics.

2.3 Theoretical Framework

The decision to adopt traditional agriculture, solar-only systems, or agrivoltaics presents significant trade-offs for landowners in California's Central Valley, but the value of these tradeoffs is uncertain, varying by crop type and spatially heterogeneous physical and economic characteristics. Production systems focused on solar, crop production, or a combination of the two will offer distinct benefits and costs that are subject to a variety sources of uncertainties, including market conditions, weather variability, water availability, and potential policy constraints. Traditional agriculture is particularly sensitive to market fluctuations and climate risks, including rising irrigation costs and changes in yield due to severe weather events. Solar-only systems offer a stable income through power purchase agreements (PPAs) or land leases with solar developers over longer contract terms (sometimes decades). If landowners sell power, however, this requires significant upfront investments and displaces agricultural production activities entirely. Agrivoltaics creates a diversified

income stream for landowners but also incurs higher establishment costs. Besides, while agrivoltaics can reduce water use and protect crops from heat stress, it may negatively affect yields for certain crops due to shading or altered growing conditions.

The potential water savings of agrivoltaics is what makes it particularly appealing to CV landowners facing increasing water scarcity and policy restrictions under SGMA. However, the extent to which these savings offset the higher costs remains highly site- and crop-specific, adding another layer of complexity to land-use decisions. Additionally, land-use decisions are influenced by external factors such as renewable energy incentives, water management policies, and the evolving profitability of crops. Together, these layers of complexity create uncertainty and highlight the need for a structured, data-driven approach to evaluate land-use decisions.

To address these challenges, we develop a stochastic dynamic programming (SDP) framework that incorporates a real-options approach. This model captures uncertainties in economic, environmental, and exogenous policy factors while accounting for the irreversibility of land-use transitions, such as installing solar panels. By simulating outcomes over time, this framework evaluates the trade-offs and identifies optimal land-use strategies under uncertainty. Through this approach, we aim to provide insights into the economic and environmental conditions under which landowners might adopt different land-use regimes, as well as the role of policy in influencing these decisions.

2.3.1 Regime Switching Framework

For this analysis, we consider three alternative land management regimes: purely agricultural production (AO), purely solar production (SO), and agrivoltaic production (AV). Each regime represents a different land-use strategy with a different future income stream. In the first regime AO, the land is used exclusively for agricultural production, which is

the current state and the initial state in the model. Under this regime, the land manager maximizes returns to agricultural production and is typically preferred when farming yields high economic returns relative to solar or agrivoltaics or in cases where solar installation is not viable due to various constraints such as grid infrastructure, high site preparation cost, policy constraints, or community preferences.

The SO regime focuses exclusively on generating income from solar energy production. For this analysis, we assume that landowners lease their land for solar installations, prioritizing energy revenue over agricultural output. This regime is most beneficial in areas with higher solar compatibility and may be preferred due to low agricultural profitability, high irrigation cost, or high solar incentives.

Finally, the AV regime integrates solar with crop production on the same land, which means that solar and agricultural activities will affect management options and cost structures for each system. For instance, the shade from solar panels helps reduce irrigation usage, and protects the crop from heat stress, but depending on the crop, the shading may decrease crop yield. The crop underneath solar panels helps lower the temperature, which benefits solar productivity, while routine farmwork may cause dust accumulation on the solar panels, which can affect the performance of solar panels.

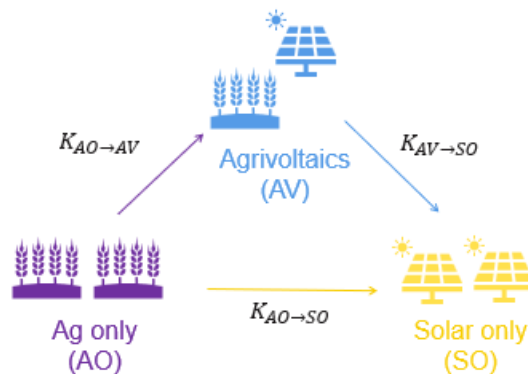


Figure 2.1: Illustration of the Regime Switching Model

Due to the irreversibility of solar installations, which remain in place typically for decades, we only allow land use conversion into SO or AV in one direction, consistent with Figure 2.1. The starting regime is always AO, a representative agricultural landowner that can choose to remain in agricultural production or switch either to AV or SO. Starting from AV, the landowner may choose to give up agriculture production and switch to SO, or stay in AV, but they do not have the option to remove solar panels and switch back to AO. Finally, the SO regime is the absorbing regime, and once achieved, the land will be committed to solar production for the remainder of the simulation horizon.

Our approach adopts a stochastic dynamic programming framework that is well-suited for problems where decisions must be made sequentially and where outcomes are uncertain. In a deterministic framework, switching from regime X to Y would occur when the net present value (NPV) is higher than the NPV of regime X plus the switching cost $K^{X \rightarrow Y}$. By introducing uncertainty, the framework accounts for the value of waiting or deferring the switch until conditions become more favorable. Additionally, since the transitions are irreversible, the adoption decisions must account for the uncertainty of future states, ensuring that landowners can dynamically adjust their strategies in response to fluctuations in market conditions and other stochastic factors.

We employ a discrete-time setup that is aligned with annual agricultural production cycles. To minimize crop disruption, and to allow for specific site preparation adjustments, the installations of solar panels are usually scheduled during the off-season, which depends on the crop. In California, the standard off-season is considered winter (Dec to Feb), so we assume the adoption decision will be made annually. Furthermore, while the finite lifespan of solar panels (typically 30 years) might suggest a finite-horizon model, we adopt an infinite-horizon framework for several reasons. First, a finite horizon model requires specifying a terminal condition, which introduces artificial constraints that may not reflect realistic long-term decision-making. Second, from a theoretical perspective, the infinite

horizon ensures that the solution converges to a stationary policy function, where optimal decisions depend on the current state and expected future values. This convergence is supported by the inclusion of a discount factor (β), which reflects the landowner's time preference and ensures that future rewards are appropriately discounted. With $\beta < 1$, the model avoids the problem of infinite accumulation of rewards, so that the policy function remains stable over time. By adopting this approach, the model captures the dynamic and recursive nature of land-use decisions under uncertainty. In the next section, we will define the reward functions in each regime, which is key to understanding the trade-offs and opportunity costs associated with land-use transitions.

2.3.2 Reward Functions

The reward functions represent the landowner's income streams under each regime and serve as the foundation for evaluating the comparative benefits of different land-use strategies. These functions allow the model to quantify the trade-offs and opportunity costs associated with switching between regimes.

In the SO regime, the landowner's net income can take two forms depending on the ownership of the solar panels. If the landowner installs the solar panels on their own, the net benefit of solar at each period can be written as $p_t^e E_t - m_t$, where p_t^e represents the price of solar power purchase agreements (PPAs) at year t , and E_t is the electricity generated, m_t is the annual operation and maintenance cost for solar. Alternatively, under third-party ownership, the solar panels are owned, installed, and maintained by a solar developer, who leases the land from the landowner. In this case, the landowner receives a fixed annual rent for leasing their land. For simplicity, we assume a static solar rent in this analysis, reflecting 2019 USD values. The net income for the landowner under third-party ownership can therefore be written as:

$$\Pi_t^{SO} = R_t^{\text{solar}} \quad (2.1)$$

The assumption of third-party ownership is a reasonable representation of a common and plausible approach in the CV. As noted in the interviews conducted by Buckley Biggs et al. (2022), third-party ownership models are attractive to agricultural landowners in California due to their simplicity and the guaranteed income stream they will provide over the contract period.

In the AO regime, the representative landowner's net income is their crop revenue R_t^{ag} subtracted by costs, which includes irrigation cost C_t^{irr} and other expenses C^{oth} like labor, machinery, fertilizers, pesticides, etc, which varies across crops. We write the reward from the AO regime as:

$$\Pi_t^{AO}(\mathbf{S}_t) = R_t^{\text{ag}} - C_t^{\text{irr}} - C^{\text{oth}} \quad (2.2)$$

The main uncertainties we consider in this model come from the crop income and weather, which affects water requirements for irrigation. Thus we define the state space $\mathbf{S}_t \equiv (\log R_t^{\text{ag}}, \log C_t^{\text{irr}})$. This approach allows us to model the temporal dependencies and fluctuations in agricultural income and irrigation costs, providing a realistic simulation of how these variables might evolve over time under different scenarios.

Finally, in the AV regime, solar and crops are jointly produced and have impacts on each other. The agricultural revenue in this regime is reduced by a factor α due to partial shading by the solar panels or due to larger spacing for solar arrays, while irrigation cost is reduced by a factor ρ due to decreased evapotranspiration. These factors vary across crops due to different crop shade-tolerance and compatibility for different agrivoltaic designs. In this regime, the landowner also gains additional income from solar leasing, whereas the lease rate is usually lower than a traditional solar farm rent due to lower power density. The

reward function in the AV regime is written as:

$$\Pi_t^{AV}(\mathbf{S}_t) = (1 - \alpha)R_t^{\text{ag}} - (1 - \rho)C_t^{\text{irr}} - C^{\text{oth}} + \gamma R_t^{\text{solar}} \quad (2.3)$$

The model accounts for stochastic transitions in the state variables \mathbf{S}_t , driven by the VAR(1) process described above. These transitions influence the expected future rewards in the Bellman equations, as the landowner bases their decisions on the probabilistic evolution of crop revenues and irrigation costs.

2.3.3 Bellman Equations

To solve for the optimal switching decision recursively, we utilize Bellman Equations. For the SO regime, if we consider the stochasticity in solar income, the value functions expressed as: $V^{SO}(R_t^{\text{solar}}) = \Pi_t^{SO} + \beta \mathbb{E}[V^{SO}(R_{t+1}^{\text{solar}}) | R_t^{\text{solar}}]$, where β is the discount factor. As the stochasticity in solar rents are not considered in this analysis, it is simply the NPV of the solar rent in 30 years, $V^{SO} = R^{SO}/(1 - \beta)$. Based on the reward functions of agrivoltaics, the value function for the AV regime is expressed as:

$$V^{AV}(\mathbf{S}_t) = \max \left\{ \underbrace{\Pi_t^{AV}(\mathbf{S}_t) + \beta \mathbb{E}[V^{AV}(\mathbf{S}_{t+1}) | \mathbf{S}_t]}_{\text{stay in AV}}, \underbrace{V^{SO} - K_{AV \rightarrow SO}}_{\text{switch to SO}} \right\} \quad (2.4)$$

This function captures the decision to either stay in the AV regime, earning the immediate reward from AV and the discounted expected net present value (ENPV) of staying in the AV regime in the next period conditional on the current state \mathbf{S}_t ; or to switch to the SO regime, which the value equals to the value of SO regime subtracted by the switching cost $K_{AV \rightarrow SO}$.

Switching costs, $K_{X \rightarrow Y}$, represent the economic costs associated with transitioning between land-use regimes. These costs capture the physical and financial investments

required for infrastructure adjustments, as well as potential foregone income during the transition period. Including these costs ensures that the model accurately reflects the economic barriers to land-use changes.

Finally, in the AO regime, the landowner faces three options: the option to continue with purely agricultural operations, switch to solar production, or to joint agrivoltaic production. The value function is given by:

$$V^{AO}(\mathbf{s}_t) = \max \left\{ \underbrace{\Pi_t^{AO}(\mathbf{s}_t) + \beta \mathbb{E}[V^{AO}(\mathbf{s}_{t+1}) | \mathbf{s}_t]}_{\text{stay in AO}}, \underbrace{V^{SO} - K_{AO \rightarrow SO}}_{\text{switch to SO}}, \underbrace{V^{AV}(\mathbf{s}_t) - K_{AO \rightarrow AV}}_{\text{switch to AV}} \right\} \quad (2.5)$$

In each period, the landowner evaluates the value of the three options, and if the immediate reward from AO plus the ENPV of AO is the highest, then it is optimal to stay in AO. If the value of SO subtracted by the switching cost $K_{AO \rightarrow SO}$ is the highest, then the landowner's optimal decision is to sink the cost and switch to SO. If it is optimal to switch to AV, the value function is determined by the value function from equation (2.4).

The recursive structure of the Bellman equations ensures that decisions at each period account for both immediate reward and the expected future value. The structure also ensures the irreversibility constraints: once the landowner commits to the solar-only regime, no further decisions can be made. In section 2.4, we describe in detail the computational methods used to solve the Bellman equations.

2.4 Computational Method

The theoretical framework outlined above provides the mathematical foundation for modeling the landowner's decision-making under uncertainty. Solving the Bellman equations in this context involves numerical methods due to the stochastic nature of the problem and the continuous state space. This section describes the computational techniques used to

discretize the state space, integrate stochastic shocks, and solve the dynamic programming model efficiently.

State Space Discretization To approximate the continuous state space of agricultural revenue and irrigation costs, the model employs a grid-based discretization technique using linear basis functions. Since agricultural revenue and irrigation costs exhibit significant variation over time, the model operates in the logarithmic space of these variables, denoted as $\mathbf{S}_t = (\log R_t^{\text{ag}}, \log C_t^{\text{irr}})'$. The state space is defined over a range determined by the steady-state values of the stochastic variables:

$$\mathbf{S}^* = (\mathbf{I} - \Phi)^{-1} \boldsymbol{\mu} \quad (2.6)$$

where $\boldsymbol{\mu}$ is the mean vector, and Φ is the matrix governing the autoregressive process. The range of the state space is expanded to include potential deviations caused by the stochastic shocks. The grid points or nodes are evenly distributed to ensure sufficient coverage of the relevant decision space. To maintain computational traceability while capturing the thresholds for regime-switching, the grid solution (N) is chosen to balance precision and efficiency.

Numerical Integration Uncertainty in agricultural revenue ($\log R_t^{\text{ag}}$) and irrigation costs ($\log C_t^{\text{irr}}$) is modeled using a first-order vector autoregressive process:

$$\mathbf{S}_t = \boldsymbol{\mu} + \Phi \mathbf{S}_{t-1} + \boldsymbol{\varepsilon}_t, \quad \boldsymbol{\varepsilon}_t \sim N(0, \Sigma), \quad (2.7)$$

where \mathbf{S}_t is the vector of state variables, $\boldsymbol{\varepsilon}_t$ is a multivariate normal shock, and Σ is the covariance matrix. The expected future values (ENPVs) under this stochastic process are computed using Gaussian quadrature. A total of M^2 quadrature points are used to approxi-

mate the integrals, ensuring numerical accuracy. This method approximates integrals using weighted sums of function values at predetermined quadrature points:

$$\mathbb{E}[V_{t+1}(\mathbf{S}_{t+1})] \sim \sum_{i=1}^{M^2} w_i V_{t+1}(\mathbf{S}_{t+1}^i) \quad (2.8)$$

where w_i are quadrature weights, and \mathbf{S}_{t+1}^i are the future states associated with each quadrature point. To enhance computation efficiency, the future states for all quadrature points are precomputed for each grid node.

Value Iteration The Bellman equations for the three regimes (AO, AV, and SO) are solved iteratively using value iteration. The value functions are updated until convergence, producing a stationary policy function that remains constant across time periods. The process starts with an initial guess for the value functions based on each regime's immediate rewards and expected values under the assumption of infinite horizon. For the SO regime, the value function is initialized as the discounted sum of solar rents (V^{SO}) over a 30-year lease, reflecting the static income generated in this regime. For the AV and AO regimes, the initial value functions incorporate the maximum of the immediate rewards and the discounted expected future value of switching to another regime, accounting for the relevant switching costs.

The iterative process involves recursively solving the Bellman equations (Equations 2.4 and 2.5) at each grid point in the discretized state space. At each step, the expected future values of the state variables, $\mathbb{E}[V_{t+1}(\mathbf{S}_{t+1})]$, are computed using Gaussian quadrature to approximate the stochastic shocks affecting agricultural revenue and irrigation costs. This integration is essential for capturing the effects of uncertainty in the decision-making process. Convergence is determined by monitoring the maximum absolute difference between the value function estimates from consecutive iterations across all grid points.

The iteration process continues until this difference falls below a threshold ($\epsilon = 10^{-3}$). Once the value function converges, the stationary policy functions can be derived.

Policy Function At each grid point, the optimal decision is determined by comparing the value of continuing in the current regime with the value of switching to other regimes subtracted by the switching costs. For the AO regime, the optimal decision is determined by evaluating whether staying in AO, transitioning to AV, or transitioning to SO yields the highest value:

$$X^{AO}(\mathbf{S}_t) = \arg \max_{\mathbf{X}^{AO}} \{V_t^{AO}, V_t^{AV} - K_{AO \rightarrow AV}, V_t^{SO} - K_{AO \rightarrow SO}\}. \quad (2.9)$$

Similarly, the policy function for the AV regime is determined by comparing the value of staying in AV to the value of switching to SO:

$$X^{AV}(\mathbf{S}_t) = \arg \max_{\mathbf{X}^{AV}} \{V_t^{AV}, V_t^{SO} - K_{AV \rightarrow SO}\}. \quad (2.10)$$

The policy values $\mathbf{X}^{AO} = \{0, 1, 2\}$, where 0 represents staying in AO, 1 represents switching to AV, and 2 represents switching to SO. And for $\mathbf{X}^{AV} = \{0, 1\}$, where 0 represents staying in AV, and 1 represents switching to SO. These policy functions are stored at each grid point in the state space, enabling the simulation of optimal decision paths. There is no policy function for the SO regime because once the SO regime is achieved, no further decisions can be made.

2.5 Data and Empirical Analysis

This section describes the data and parameterization framework used to apply the regime-switching model to the agricultural context of the Central Valley. To capture the diversity of

crops and land-use scenarios, we parameterize the model using data on major crops grown in the Central Valley and develop representative scenarios to capture variability in crop revenues and irrigation costs, and then we test the model sensitivity to other parameters like transition costs, shade tolerance, solar intensities, etc. Additionally, we incorporate policy and market scenarios to test the model’s sensitivity to future uncertainties that could shift the revenue potential for the different land use regimes. The following section details the data sources, parameter values, and policy scenarios considered in the analysis.

2.5.1 Data

For the key stochastic variables, agricultural revenue, and irrigation cost, our data relies on multiple sources: Agricultural data, including crop yields and prices for California, are collected from the USDA National Agricultural Statistics Service (NASS) annual survey data. State averages are used to represent Central Valley conditions, as these crops are predominantly grown in this region. Crop revenue is calculated as the product of yield and price, providing a measure of economic output for each crop. This revenue variable captures the economic risk associated with market volatility and yield fluctuations.

To calculate irrigation costs, weather-related data is obtained from the Central Valley Hydrologic Model (CVHM; Faunt 2009), which provides monthly observations of precipitation and reference evapotranspiration (ET_o) for the CV region. Effective rainfall is calculated following FAO guidelines (Allen 2000), which account for the fraction of rainfall usable for crops. Crop coefficients (K_c) from FAO are applied to ET_o values to determine crop water requirements. The net irrigation need is computed as the difference between crop water requirements and effective rainfall. After calculating monthly irrigation needs, they are aggregated into annual values². These annual irrigation needs are then multiplied by

²Irrigation need_t^c = $\sum_m \text{ETo}_{m,y} \cdot \text{Kc}_m - \sum_m \text{effective rainfall}_{m,y} \cdot I(\text{Kc}_m > 0)$

irrigation water costs per unit, derived from UC Davis Cost and Return Studies, to provide crop-specific annual irrigation costs for use in the model. This variable captures the influence of weather and climate variability on both yields and irrigation demands/costs, introducing additional uncertainty and risk into land-use decisions.

The variability in agricultural revenue and irrigation costs is modeled using a first-order autoregressive process, capturing the dynamic relationships between the logarithms of revenue and irrigation costs. The estimated VAR(1) parameters (in Table A.2, A.3) are used to simulate the future evolution of revenue and irrigation costs under uncertainty. Figure 2.3 presents the simulated values for each crop.

Secondly, the agrivoltaics parameters used in the model, including shading effects (α), water savings (β), and solar intensities (γ), are derived from various field studies of agrivoltaic designs. The values and sources are summarized in Table A.2, A.3. These parameters reflect the income stream for the integrated land-use type and capture the interaction of agricultural and solar production. As shown in table A.2, A.3, we assume that crops with higher shade tolerance such as grapes are minimally affected by agrivoltaics practice; and that for field crops that need large farm machinery, and require large space between solar arrays, the solar capacity is lower than those crops that can be grown underneath the solar panels with normal inter-row spacing. For perennial tree crops such as almonds and oranges, agrivoltaics is particularly challenging due to the structural and operational constraints associated with integrating solar panels with tree canopies. While there are field studies conducted for tree crops (Fernández-Solas et al. 2023; Magarelli et al. 2024), they show much higher installation costs and yield losses. As a result, we assume that agrivoltaics adoption for these crops results in the complete loss of agricultural revenue, as the existing orchard setup would need to be fully converted to accommodate the solar infrastructure. This assumption reflects the practical and economic barriers to integrating agrivoltaics with tree-based crops.

Parameter values from these studies may vary depending on site-specific conditions, including crop types, solar configurations, soil properties, and local climate. It is worth emphasizing that the focus of this study is not to identify the optimal agrivoltaic configuration. Instead, we assume that configurations are optimized for each site to ensure realistic parameterization within the modeling framework.

Transition costs between land use regimes represent both direct and indirect costs of the transitioning, including direct investments in capital and inputs to facilitate the transition and opportunity (or "sunk") costs of machinery or natural assets that are no longer usable. These costs vary depending on the infrastructure required and the adjustments made to the existing operations on the land. Since our model assumes third-party solar ownership for both agrivoltaics and solar-only regimes, the direct transition costs do not include the module costs and installation labor. However, they account for land preparation costs and other adjustments. Based on the Horowitz et al. (2020) capital cost estimates, the per-acre cost for dual-use agrivoltaics (crop + PV) is approximately \$16,990. This estimate includes specialized site investigation, soil preparation, column foundation, and other modifications required for dual land use. For purely solar systems, the preparation cost is lower as it does not involve accommodating agricultural activities, but this transition does need to account for the sunk cost of farm machinery and other displaced agricultural infrastructures.

Using these benchmarks, we assume transition costs of \$35,000 per acre for switching from AO to AV, \$30,000 for AO to SO, and \$10,000 for AV to SO. The higher cost of AO to AV reflects the complexity and additional investments required to integrate solar infrastructure with agricultural operations. The AO to SO cost is lower due to the simpler requirements for establishing a solar-only system, while the AV to SO transition cost is much lower, as we assume that the existing solar infrastructure only requires adjustments to cease crop production, plus the sunk cost of the displaced agricultural machinery. In later sections 2.6.4, we test the sensitivity of these assumed transition costs to assess their impact on

land-use decisions and the adoption of agrivoltaics and solar-only systems.

2.5.2 Parameterization

To evaluate the economic and environmental trade-offs in land-use decisions, we categorize crops into four groups based on their revenue and irrigation cost characteristics: Low Revenue-Low Irrigation Cost, Low Revenue-High Irrigation Cost, High Revenue-Low Irrigation Cost, and High Revenue-High Irrigation Cost. For simplicity, these groups are represented by Corn, Alfalfa, Tomatoes, and Grapes, respectively, to represent general conditions, though similar proxy crop categories could be developed using multiple crops with similar revenue and cost structures. The VAR(1) parameters estimated from historical data, as described in the previous section, are used to capture the stochastic nature of agricultural revenue and irrigation costs for these crops. Other agrivoltaics-associated parameters, including shading effects (α), water savings (β), and solar intensity (γ), are set to reflect moderate impacts of agrivoltaics on crop and solar productivity, as summarized in Table A.1.

To control for other factors, we first assume a uniform profit margin for purely crop production for each crop group. This assumption aligns with the average agricultural land rent in California according to USDA NASS data. Operational cost data are derived from sample cost and return studies conducted by the University of California Agriculture and Natural Resources Cooperative Extension. The non-irrigation expenses are assumed to be constant and calibrated to align with this profit margin under steady-state conditions. This parameterization approach provides a flexible framework that can be adapted for other crops or extended to analyze additional site-specific conditions as more data becomes available.

2.5.3 Scenario Analysis

To explore how land-use decisions respond to varying economic, environmental, and policy conditions, we develop a set of scenarios that test changes in key parameters in this model. These scenarios are designed to simulate different policy and environmental conditions, allowing us to assess how exogenous factors influence the optimal timing and decision of transitions between AO, AV, and SO regimes. Each policy scenario is evaluated and compared to baseline model outcomes with no additional policy or market considerations, i.e., where land use decisions are driven purely by expectations of stochastic future inputs.

First, as SGMA in California proceeds to the next stage, accomplishing the Groundwater Sustainable Plans (GSPs), it is likely that the irrigation costs for CV farmers will increase due to restrictions on groundwater extraction or enforcement mechanisms that raise the costs of groundwater extraction. To test the impact of different stringency levels of SGMA, we include scenarios where irrigation costs rise relative to the current baseline by 20%, 50%, and 100%.

Second, we investigate how changes in the volatility of economic and environmental conditions affect land-use decisions. Scenarios with higher economic volatility increase the variability of agricultural revenue, reflecting higher market uncertainty due to fluctuating crop prices or demand. Scenarios with higher weather volatility increase the variability of irrigation costs, stimulating the effects of irregular rainfall and evapotranspiration due to climate change. Additionally, a combined volatility scenario increases both economic and weather volatility simultaneously. These scenarios test how the timing of landowner decisions may change under less predictable market and environmental conditions.

Finally, we test solar rent scenarios to examine the impact of policy and market conditions on the profitability of solar systems. In scenarios with increased solar rent, higher lease payments from solar developers reflect conditions where solar becomes more profitable

either due to lower cost or favorable solar policy incentives. Conversely, scenarios with decreased solar rent simulate reduced incentives or adverse market conditions, potentially making traditional AO uses more competitive. Specifically, we simulate annual solar rents of \$500, \$1000, \$1500, and \$2000 per acre, which are realistic solar rents based on landowner surveys in the Central Valley (Buckley Biggs et al. 2022).

2.6 Results

2.6.1 Representative Crops

This section presents the results of the regime-switching model for the four representative crops: Low Revenue-Low Irrigation Cost, Low Revenue-High Irrigation Cost (LH), High Revenue-Low Irrigation Cost (HL), and High Revenue-High Irrigation Cost (HH). The parameters used for each representative crop are detailed in Table A.1. For each crop, we analyze the functions derived from the model, illustrating the optimal land-use decisions over the state space of agricultural revenue and irrigation costs.

The policy functions for each representative crop are plotted in Figure 2.5. In each subplot, the x-axis represents the log of agricultural revenue ($\log R_t^{\text{ag}}$), and the y-axis represents the log of irrigation costs ($\log C_t^{\text{irr}}$). This defines the state space within which land-use decisions are made. Each row (subplot) consists of two panels: the left panel shows the policy function for the AO regime, and each color represents the optimal regime at the state. The agricultural landowners can choose from staying AO, switching to AV, or switching to SO directly. The right panel shows the policy function for the AV regime, had the landowner already transitioned to AV from AO. The conversion surface in each plot defines the economic conditions in which the switching between regimes is optimal.

For low-revenue crops (LL and LH), the policy functions indicate that it is optimal to

remain in AO under the state space. This is consistent with the intuition, as low revenues do not justify the high upfront costs associated with transitioning to AV or SO. If a transition to AV does occur, the policy function suggests that it is optimal to remain in AV, reflecting the stability and reduced irrigation costs associated with the dual-use system. The combination of low agricultural profitability and moderate water savings from AV makes staying in AV economically viable but limits incentives for further transition.

For high-revenue crops (HL and HH), the policy functions show that agricultural revenue is the primary driver of land-use decisions. Under high agricultural revenue, it is optimal to stay in AO, as the profitability of farming outweighs the benefits of transitioning to AV or SO. However, for high irrigation need crops (HH), the AV regime becomes more favorable in the majority of state space, reflecting the incentives provided by the water-saving benefit of AV, as well as the income-diversification benefits of AV systems in the presence of high water demands and supply volatility.

To further explore the sensitivity of land-use decisions to crop-specific characteristics, we tested all four representative crops under the assumption of low shade tolerance. In this case, the shading effects of agrivoltaics significantly reduce agricultural revenue, with the parameter α set to 0.6. This implies a 60% reduction in crop revenue due to shading or changes in planting density required for agrivoltaic systems, which makes agrivoltaic systems less attractive.

Under this assumption, for low-value crops and High Revenue-Low Irrigation Cost crops, it is consistently optimal for landowners to remain in the AO regime across the entire state space. Even for HL crops, which typically present higher profitability and might be incentivized to adopt AV systems under baseline conditions, the reduction in revenue eliminates the viability of switching to AV, meaning that the water-saving benefit does not offset the revenue loss and thus does not justify the transition.

However, for High Revenue-High Irrigation Cost crops, the results differ. As shown in

Figure 2.6, there remains a conversion surface where switching from AO to AV remains optimal. In the left panel, this occurs in regions of the state space with low agricultural revenue and high irrigation cost levels. The combined benefit of solar rent and reduced water costs under AV can still outweigh the diminished agricultural returns caused by shading. However, as revenue increases or irrigation costs decrease, the optimal decision shifts back to remaining in AO.

The right panels of Figure 2.6 illustrate the decisions starting from the AV regime. Under most conditions, it remains optimal to stay in AV once the transition is made. Nevertheless, in cases of extremely low agricultural revenue and very high irrigation costs, the model projects a transition to SO. This reflects a scenario in which AV no longer provides sufficient economic benefits to justify continuing dual land use, and landowners may prefer fully dedicating their land to solar production and certain income streams.

2.6.2 Scenario Analysis

Scenario analysis allows us to explore how land-use decisions respond to exogenous factors like policy, market, and environmental conditions. In this section, we focus on the High Revenue-Low Irrigation Cost (HL) category, as it represents the most dynamic and illustrative case for understanding land-use decision-making under uncertainty. Unlike other categories, where a single regime dominates under the majority of the state space, the HL category reveals nuanced trade-offs between AO, AV, and SO regimes. This category, represented by tomatoes, also holds significant economic relevance in the Central Valley. To evaluate the impact of SGMA, we simulate state variable paths over 30 years for 1000 times, analyzing how irrigation cost increases influence land-use transitions. These scenarios include the baseline and three SGMA-induced cost increases by: 20%, 50%, and 100% (labeled SGMA-20, SGMA-50, and SGMA-100). Figure 2.7 presents the optimal regime

percentages over time for each scenario.

Under baseline conditions (status quo), more than 90% of simulations remaining the AO regime after 30 years, with fewer than 10% transitioning to AV. However, as irrigation costs increase due to SGMA, the more stringent the policy is, the faster it transitions to AV. In the SGMA-100 scenario, where irrigation costs double, over 40% of the simulations adopt AV by the end of the 30-year period. These results highlight the critical role of groundwater-oriented policies that could increase irrigation costs in driving future land use decisions in the Central Valley.

To analyze the impact of increased market and weather volatility on land use decisions, we introduce scenarios that reflect higher levels of uncertainty in agricultural revenue and irrigation costs by introducing increased variance (Σ). These scenarios, denoted as HMR (High Market Risk), HWR (High Weather Risk) and HMR+HWR (combined high risks), allow us to explore how volatility affects the transitions between AO, AV, and SO regimes. Figure 2.9 shows the percentage of simulations in each regime under baseline conditions and the higher volatility scenarios.

Compared with the baseline scenario, when market (HMR) or weather (HWR) volatility increases, the pace of adoption slows, and the AO regime retains dominance for longer periods. The combined HMR+HWR scenario exhibits the most significant delay in transitions compared to the baseline. This indicates that when volatility in agricultural revenue or irrigation costs increases, landowners may prefer to delay transitions to AV or SO because these changes involve sunk costs and irreversible decisions. This delay reflects the greater value of waiting for more information before committing to a new regime under uncertain conditions.

In the HWR scenario, we also observe a small percentage of simulations transitioning to the SO regime. This shift can be attributed to the stability provided by solar rent income, which provides a hedge against the uncertainty in irrigation costs driven by adverse weather.

Unlike AV, which requires significant investments and exposes landowners to market risks, the SO regime offers predictable income, making it more appealing under weather-related volatility. This shift emphasizes the role of stable income sources in mitigating risk and highlights how uncertainty delays transitions to regimes with higher upfront costs.

Figure 2.10 presents the policy functions under these scenarios. Under the baseline, it is optimal to remain in the AO regime when agricultural revenues are high. However, under high market volatility (HMR), the conversion threshold to AV decreases, shifting from approximately 7.5 to slightly above 6, while switching to AV remains optimal under low revenue conditions. However, in the HWR scenario, as irrigation costs increase, it initially becomes optimal to remain in AV, but beyond that, switching directly to SO becomes optimal. This reflects the stabilizing role of SO in mitigating high irrigation cost risks. Similarly, in the policy function of the AV regime, high irrigation costs drive transitions to SO. Under the combined HMR+HWR scenario, these patterns persist, with the combined impact of market and weather volatility.

Finally, solar rent is critical for the trade-offs in different regimes. To test how solar incentives change land-use decisions, we simulate scenarios with varying annual solar payment levels, labeled SR-500, SR-1000, SR-1500, SR-2000, with SR-1500 representing the baseline scenario in the model. Figure 2.8 presents the percentage of simulations in each regime over a 30-year period under these scenarios. For low solar rents (SR-500 and SR-1000), it remains optimal for all simulations to stay in the AO regime, as the additional income from solar systems does not justify the transition costs. At the baseline rent (SR-1500), around 10% of the simulations adopt AV by the end of the period, reflecting the threshold at which solar incentives begin to compete with agriculture. However, at SR-2000, the transition to AV accelerates, with all simulations converging to AV by the end of the 30 years, as the higher solar payments outweigh the costs and opportunity losses from switching. These results highlight a critical tipping point in solar rent, where increasing

incentives could significantly accelerate the adoption of AV systems and shift land-use strategies in favor of solar-integrated farming.

2.6.3 Crop-specific Analysis

We extended the model to include eight additional crops widely grown in the Central Valley. The policy functions for these crops are presented in Figure 2.11 and 2.12. These results further support the findings from the representative crops. In Figure 2.11, we plotted the four low-value crops alfalfa, corn, rice, and wheat, and it shows that it is optimal to stay in AO for the entire state space for all these four crops, reflecting the limited economic incentives to transition to alternative land-use regimes when agricultural returns are relatively low. For high-value crops, such as tomatoes and grapes in Figure 2.12, it becomes optimal to switch to AV under lower revenue and high irrigation costs. Compared with tomatoes, grapes have higher irrigation needs, therefore, are more prone to adopting agrivoltaics. Conversely, for almonds and oranges, since we assume a total loss of agricultural revenue (in addition the sunk costs of forgone natural assets), AV does not appear optimal for these crops across the entire state space. For higher-value crop almonds, it is optimal to stay in AO, but for oranges, it is optimal to switch to SO directly when net revenue is low.

These results are consistent with the findings from the representative crops, and the crop-specific analysis provides more actionable and localized insights into the Central Valley context, as they reflect the unique characteristics of key crops that dominate the region.

2.6.4 Sensitivity Analysis

Building on the crop-specific analysis in the previous section, we now examine how variations in key parameters influence the optimal land-use decisions. This sensitivity analysis

provides deeper insights into the robustness of the findings and highlights how different crops may respond to changes in agrivoltaic performance, economic factors, and transition costs.

First, to evaluate the impact of shading on land-use decisions, we tested a series of α s from -0.2 (20% yield increase) to 0.9 (90% loss of revenue). Table 2.1 summarizes the optimal regimes under steady-state conditions for each crop and (α) value. The results reveal that for low-value crops like alfalfa, corn, rice, and wheat, the optimal regime remains AO across all tested α values. These crops have low economic returns, and even under scenarios where AV increases agricultural income, it is not enough to cover the high upfront costs. Almonds, a high-revenue perennial crop, only switch to AV when α is negative, suggesting that agrivoltaics needs to enhance yields for this transition to be optimal. Grapes, known for their shade-tolerance, are suitable for AV adoption; however, as α increases, the economic loss from shading outweighs the benefit, and staying in AO becomes dominant. Tomatoes present a similar but more resistant pattern; AV is optimal for tomatoes when $\alpha \leq 0.3$, but beyond that, the revenue losses outweigh the benefits. For oranges, AV is never optimal due to the profitability of the crop. Instead, at $\alpha \geq 0.3$, the stable returns from solar make switching directly to SO the optimal decision.

Second, we tested the sensitivity of land-use decisions to ρ (shown in Table 2.2), the water-saving coefficient, ranging from -0.2 (increases irrigation need) to 0.8 (saves 80% water), with the baselines presented in Table A.2 based on field studies. The results show that ρ has a limited impact on most crops grown in Central Valley, with the optimal regime remaining AO for low-value crops and AV never emerging as optimal for almonds or oranges. However, for high-value, high-irrigation crop grapes, ρ plays a critical role; when $\rho \geq 0\%$, it becomes optimal to adopt AV, reflecting its high sensitivity to water-saving benefits.

Next, we examined the model sensitivity to γ , the solar intensity coefficient in the AV regime (Table 2.3). The results indicate that for high-revenue crops like grapes and tomatoes,

a higher γ is required to make the transition to AV economically viable. This suggests that for AV to compete with AO, especially for these crops, sufficient solar income must offset the shading and transition costs.

For transition costs, we tested the sensitivity by scaling the baseline values of $K_{AO \rightarrow AV} = 35k$, $K_{AO \rightarrow SO} = 30k$, $K_{AV \rightarrow SO} = 10k$, using a range of multipliers. This approach allows us to explore how changes in sunk costs impact optimal land-use decisions. From Table 2.4, we find that for low-value crops, reducing transition costs encourages transitions from AO to SO, as the economic barrier to adopting solar systems becomes lower. Similarly, for high-value crops, lower transition costs facilitate switches to AV. These findings underscore the critical role of transition costs in shaping land-use decisions and highlight how policy mechanisms, such as subsidies or financial incentives, could influence the adoption of renewable energy systems in agricultural settings.

2.7 Discussions

2.7.1 Key Findings

This study examines the complex trade-offs of economic, environmental, technological, and policy factors in shaping land use decisions in the Central Valley. From the model results, we have several important findings. Under baseline scenarios, the AO regime is the dominant choice for high-value crops due to the profitability of farming. In contrast, low-value crops show limited transitions to AV or SO regimes, as their economic returns are insufficient to justify the high upfront costs associated with these investments. For high-revenue, high-irrigation crops like grapes, the AV regime becomes a favorable choice across a majority of the state space, reflecting the value of water-saving benefits in offsetting irrigation costs.

Scenario analysis indicates that increased volatility in market and weather conditions significantly slows transitions to AV or SO regimes. The AO regime remains dominant for a longer period, especially under the combined HMR+HWR scenario, as uncertainty increases the value of waiting before committing to irreversible investments associated with sunk cost. Despite this, under HWR scenarios, higher irrigation costs induce a small percentage of landowners to transition to the SO regime. This finding highlights the stabilizing role of solar income (under the assumption that solar developments are conducted and owned by a solar partner), which provides a predictable income stream and reduces exposure to uncertain irrigation costs. The results also highlight the critical role of solar policy incentives, with higher rents accelerating transitions to AV, particularly for the crops with higher irrigation demand.

The sensitivity analysis highlights the nuanced ways in which key parameters influence land-use decisions. The results demonstrate that the shading effect α , and transition costs play critical roles in determining the optimal regime for different crops. For instance, the analysis reveals that crops with lower economic returns remain in AO regardless of parameter changes, emphasizing the economic limitations of AV adoption for these crops. Conversely, high-revenue crops like grapes and tomatoes exhibit greater sensitivity to parameters such as α, ρ, γ , highlighting the potential for targeted policies to incentivize transitions to AV under favorable conditions. The influence of transition costs further underscores the importance of addressing economic barriers through subsidies or financial incentives to encourage renewable energy adoption. Overall, these findings suggest that land-use decisions are highly crop-specific and sensitive to both agronomic and economic factors, underscoring the need for tailored strategies that consider the unique characteristics and constraints of different crops and regions.

2.7.2 Policy Implications

The results have several implications for resource management and policy design in the Central Valley. First, policies that reduce the upfront costs of adopting AV systems, such as subsidies or low-interest financing, could mitigate the delays caused by market and weather uncertainties. With measures to lower the economic barrier to transition, it could enhance the adoption of dual-use systems, particularly in regions with high irrigation costs.

Second, the analysis highlights the importance of aligning water management policies like SGMA with incentives for AV adoption. The results indicate that rising irrigation costs under SGMA could accelerate transitions to water-saving technologies, but complementary measures - such as technical assistance and education on AV systems - would be necessary to promote wide adoption.

Third, solar incentives are shown to be a critical driver of transitions. While the results demonstrate that higher solar rents incentivize transitions to AV, it is important to note that the model assumes full information for landowners, meaning that decisions are made based on a comprehensive understanding of all costs and benefits. In reality, informational barriers could lead to suboptimal decisions, particularly under high solar rents. Policymakers and stakeholders should therefore prioritize outreach and educational efforts to ensure landowners are fully informed about the opportunities and trade-offs associated with AV systems.

Fourth, the sensitivity analysis findings highlight the importance of AV configurations that minimize the negative impacts on crop production. Optimized designs, such as elevated panels, adjustable mounting systems, or strategic spacing, could mitigate the shading effect and maintain agricultural productivity, preserving the economic advantages of AV systems. This also points to the need for continued research and technological advancements to refine AV configurations that balance energy generation with crop yields. For

policymakers and industry stakeholders, demonstration projects and pilot studies could help identify best practices and build confidence among landowners, ensuring that AV systems deliver on their potential without compromising agricultural returns.

Finally, crop insurance policies could provide a critical buffer against market and weather volatility by stabilizing agricultural revenue. By guaranteeing a minimum level of income during adverse conditions such as excessive droughts, crop insurance reduces the uncertainties the landowners are exposed to, thus enabling them to make long-term investment decisions. More specific insurance products, including those that target the specific risks and benefits of AV systems, could further encourage adoption by providing landowners with financial security over the transitioning period.

2.7.3 Limitations and Future Work

While this study provides valuable insights, several limitations must be acknowledged. First, the analysis relies on simplified assumptions about crop characteristics and economic parameters due to the data limitations. Future research should incorporate greater heterogeneity in crop-specific characteristics when better data becomes available. Second, the model assumes static solar rent levels, which may not fully capture the dynamic market conditions or technological advancement. Exploring sole-ownership for solar development or incorporating stochastic rent scenarios could enhance the understanding of how evolving incentives influence land-use transitions over time. Third, the model does not account for behavioral factors, such as risk preference, which may play a significant role in landowner decision-making. Incorporating these dimensions could provide a more nuanced understanding of adoption patterns and highlight non-economic drivers of land-use change. Finally, the analysis is based on generalized state-space results of a representative Central Valley landowner and does not consider spatial heterogeneity. Incorporating geographically

explicit data, such as local water availability, soil conditions, or regional market dynamics, could further refine the applicability of the findings to specific regions within the Central Valley. Addressing these limitations in future work will enhance the robustness of the model and provide more tailored recommendations for policymakers and stakeholders.

2.8 Conclusions

This study introduces a novel stochastic dynamic programming model to assess the land-use decisions involved in adopting agrivoltaics (AV), or solar-only(SO) systems on agricultural lands in California's Central Valley. Employing a regime-switching framework, the model captures how uncertainties in agricultural income and irrigation costs, combined with the irreversibility of investments, influence landowners' decisions to adopt AV or SO systems or to stay in traditional agricultural production. By focusing on representative crops with differing water needs and economic values, the model provides a nuanced analysis of trade-offs involving yield reductions, water cost savings, and solar income generation across various scenarios.

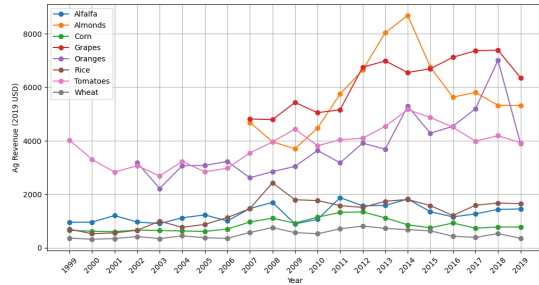
The findings reveal that the adoption of AV and SO systems is significantly influenced by market and environmental volatility, irrigation costs, and crop-specific characteristics. The analysis shows that under baseline conditions, the AO regime dominates, especially for high-value crops. However, as irrigation costs rise - particularly under the Sustainable Groundwater Management Act(SGMA), or as solar rents increase, transitions to AV and SO systems become more viable. For high-value, high-irrigation crops such as grapes, AV systems are particularly attractive due to their potential to offset rising water costs and generate stable energy income despite the potential yield loss due to partial shading. Conversely, for low-value crops like alfalfa, corn, etc, the agricultural income is not sufficient to justify the high upfront cost of adopting solar development.

Despite its contributions, this study acknowledges several limitations. The model assumes full information for landowners and does not account for behavioral factors such as risk aversion, which could influence decision-making. Additionally, operational costs and solar rent dynamics are simplified, and the analysis focuses on a representative landowner, limiting the generalizability of results to larger or more diverse agricultural operations. Spatial heterogeneity, such as variations in groundwater availability and opportunity costs across the Central Valley, is also not explicitly modeled, which could further refine predictions.

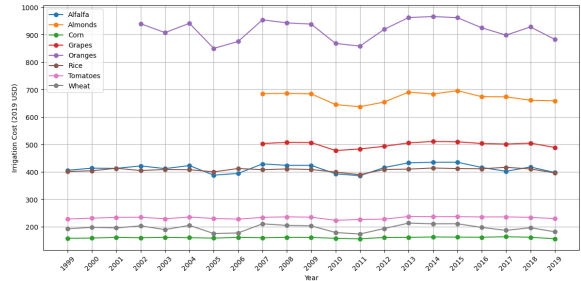
Future research should address these limitations by incorporating more dynamic and spatially explicit factors, exploring behavioral dimensions of land-use decisions, and expanding the scope to include additional crop types and larger agricultural scales. Such efforts will improve our understanding of the economic and operational feasibility of AV systems and their role in sustainable agriculture.

As California seeks innovative solutions to address climate change, water scarcity, and agricultural sustainability, this study provides valuable insights into the potential of AV systems. By balancing agricultural productivity with renewable energy generation, AV systems offer a promising pathway to enhance the resilience of food production while advancing toward a zero-carbon future.

2.9 Tables and Figures



(a) Historical Agricultural Revenue



(b) Historical Irrigation Cost

Figure 2.2: Historical Ag Revenue and Irrigation Cost in California

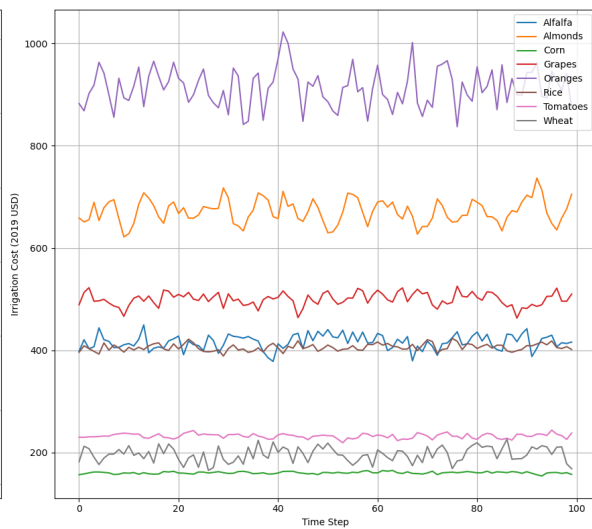
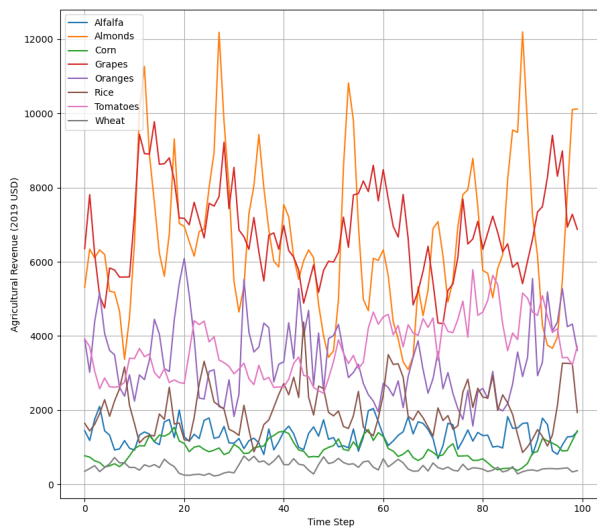


Figure 2.3: Simulated Ag Revenue and Irrigation Cost for All Crops

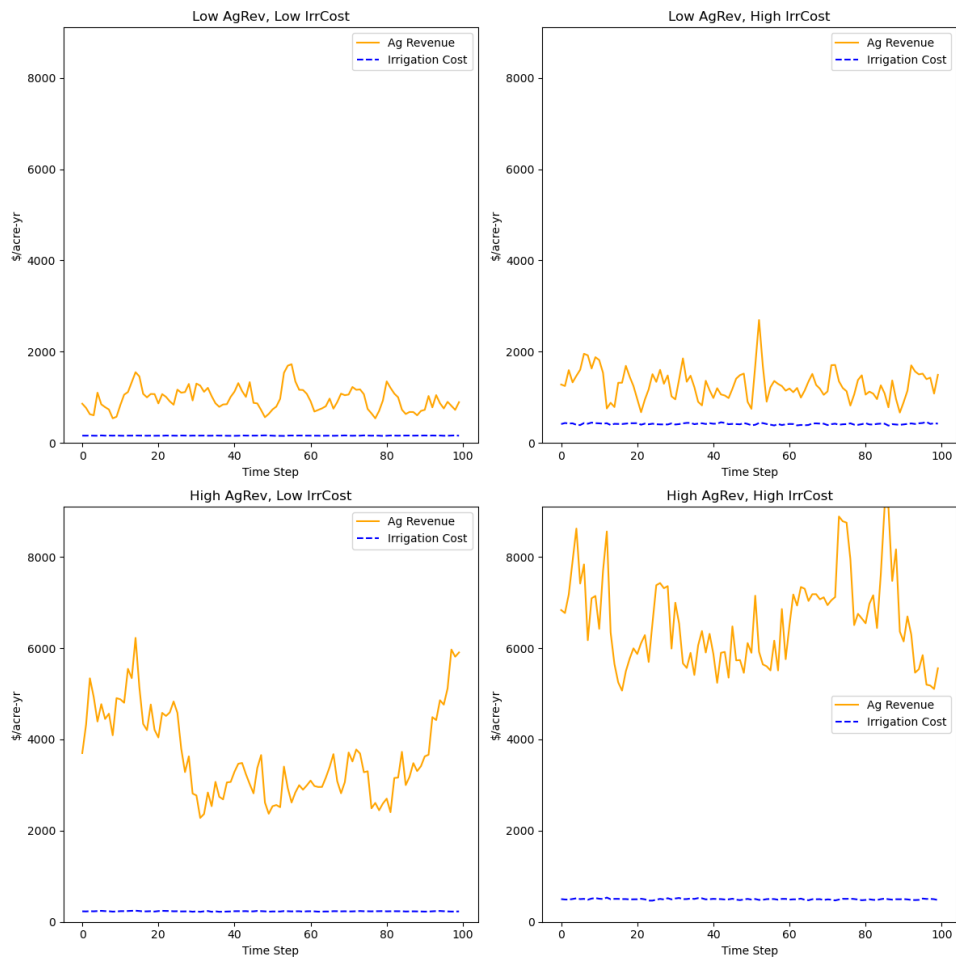


Figure 2.4: Simulated Ag Revenue and Irrigation Cost for Representative Crops

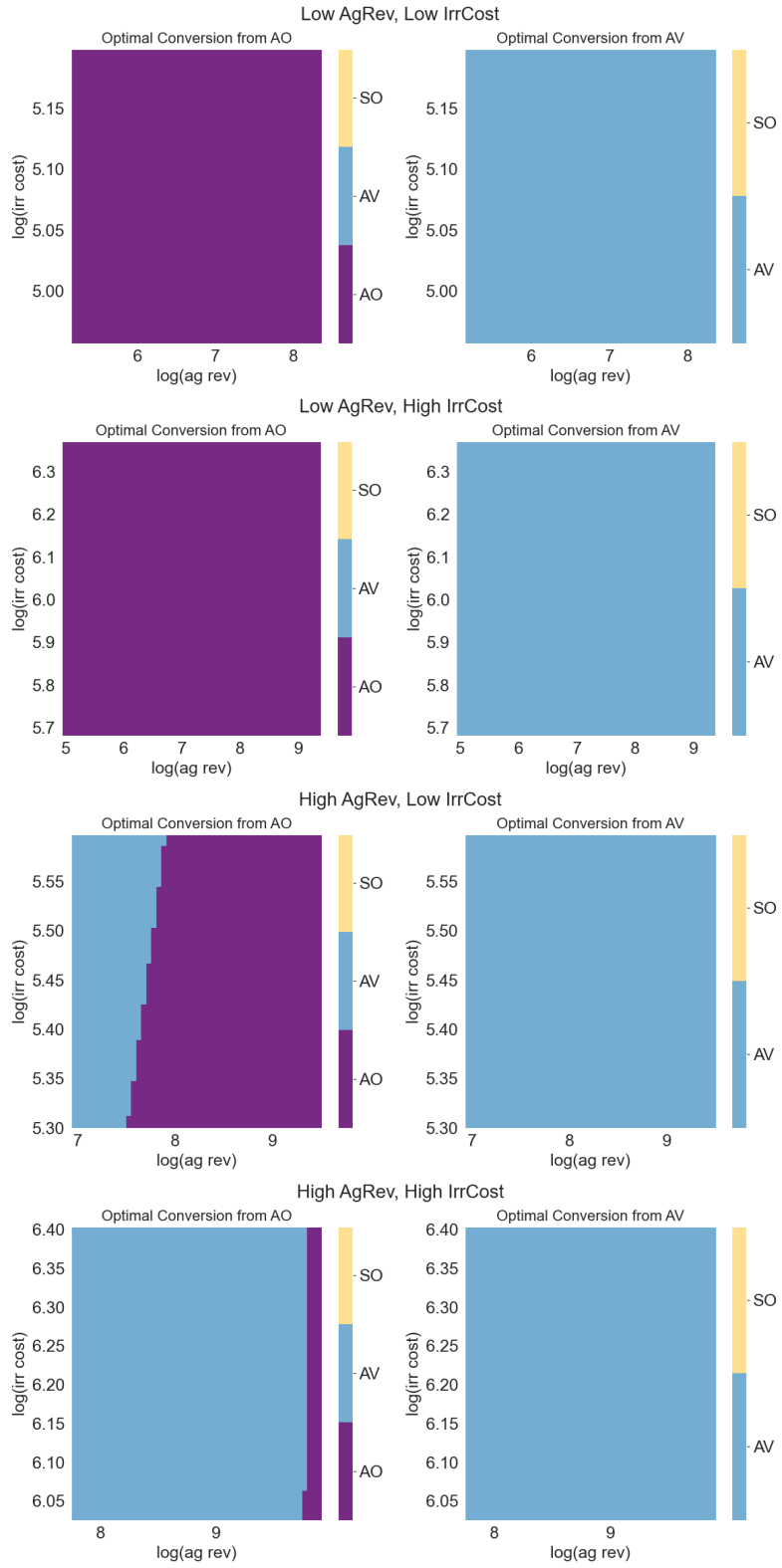


Figure 2.5: Policy Functions for Representative Crops (Baseline)

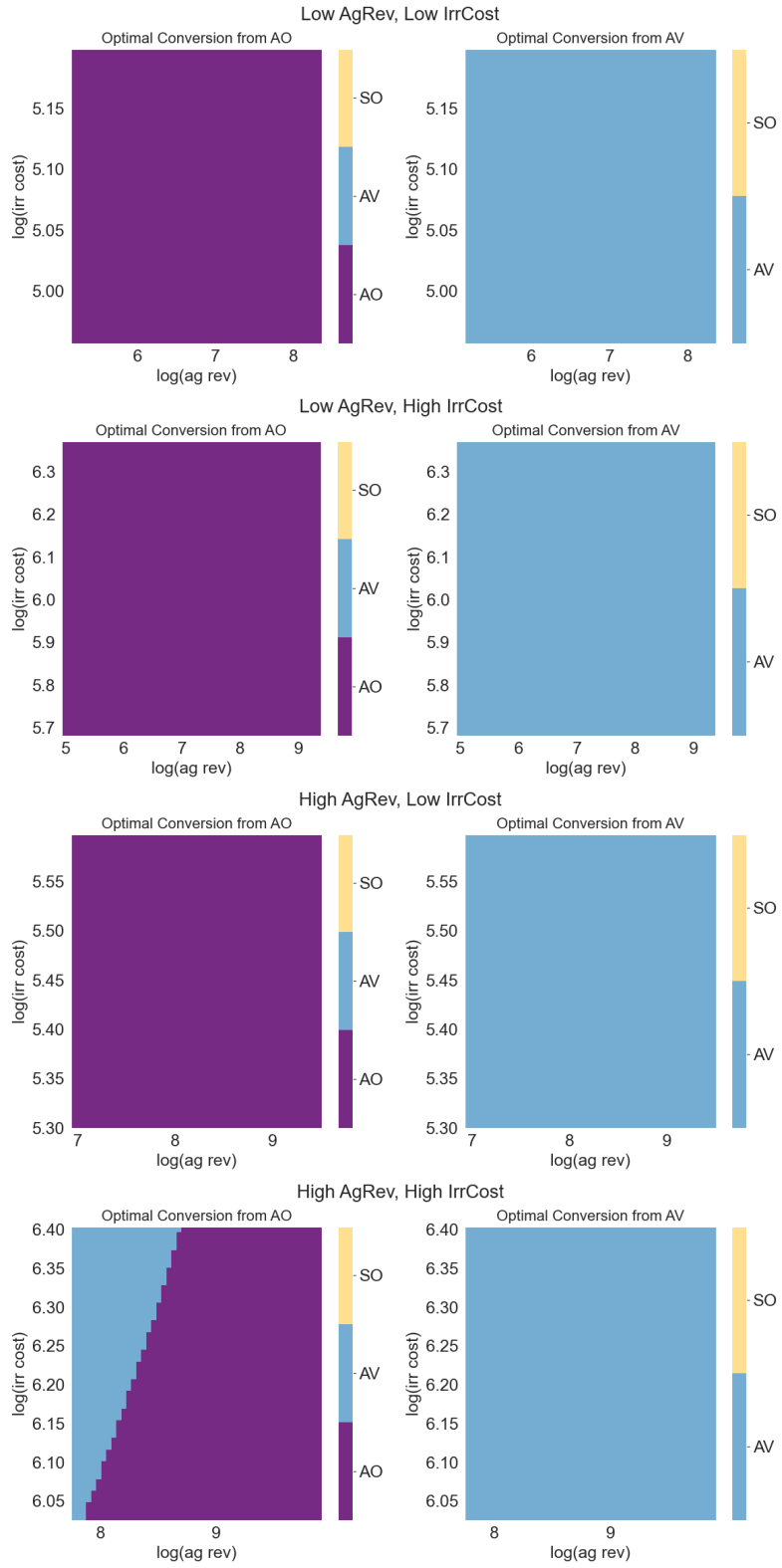


Figure 2.6: Policy Functions for Representative Crops (Low Shade Tolerance)

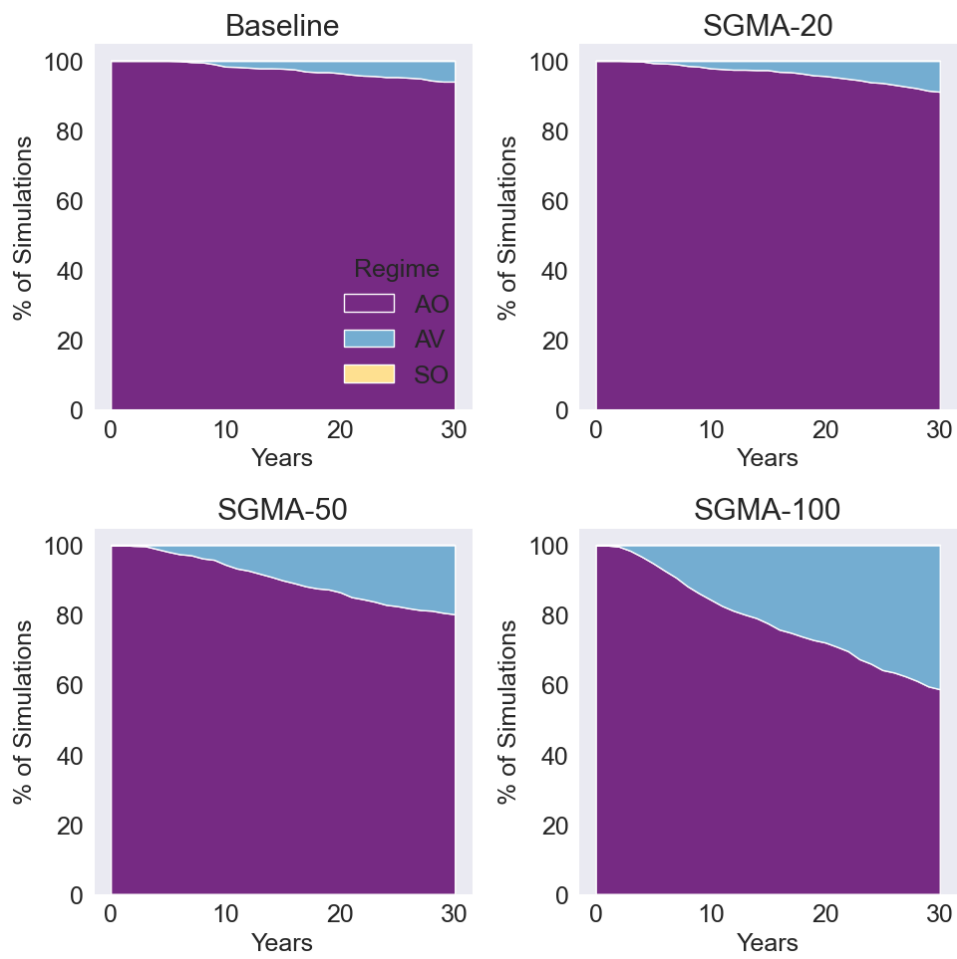


Figure 2.7: Optimal Land-Use Regime Distribution Over Time Under SGMA Scenarios

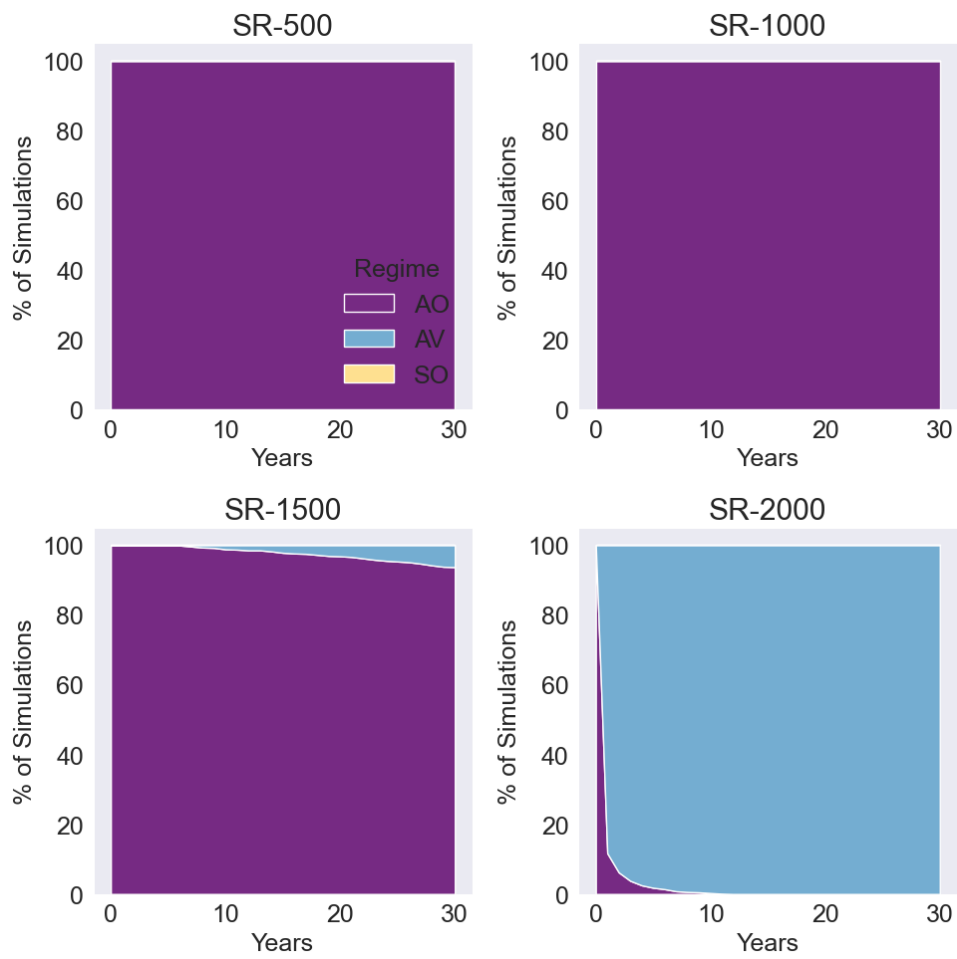


Figure 2.8: Optimal Land-Use Regime Distribution Over Time Under Solar Rent Scenarios

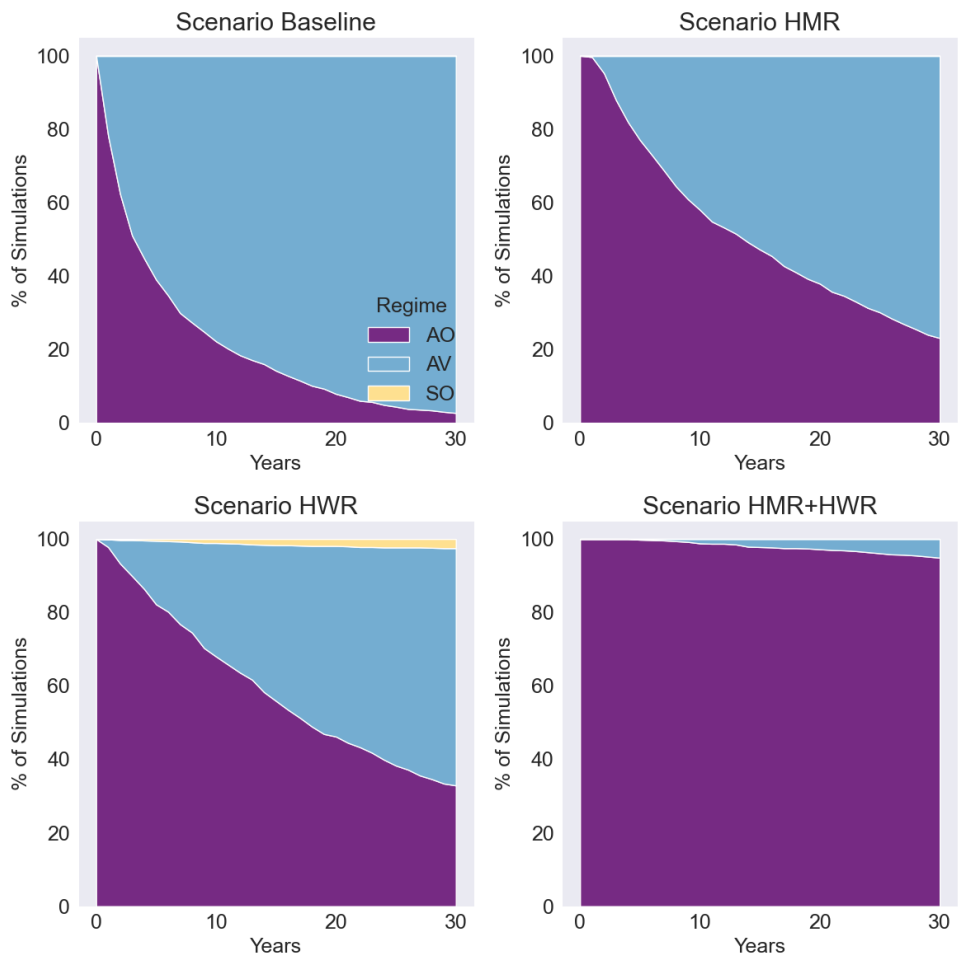


Figure 2.9: Optimal Land-Use Regime Distribution Over Time Under Risk Scenarios

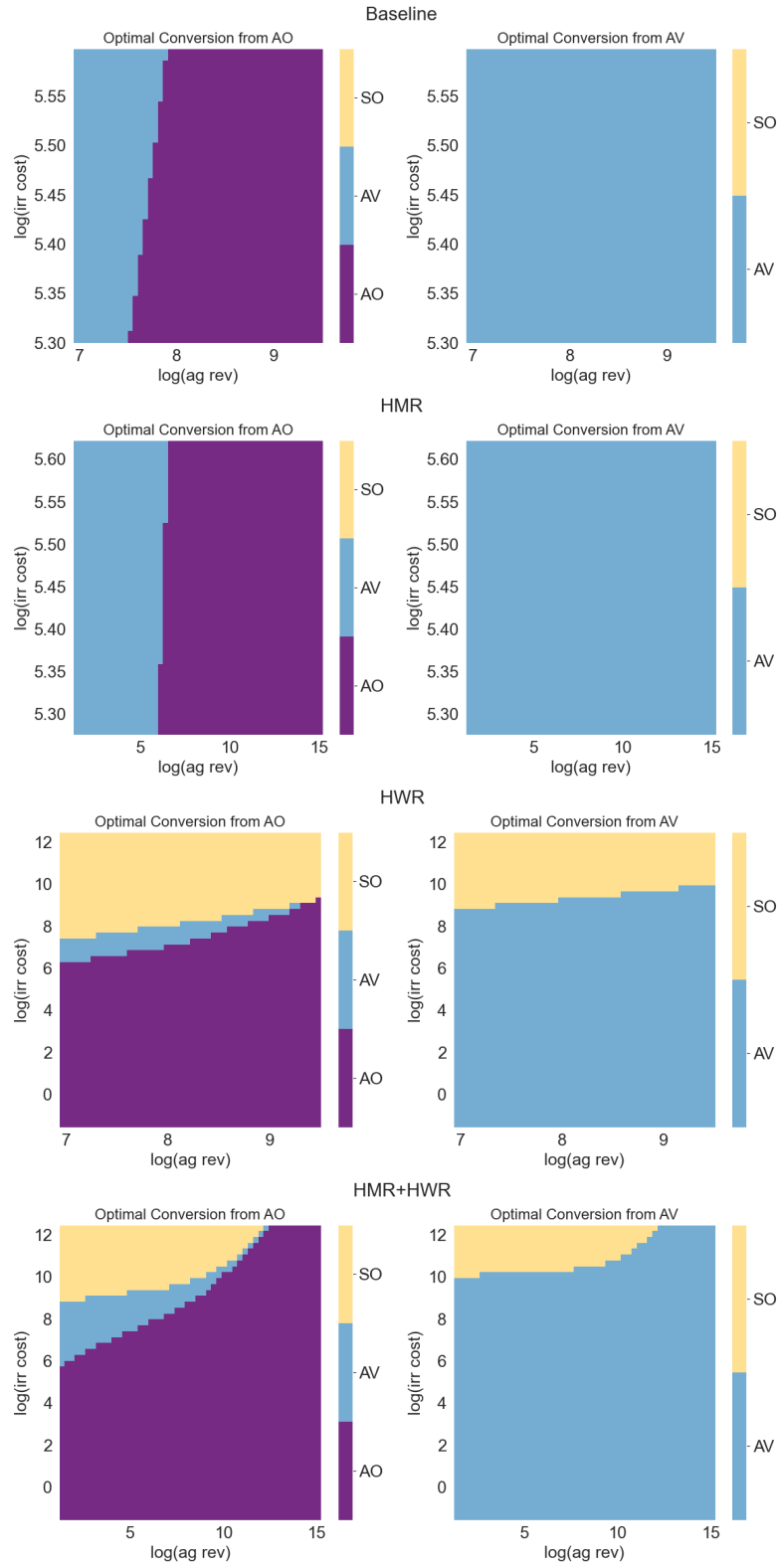


Figure 2.10: Policy Functions Under Risk Scenarios

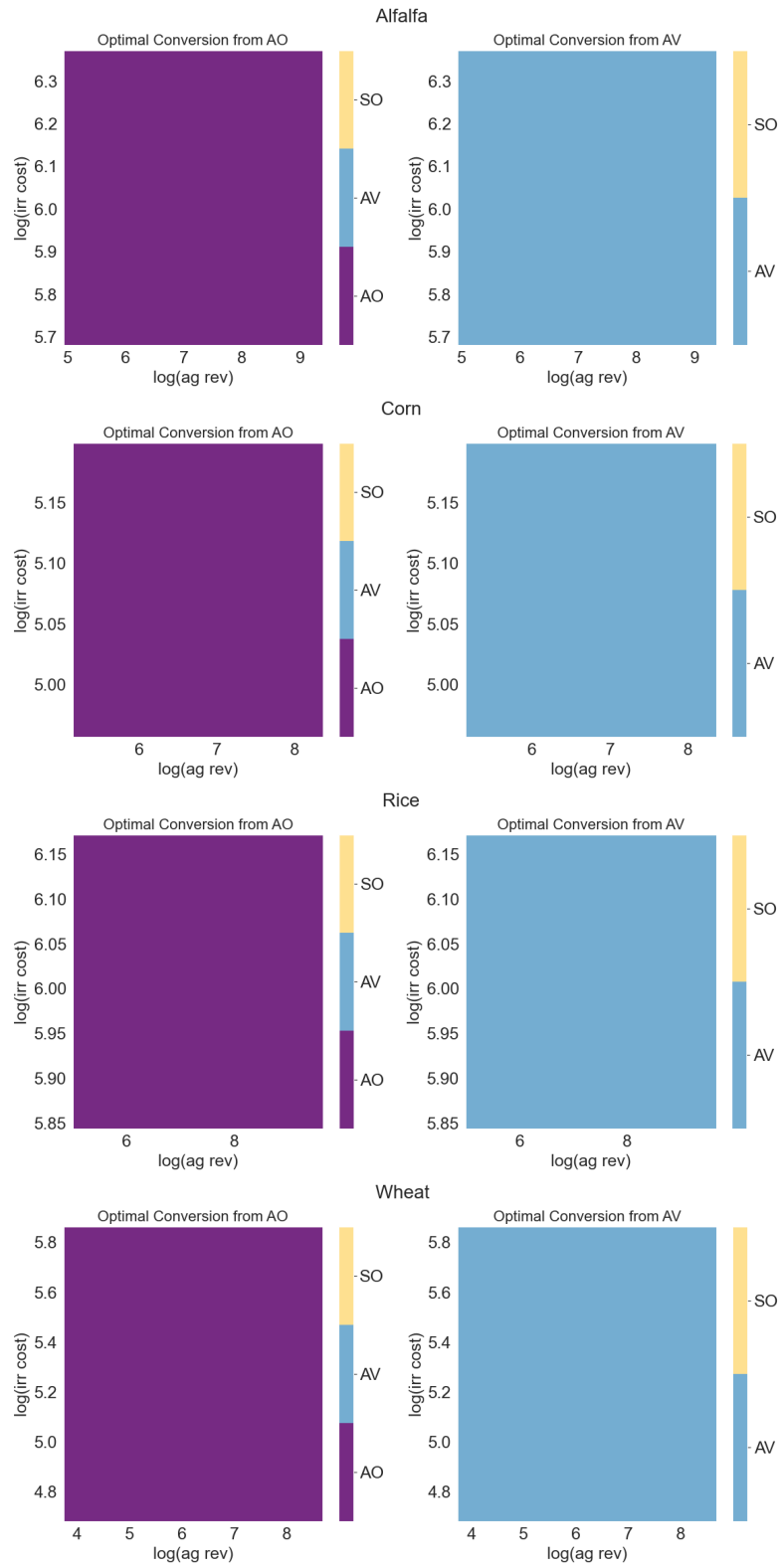


Figure 2.11: Policy Functions for All Crops

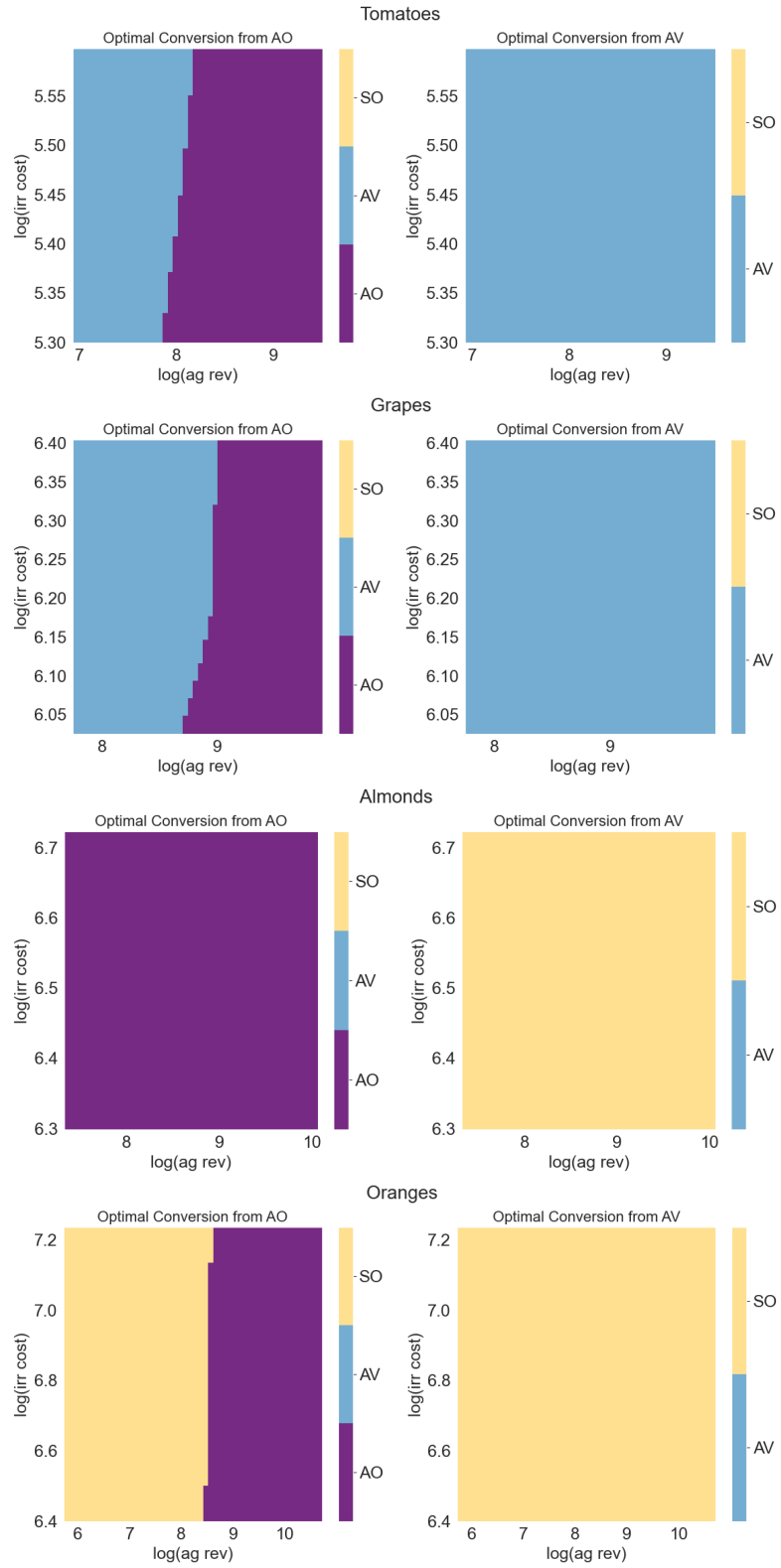


Figure 2.12: Policy Functions for All Crops (continued)

Table 2.1: Sensitivity Analysis - Optimal Regime Under Steady State (α)

α	Alfalfa	Almonds	Corn	Grapes	Oranges	Rice	Tomatoes	Wheat
-0.2	AO	AV	AO	AV	AV	AO	AV	AO
-0.1	AO	AV	AO	AV	AV	AO	AV	AO
0.0	AO	AO	AO	AV	AV	AO	AV	AO
0.1	AO	AO	AO	AV	AV	AO	AV	AO
0.2	AO	AO	AO	AO	AV	AO	AV	AO
0.3	AO	AO	AO	AO	SO	AO	AV	AO
0.4	AO	AO	AO	AO	SO	AO	AO	AO
0.5	AO	AO	AO	AO	SO	AO	AO	AO
0.6	AO	AO	AO	AO	SO	AO	AO	AO
0.7	AO	AO	AO	AO	SO	AO	AO	AO
0.8	AO	AO	AO	AO	SO	AO	AO	AO
0.9	AO	AO	AO	AO	SO	AO	AO	AO

Table 2.2: Sensitivity Analysis - Optimal Regime Under Steady State (ρ)

ρ	Alfalfa	Almonds	Corn	Grapes	Oranges	Rice	Tomatoes	Wheat
-0.2	AO	AO	AO	AO	SO	AO	AO	AO
-0.1	AO	AO	AO	AO	SO	AO	AO	AO
0.0	AO	AO	AO	AO	SO	AO	AO	AO
0.1	AO	AO	AO	AV	SO	AO	AO	AO
0.2	AO	AO	AO	AV	SO	AO	AO	AO
0.3	AO	AO	AO	AV	SO	AO	AO	AO
0.4	AO	AO	AO	AV	SO	AO	AO	AO
0.5	AO	AO	AO	AV	SO	AO	AO	AO
0.6	AO	AO	AO	AV	SO	AO	AO	AO
0.7	AO	AO	AO	AV	SO	AO	AO	AO
0.8	AO	AO	AO	AV	SO	AO	AO	AO

Table 2.3: Sensitivity Analysis - Optimal Regime Under Steady State (γ)

γ	Alfalfa	Almonds	Corn	Grapes	Oranges	Rice	Tomatoes	Wheat
0.0	AO	AO	AO	AO	SO	AO	AO	AO
0.1	AO	AO	AO	AO	SO	AO	AO	AO
0.2	AO	AO	AO	AO	SO	AO	AO	AO
0.3	AO	AO	AO	AO	SO	AO	AO	AO
0.4	AO	AO	AO	AO	SO	AO	AO	AO
0.5	AO	AO	AO	AO	SO	AO	AO	AO
0.6	AO	AO	AO	AO	SO	AO	AO	AO
0.7	AO	AO	AO	AV	SO	AO	AO	AO
0.8	AO	AO	AO	AV	SO	AO	AV	AO
0.9	AO	AO	AO	AV	SO	AO	AV	AO

Table 2.4: Sensitivity Analysis - Optimal Regime Under Steady State (K)

K multiplier	Alfalfa	Almonds	Corn	Grapes	Oranges	Rice	Tomatoes	Wheat
0.0	AV	AO	AV	AV	SO	AV	AV	SO
0.1	AV	AO	SO	AV	SO	AV	AV	SO
0.5	AO	AO	SO	AV	SO	AO	AV	SO
0.75	AO	AO	AO	AV	SO	AO	AV	AO
1.0	AO	AO	AO	AV	SO	AO	AO	AO
2.0	AO	AO	AO	AO	AO	AO	AO	AO
5.0	AO	AO	AO	AO	AO	AO	AO	AO
10.0	AO	AO	AO	AO	AO	AO	AO	AO

CHAPTER

3

OPTIMIZING AGRIVOLTAICS ADOPTION
TO SUPPORT GROUNDWATER
CONSERVATION IN CALIFORNIA'S
CENTRAL VALLEY

3.1 Introduction

California's Central Valley (CV) is one of the most productive agricultural regions in the world, supplying 8% of the US foods and 40% of the table foods and generating more than \$50 billion annually in farm revenue (Newsom 2022). Its high productivity depends on extensive irrigation, with groundwater supplying around half of its total irrigation in an average year and up to 75% during droughts (Liu et al. 2022). This heavy reliance on groundwater has led to a long-term depletion rate of $2\text{km}^3\text{yr}^{-1}$ (Levy et al. 2021), which have resulted in increased pumping cost, degradation of groundwater quality, and land subsidence. In response, California enacted the Sustainable Groundwater Management Act (SGMA) that mandates sustainable aquifer management by 2040, primarily through forming Groundwater Sustainable Agents (GSAs) tasked with implementing Groundwater Sustainable Plans. However, compliance with SGMA is expected to necessitate large scale reduction in irrigated farmland (Escriva-Bou et al. 2023; Hanak et al. 2019). This land retirement poses significant economic and food security challenges.

At the same time, California's clean energy policies, including SB100 aiming at 100% carbon neutrality are driving rapid growth in renewable energy like utility-scale solar development. This expansion introduces land-use competition between renewable energy production and agricultural production. As a result, agrivoltaics (AV), the co-location of solar and agricultural practices has gained increasing attention as it, in some contexts, can provide water savings by reducing evapotranspiration and lowering irrigation demand through shading, which provides the potential to balance food production, water conservation, and renewable energy expansion (Barron-Gafford et al. 2019).

This study builds on the analysis presented in Chapter 2 by developing and applying a regional spatiotemporal economic optimization model of land and water resource allocation in CV at the intensive and extensive margin to explore potential interactions between solar

and AV adoption and regional groundwater conservation objectives. Specifically, this study seeks to understand to what extent solar land use change or the adoption of AV production decisions could impact irrigation decisions. Through extensive sensitivity analysis, we quantify the impact of solar and AV adoption on the spatiotemporal distribution of water use using a new hydro-economic framework that captures groundwater dynamics and crop irrigation possibilities at the intensive and extensive margins. We also explore how the solar and AV adoption decisions change in the presence of groundwater conservation incentives (both price and quantity instruments). Results from this study highlight how AV can complement groundwater conservation goals, but only at high levels of land use change that may be incompatible with energy sector demands for regional solar production. Further, we highlight potential "water leakage" effects of solar and AV adoption, in which concentrated solar production in one region causes crop mix changes and irrigation intensification in other regions, potentially exacerbating groundwater management challenges.

3.2 Literature Review

There is an extensive theoretical and applied economic literature focused on groundwater management, including research that explores optimal intertemporal management of groundwater supplies (Worthington et al. 1985), groundwater management under uncertainty (Krishnamurthy 2017), conjunctive water allocation and quality modeling (Das and Datta 2001), and the effects of policy, technology, and management interventions on groundwater conservation outcomes (Wang et al. 2015; Mustaq Shaikh and Farjana Birajdar 2024).

Pertinent to this manuscript, other research has applied empirical or modeling frameworks to explore the potential implications of production technologies or related management interventions in supporting groundwater conservation goals. For example, Pfeiffer

and Lin (2014) shows that incentives designed to increase the adoption of more efficient irrigation systems may exacerbate water management challenges, leading to increased groundwater consumption. In the solar-agriculture nexus domain, recent economic literature has focused on solar-powered pumps and interactions between off-grid solar electrification and agricultural development, primarily in the global south. This work addresses potential intertemporal externalities resulting from low (or zero) marginal cost groundwater extraction from solar pumps, which can drive future resource scarcity (Closas and Rap 2017; El Mahdi BENTALEB et al. 2024).

While previous research has focused on technologies that increase water use efficiency, or reduce groundwater pumping costs, AV production patterns offer a unique technological intervention that reduces the derived demand for water at the crop level, while potentially diversifying income streams for farmers. Our analysis builds on the groundwater management literature by incorporating this joint production technology and exploring potential synergies and tradeoffs between renewable energy development and groundwater conservation goals using illustrative regional policy simulations.

3.2.1 Agrivoltaics and Regional Groundwater Management

Despite the hype about the potential of agrivoltaics in increasing land use efficiency and water conservation (Dinesh and Pearce 2016), the widespread adoption of agrivoltaics involves complex trade-offs within the food-water-energy nexus, as it affects crop production potential, water availability, and regional land-use priorities. High initial capital cost, uncertainties in long-term returns, and the increased complexity in operating both solar and farm work create barriers to landowners (Macknick et al. 2022). Additionally, the suitability of agrivoltaics varies by crop type, as some crops benefit from shading while others experience higher yield reductions under solar panel shading. These challenges are analyzed in depth

in Chapter 2, which examines agrivoltaics adoption from a representative CV landowner's perspective, focusing on the conditions where AV adoption would be optimal, and analyzes how uncertainties influence landowners' adoption decisions under a stochastic dynamic programming framework.

While landowner decisions drive localized agrivoltaic adoption, the regional implications -particularly in the context of groundwater conservation - remains underexplored. Existing modeling efforts in agrivoltaics have primarily focused on micro-scaled analysis, such as optimizing panel configurations for crop yield (Dupraz et al. 2011), and analyzing its financial feasibility and energy-agricultural trade-offs under different economic conditions Yajima et al. (2023). For instance, Bhandari et al. (2021) adopts a case study in Niger covering four types of irrigation strategies to analyze the economic feasibility of agrivoltaics practices. While these studies evaluate the agrivoltaics' economic implications and potential in balancing trade-offs in the Food-Water-Energy Nexus, their model does not account for aquifer dynamics or the feedback effects of pumping restrictions on regional-scale land-use decisions. Similarly, Alam et al. (2023) proposes a modeling framework for stakeholders to assess the profitability to optimize AV system design, but it prioritizes farm-level profitability over regional resource sustainability. This leaves critical questions unanswered about how widespread adoption could stabilize groundwater reserves or mitigate SGMA-mandated land retirement, which threatens both food security and rural economies.

3.2.2 Hydrologic and Hydroeconomic Models in the Central Valley

Due to its economic significance and hydrologic complexity, California's Central Valley has been the focus of extensive modeling efforts that aim to simulate water dynamics, optimize land and water allocation, forecast aquifer responses, and inform policy decisions. Hydro-

logic models such as the Central Valley Hydrologic Model (CVHM; Faunt 2009) developed by the U.S. Geological Survey (USGS) and C2VSim (Brush et al. 2013) developed by the California Department of Water Resources (DWR), have become foundational tools for simulating groundwater-surface water flows, recharge dynamics, and subsidence trends. These models have been widely applied in groundwater sustainability research and used to evaluate the hydrologic impacts of climate change and drought response policies (Alam et al. 2019). While these hydrologic models offer granular insights into groundwater storage and depletion and provide valuable data inputs for policy insights, they primarily simulate the physical processes rather than economic decision-making.

Complementing these hydrologic tools, hydroeconomic models like Statewide Agricultural Production (SWAP) Model (Howitt et al. 2009) integrate economic decision-making into water management. SWAP simulates how farmers allocate land and water across crops to adapt to water scarcity, offering insights into the economic trade-offs of policies like water pricing or water rights. Similarly, the CALVIN model (Draper et al. 2003) is a large-scale hydroeconomic model that optimizes statewide water infrastructure, incorporating agricultural, urban, and environmental demands. These frameworks offer insights into how CV agriculture adapts to water scarcity, navigates regulatory constraints like SGMA, and optimizes crop choices under fluctuating water availability and market conditions.

Despite the advancements in hydroeconomic modeling, the interaction between land-use change, renewable energy integration, and groundwater sustainability remains a gap. While recent studies incorporate agrivoltaics in land-use decisions within partial equilibrium models (i.e. Van Der Horst 2019), they do not integrate groundwater dynamics and its impact on land-use decisions. This is particularly important in the context of Central Valley, where groundwater depletion alters the economic viability of both agricultural and solar infrastructure. For example, falling aquifer levels increase pumping costs, and could disproportionately affect water-intensive crops like alfalfa, while solar farms or agrivoltaics could

reduce irrigation demand but remain unmodeled in current hydroeconomic frameworks.

This study extends existing modeling efforts by incorporating agrivoltaics within a hydro-economic framework to explore how this technological intervention can influence both groundwater sustainability and agricultural productivity under both business as usual water management and stringent controls imposed by SGMA. By merging groundwater dynamics with land-use decisions at the intensive and extensive margin, the primary objective of this is to assess the extent to which agrivoltaics can contribute to groundwater sustainability goals without excessively compromising agricultural productivity. The results suggest that agrivoltaic adoption has the potential to reduce water withdrawals, moderate land retirement under SGMA-imposed constraints, and provide economic diversification for landowners, offering a market-driven alternative to large-scale fallowing. However, the extent of adoption and conservation benefit varies across regions, showing a potential water leakage effect, where solar and agrivoltaics adoption in one area shifts groundwater extraction pressures elsewhere.

The remainder of this study is structured as follows: Section 3.3 details the methodological framework, outlining the dynamic optimization model and key economic and hydrologic constraints. Section 3.4 describes the data sources used for model calibration. Section 3.5 presents the results, comparing land-use and water-use outcomes across different policy scenarios. Section 3.6 discusses the implications, and Section 3.7 concludes.

3.3 Methodology

This study develops a dynamic, spatially explicit hydroeconomic optimization model to evaluate land-use strategies in California's Central Valley (CV) under competing demands for agricultural productivity, renewable energy expansion, and groundwater sustainability.

The model simulates land-use decisions and irrigation strategies over a 30-year horizon ¹, integrating the trade-offs between crop revenue, solar lease payments, and groundwater extraction costs. The framework is formulated as a dynamic nonlinear programming model, implemented in GAMS, GAMSPy, and Pyomo, optimizing land allocation among three competing land uses: traditional agriculture (AO), agrivoltaics (AV), and ground-mounted solar (SO). Additionally, the model optimizes the allocation of groundwater and surface water for irrigation, allowing for adaptive water-use decisions in response to land-use transitions.

3.3.1 Objective Function

The objective of the model is to maximize the present value of net benefits derived from land use decisions over the time horizon (T). The total economic return is defined as:

$$W = \max \sum_t^T \beta^t \sum_r [\sum_{c,i} (L_{r,c,i,t}^{AO} \Pi_{r,c,i,t}^{AO} + L_{r,c,i,t}^{AV} \Pi_{r,c,i,t}^{AV}) + L_{r,t}^{SO} \Pi_{r,t}^{SO}] \quad (3.1)$$

where the indices r, c, i, t denote region, crop, irrigation level, and time step (year), respectively. The spatial unit r corresponds to hydrologically and economically distinct agricultural zones derived from the Central Valley Production Model (CVPM). The crops considered in this model include alfalfa, corn, cotton, grapes, pistachios, rice, tomatoes, walnuts, and Idle land. Irrigation index i includes four levels: low, medium, high, and potential, and is associated with crop yields. The parameter β is the discount factor, L denotes the land allocated for different uses, and Π represents the net profit per unit area, defined separately for agricultural only (AO), agrivoltaics (AV), and Solar-only (SO), detailed below:

$$\Pi_{r,c,i,t}^{AO} = P_{c,t} Y_{r,c,i,t}^{AO} - p_r^s w_{r,c,i,t}^{s,AO} - C(h_{r,t}, w_{r,c,i,t}^{g,AO}) - C_c^{\text{oth}} \quad (3.2)$$

¹corresponds with the typical lifespan of solar panels

where $P_{c,t}$ is the crop price that follows a constant annual growth $g^c = 2\%$, $Y_{r,c,i,t}^{AO}$ represents the yield associated with the irrigation level, p_r^s denotes the unit price for surface water in region r , and $w_{r,c,i,t}^{s,AO}$, $w_{r,c,i,t}^{g,AO}$ each represents the volume of surface water and groundwater withdrawn. Function $C(h, w^g)$ is the groundwater pumping cost function, which depends on the depth to water $h_{r,t}$ and the volume of groundwater extracted. The term C_c^{oth} accounts for other production costs.

For agrivoltaics (AV) where crops are grown underneath or in-between solar arrays, its net profit includes an additional solar revenue term $\gamma R_{r,t}^{SO}$ which is a fraction of the solar lease payment as a solar farm, but incurring crop-specific yield penalties due to shading of infrastructure constraints $(1 - \alpha_c)$

$$\Pi_{r,c,i,t}^{AV} = P_{c,t} \cdot (1 - \alpha_c) Y_{r,c,i,t}^{AV} - p_{r,t}^s w_{r,c,i,t}^{s,AV} - C(h_{r,t}, w_{r,c,i,t}^{g,AV}) - C_c^{oth} + \gamma R_{r,t}^{SO} \quad (3.3)$$

The groundwater pumping cost function is given by:

$$C(h, w^g) = (k_r + e_r \sigma_r) w^g + e_r w^g h_r + \frac{e_r}{A \cdot s y_r} \frac{w^{g2}}{2} \quad (3.4)$$

where k_r represents the fixed pumping cost, e_r is the energy cost coefficient, and σ_r is the drawdown, which accounts for localized water table declines caused by pumping. The term h_r represents the depth to water, defined as the vertical distance from the ground surface level to the groundwater table level. This depth determines the baseline energy required to lift water to the surface, with greater depths increasing the total pumping cost, and is bounded by the well depth in each region. The inclusion of σ follows Knapp et al. (2003), which accounts for additional pumping costs due to localized well interference and transient declines in water level caused by active groundwater extraction. The final term in the equation captures the nonlinear cost of pumping, where the extraction becomes

increasingly expensive as the volume of extraction becomes higher. Here, $A \cdot s y_r$ represents the product of total area² and specific yield of the aquifer, determining how much groundwater level declines in response to withdrawals, also used in the groundwater dynamics equation 3.9.

3.3.2 Constraints

The optimization framework incorporates constraints to reflect the physical, economic, and hydrological realities of the Central Valley. The physical constraints include land availability, surface water availability constraints, and the water balance constraint. Land Use Constraint ensures that total land use does not exceed the initial land endowment in each region (L_r), and is defined as:

$$\sum_{c,i} (L_{r,c,i,t}^{AO} + L_{r,c,i,t}^{AV}) + L_{r,t}^{SO} \leq L_r \quad (3.5)$$

Surface water withdrawals for irrigation are constrained by regional water availability, accounting for conveyance losses:

$$\sum_{c,i} (w_{r,c,i,t}^{s,AO} \cdot L_{r,c,i,t}^{AO} + w_{r,c,i,t}^{s,AV} \cdot L_{r,c,i,t}^{AV}) \leq \bar{w}_r^s (1 - \lambda^{\text{conv}}) \quad (3.6)$$

where \bar{w}_r^s is the total available surface water in region r , subject to a conveyance efficiency factor λ^{conv} . Additionally, we set the lower bound to the surface water usage in each CVPM region to be 10% of their available surface water. Most California water districts have use-it-or-lost-it policies, meaning that failing to utilize allocated surface water rights can lead to losing future water rights. To maintain historical water rights, we impose a minimum usage constraint.

$$\sum_{c,i} (w_{r,c,i,t}^{s,AO} \cdot L_{r,c,i,t}^{AO} + w_{r,c,i,t}^{s,AV} \cdot L_{r,c,i,t}^{AV}) \geq \eta \cdot \bar{w}_r^s \quad (3.7)$$

²Here, total area is the total land area, not the modeled area.

where $\eta = 0.1$ represents the minimum required fraction of available surface water that must be utilized to prevent reductions in future allocations. Finally, total irrigation water use (from groundwater and surface water sources) must satisfy the water balance equation, ensuring that all applied water satisfies the irrigation requirements:

$$\begin{aligned} w_{r,c,i} &= w_{r,c,i,t}^{g,AO} + w_{r,c,i,t}^{s,AO} \\ w_{r,c,i}(1 - \rho_c) &= w_{r,c,i,t}^{g,AV} + w_{r,c,i,t}^{s,AV} \end{aligned} \quad (3.8)$$

where $w_{r,c,i,t}$ represents the total irrigation requirement per unit land in each region r for each crop c and irrigation level i . The parameter ρ_c captures the irrigation need reduction from AV systems due to lower evapotranspiration under solar panel shading.

In addition to physical constraints, this model also accounts for groundwater dynamics, recognizing that groundwater withdrawals impact future pumping costs and availability. Unlike surface water, which comes from rainfall and snowmelt and is considered exogenous, groundwater extraction influences the groundwater table level over time, affecting both pumping costs and long-term sustainability. The following equation demonstrates the evolution of the groundwater level affected by recharge and the volume of water pumped.

$$\begin{aligned} h_{r,t+1} &= h_{r,t} - \frac{R_{r,t} - \sum_{i,c} (w_{r,c,i,t}^{g,AO} + w_{r,c,i,t}^{s,AO})}{As^y}, \forall t > 0 \\ R_{r,t} &= \lambda_{conv} \cdot (\bar{w}_r^s - \sum_{i,c} w_{r,c,i,t}^s + PP_r) + \lambda_{perco} \sum_c (w_{r,c,i,t}^s + w_{r,c,i,t}^g) \end{aligned} \quad (3.9)$$

where $h_{r,t}$ is the depth to water in region r at time t , As^y represents the product of area and specific yield of the aquifer, which determines how groundwater levels respond to pumping and recharge. Recharges $R_{r,t}$ come from infiltration of surface water and deep percolation from applied irrigation. Surface water infiltration comes from the surface water remaining after irrigation withdrawal and precipitation PP_r . Parameter λ_{perco} represents percolation

rate, capturing how much applied irrigation seeps into the aquifer.

In addition to the physical constraints, the model also incorporates constraints to reflect economic feasibility and reality. Firstly, land-use transitions in agricultural and renewable energy are usually subject to irreversibility constraints. This reflects the long-term commitment to solar and agrivoltaic installations; once installed, the land cannot be reverted to agricultural production only due to high infrastructure costs and long-term lease agreements. This is enforced through the following constraints:

$$\begin{aligned} L_{r,t}^{\text{SO}} &\geq L_{r,t-1}^{\text{SO}} \\ \sum_i L_{r,c,i,t}^{\text{AV}} &\geq \sum_i L_{r,c,i,t-1}^{\text{AV}}, \forall t > 0 \end{aligned} \quad (3.10)$$

Certain crops, such as pistachios and walnuts, require long investment horizons and are highly sensitive to shading. As a result, these permanent crops are considered not eligible for AV integration, meaning they can only be grown under traditional agriculture (AO). This constraint is imposed as

$$L_{r,c,i,t}^{\text{AV}} = 0, \quad \forall c \in \text{permanent crops} \quad (3.11)$$

where permanent crops include all perennials with long establishment periods, ensuring that landowners do not allocate these crops to agrivoltaic systems.

To reflect practical land-use transition patterns in farming systems and prevent extreme fluctuations in crop allocation, the model enforces a crop mix stability constraint, which ensures that the total land dedicated to agriculture (AO and AV) remains within a reasonable range relative to its initial allocation:

$$(1 - \delta)L_{r,c} \leq \sum_i L_{r,c,i,t}^{\text{AO}} + \sum_i L_{r,c,i,t}^{\text{AV}} \leq (1 + \delta)L_{r,c} \quad (3.12)$$

Last but not least, the solar lease payment per acre yr-1 is modeled as a decreasing function of total land allocated to solar installations, reflecting diminishing marginal returns as landowners increase solar adoption. This constraint aims to capture market saturation effects and infrastructure constraints. For both utility-scale solar and agrivoltaics, with the saturation parameter, λ^{AV} , higher for agrivoltaics to account for its higher installment barrier. The solar lease payment functions are given by:

$$\begin{aligned}
 R_{r,t}^{SO} &= R_0^{SO} \cdot \left(1 - \lambda^{SO} \frac{L_{r,t}^{SO}}{L_r}\right) \\
 R_{r,t}^{AV} &= R_0^{AV} \cdot \left(1 - \lambda^{AV} \frac{\sum_{c,i} L_{r,c,i,t}^{AV}}{L_r}\right)
 \end{aligned}
 \tag{3.13}$$

3.4 Data

3.4.1 Data sources

This study leverages a diverse range of data spanning food, water, and energy systems. The Central Valley (AV) is divided into 26 sub-regions defined by the Central Valley Production Model (CVPM) to capture spatial heterogeneity in climate, hydrology, and agricultural practices. These regions cover the Sacramento Valley, Delta, San Joaquin Valley (North, Central, and South), and Tulare Basin. The spatial distribution of crops is derived from LandIQ, which provides high-resolution pixel data on farm locations and cropping patterns. The model includes eight major crops, collectively representing 25% of the total land in the Central Valley and 85% of the agricultural land. These crops consist of field crops such as alfalfa, corn, cotton, and rice; vineyard crops; nursery crops such as tomatoes; and tree nuts, including pistachios and walnuts. Figure 3.1 maps the spatial distribution of these crops, illustrating the proportion of land dedicated to each crop across CVPM subregions.

Agricultural economic data, including crop-specific prices, historical yields, and pro-

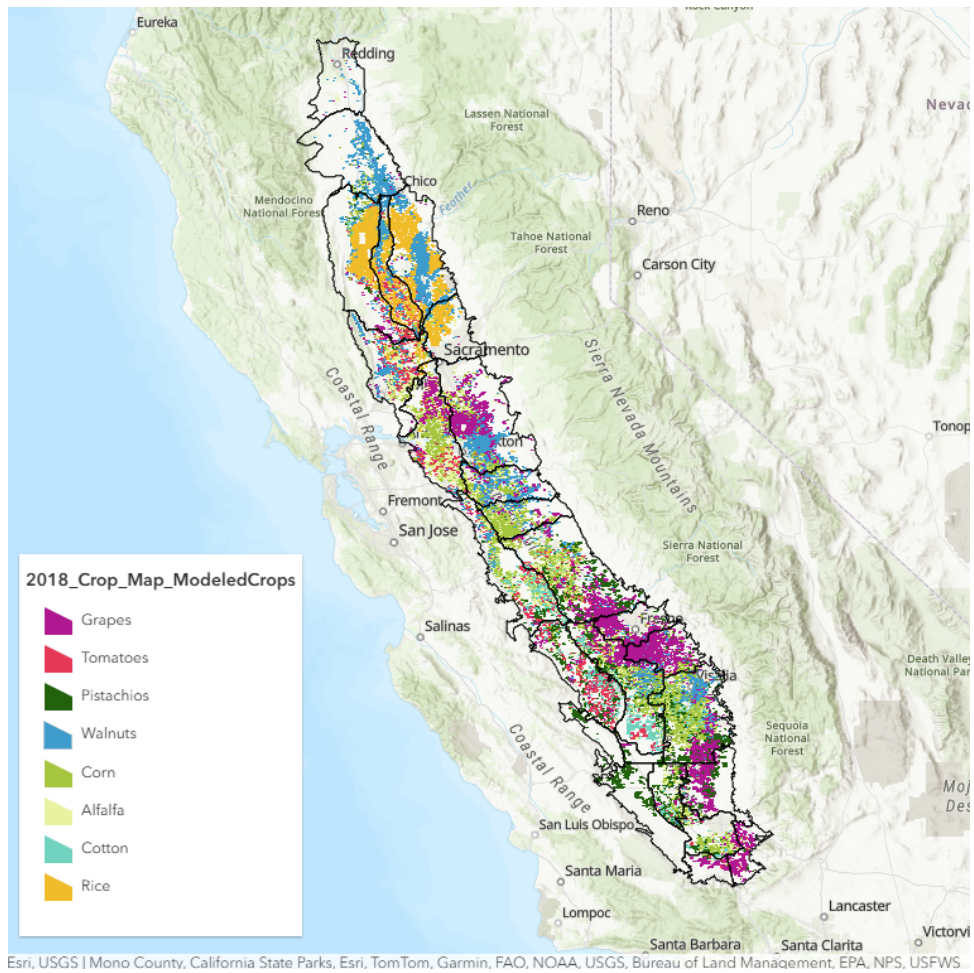


Figure 3.1: Modeled Crop Distribution in Central Valley

duction costs, are obtained from the USDA National Agricultural Statistics Service (NASS) and the UC Davis Cooperative Extension Cost and Returns Studies. The agrivoltaics parameters, including yield reduction, irrigation need reduction, and solar intensity, are from various field experiments. For alfalfa, estimates are derived from Weselek et al. (2021), while parameters for corn are based on Gupta et al. (2024). The effects on grapes are informed by field experiments performed in Italy (Ferrara et al. 2023), while rice parameters are obtained from the studies of Sojib Ahmed et al. (2022); Gonocruz et al. (2021). For tomatoes, the model relies on findings from Rabasoma et al. (2024) and Mohammedi et al. (2023).

Water availability is a critical parameter of the model, with both surface water and groundwater resources influencing land-use decisions. Surface water allocations are derived from the CALVIN model, accounting for reservoir releases and canal deliveries from the State Water Project (SWP) and the Central Valley Project (CVP). Data from the California DWR Well Completion Reports (WCR) provides groundwater level, ground surface level, and well depth data, which is extrapolated and averaged to each CVPM subregion. The surface water price data is derived from local water district records, while specific yield parameters used in groundwater dynamics are based on Williamson et al. (1989).

3.4.2 Linking Irrigation Demand to Yield Levels

Irrigation demands for each crop are calculated using reference evapotranspiration (ET_o), precipitation (PP) data from CVHM, and crop coefficient (K_c) following the FAO irrigation demand equation:

$$\text{irrigation demand}_{r,c} = \text{ET}_{o,r,c} \cdot \text{Kc}_c - \text{Pe}_{r,c} \quad (3.14)$$

where effective rainfall (Pe) is the fraction of precipitation available for plant use. Following FAO guidelines, effective rainfall is estimated using:

$$Pe = \begin{cases} 0.8 \times PP - 25, & \text{if } PP > 75\text{mm} \\ 0.6 \times PP - 10, & \text{if } PP \leq 75\text{mm} \end{cases} \quad (3.15)$$

where PP is monthly precipitation (mm). If $Kc = 0$, corresponding to non-growing periods, effective rainfall is set to zero to prevent overestimation. Yearly irrigation demand is then computed by summing over the water years to align with California's hydrological planning cycles.

Another innovation in this study is linking irrigation requirements with yield levels, allowing the model to capture the water productivity trade-offs in agricultural decision-making at the intensive production margin. To achieve this, historical yield data from USDA NASS is used to categorize yield distributions into four quantile-based levels ($Y_{c,i}$) representing different productivity scenarios: 25th percentile (Low), 50th percentile (Medium), 75th percentile (High), and 95th percentile (Potential). For each yield level, the corresponding irrigation demand is calculated using a non-linear response function:

$$w_{r,c,i} = \text{irrigation demand}_{r,c} \times \left(1 - \frac{1}{Kc_c} \times \left(1 - \frac{Y_{c,i}}{Y_c^p} \right) \right) \quad (3.16)$$

where $Y_{c,i}$ represents the observed yield level for crop c under irrigation level i , and Y_c^p is the potential yield (95th percentile). The irrigation levels $w_{r,c,i}$ are then used into the water balance equations (3.8), indicating the irrigation requirement for crop c in region r to reach the yield level corresponding to i . Figure 3.2 presents the distribution of irrigation requirements across CVPM regions for each crop and irrigation level.

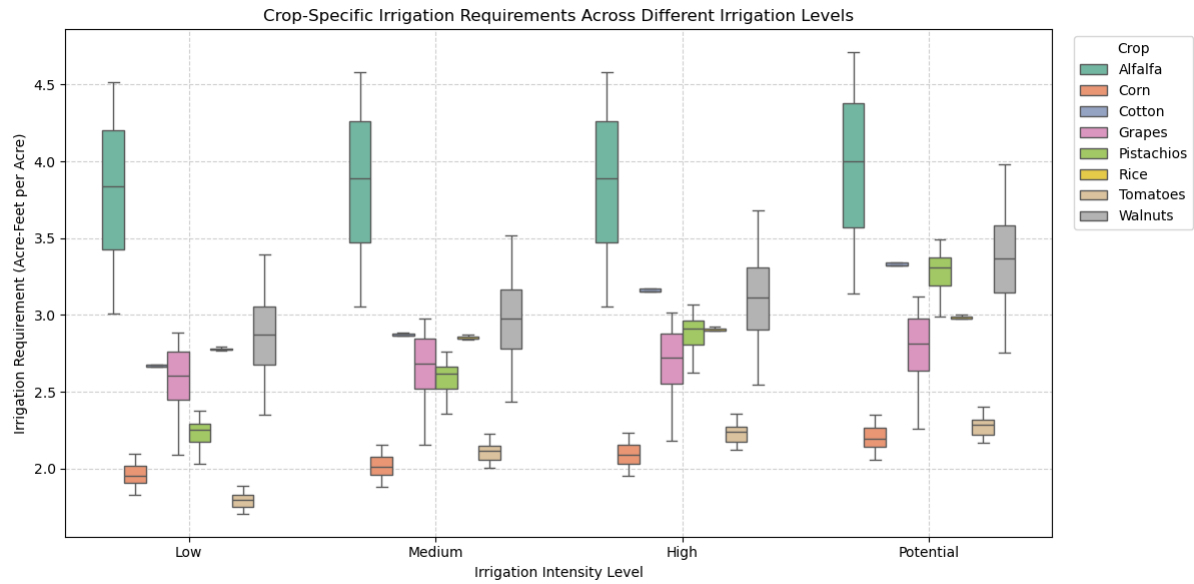


Figure 3.2: Crop-Specific Irrigation Requirements by Irrigation Intensity

3.5 Results

3.5.1 Baseline Land-Use scenarios

This section presents results from the baseline evaluation of three land-use scenarios in the Central Valley (CV) to assess how different approaches to agricultural and solar land allocation influence crop production, water use, and groundwater sustainability. The first scenario represents the status quo, where land is allocated solely to traditional agricultural production (S1: AO). In the second scenario, utility-scale solar developments (S2: AO+SO) are introduced, allowing a portion of agricultural land to be converted exclusively for energy production. The third scenario incorporates all three land uses (S3: AO+SO+AV), integrating agrivoltaic systems that enable the co-location of solar energy generation and crop cultivation.

Impact on Land-Use

We first analyze the shift in land allocation among traditional agricultural, utility-scale solar and agrivoltaics across the three scenarios. Figure 3.3 illustrates the land use by category over the 30-year simulation period for each scenario. In the status-quo scenario where land use is restricted to crop production, a substantial portion of land is left fallow over time, resulting in the highest proportion of fallowed land among the three scenarios. Introducing utility-scale solar (S2) reduces the amount of fallowed land, as some agricultural land transitions to solar energy production. By the end of the 30-year period, 12.4% of the total land is allocated to utility-scale solar. With the inclusion of agrivoltaic systems (S3), fallowed land is further reduced, with 7.6% of the total land allocated to utility-scale solar and 47.2% to agrivoltaics by the end of the simulation.

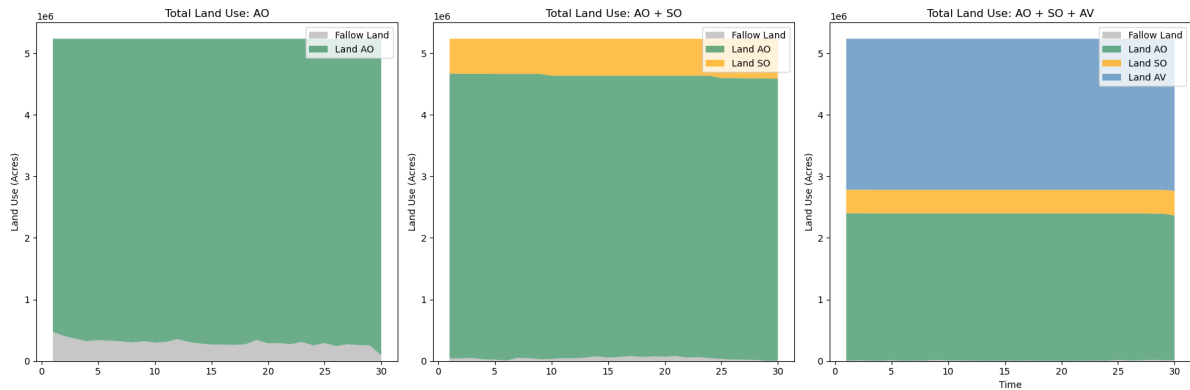


Figure 3.3: Impact of Solar and Agrivoltaics on Agricultural Land Use Over Time

Figure 3.4 compares land allocation across crops under three scenarios at the end of the 30-year simulation period. The status quo (S1) maintains the highest agricultural land use across all crops. Introducing utility-scale solar (S2) displaces significant acreage from water-intensive crops: walnuts, rice, and grapes experience the highest declines, reflecting

their vulnerability to land-use competition.

With the integration of agrivoltaics (S3), a substantial portion of agricultural land transitions to dual-use systems, with 94% of alfalfa, 98% of corn, 85% of cotton, and 82% of rice, 41% of grapes, and 27% of tomatoes land are allocated to AV. Field crops such as alfalfa, corn, rice, and cotton are the most likely to adopt AV, as they balance moderate economic returns with high compatibility under shade. In contrast, grapes exhibit lower AV adoption despite their high compatibility, likely due to their higher profitability under traditional agricultural practices. Nursery crops like tomatoes are among the less likely crops to transition to AV, reflecting their low shade tolerance.

Total agricultural land—including both AO and AV—remains lower under S3 than in S1 for most crops. However, unlike the transition from AO to AO+SO, which reduces total agricultural land, the integration of AV in S3 preserves more land for agricultural production. For all crops, total agricultural land—including both AO and AV—is higher under S3 than under S2, demonstrating that agrivoltaics helps mitigate the displacement of crop production caused by utility-scale solar expansion. Pistachios and walnuts do not have any AV adoption as they are permanent crops assumed to be incompatible with AV systems and thus remain fully dedicated to traditional agriculture.

Figure 3.5 presents the spatial distribution of land allocated to solar only (SO) and agrivoltaics (AV) across CVPM regions at time T. The left panel shows the acreage allocated to SO in the AO+SO scenario (S2), while the middle and right panels illustrate the land allocated to SO and AV, respectively, under S3. From figure 3.5, we can see that regions dominated by field crops, such as rice, corn, and alfalfa, allocated the largest shares of land to solar systems, particularly in CVPM regions 3, 4, 5, 9, 10, and 18. Regions dominated by vineyards, such as 8, 16, 17, and 21B, show minimal adoption of either SO or AV.

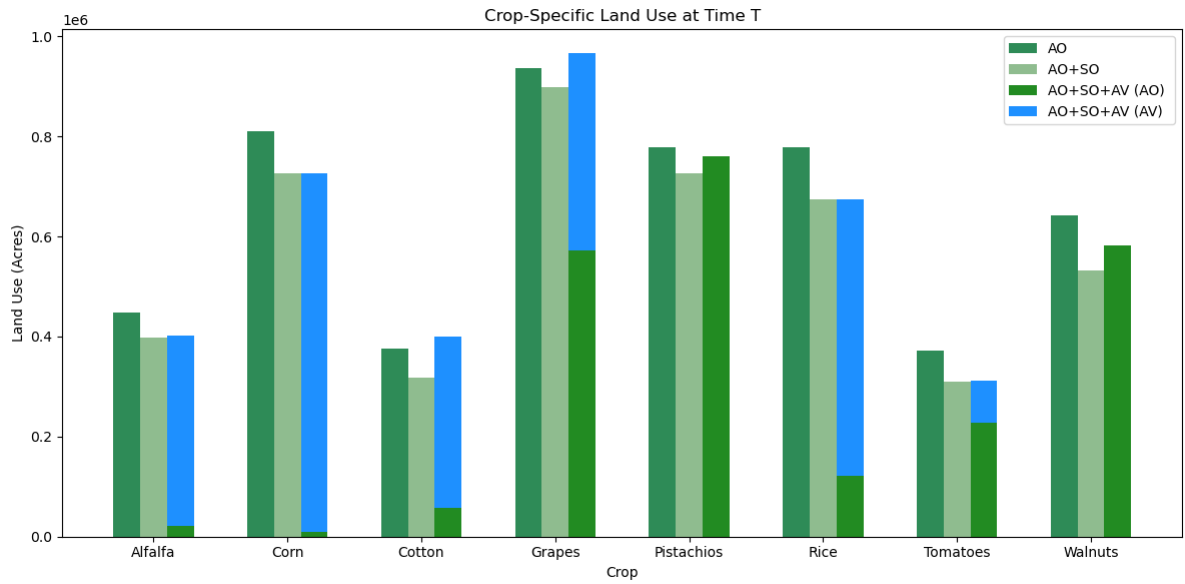


Figure 3.4: Crop-Specific Land Use Across Different Land-Use Scenarios

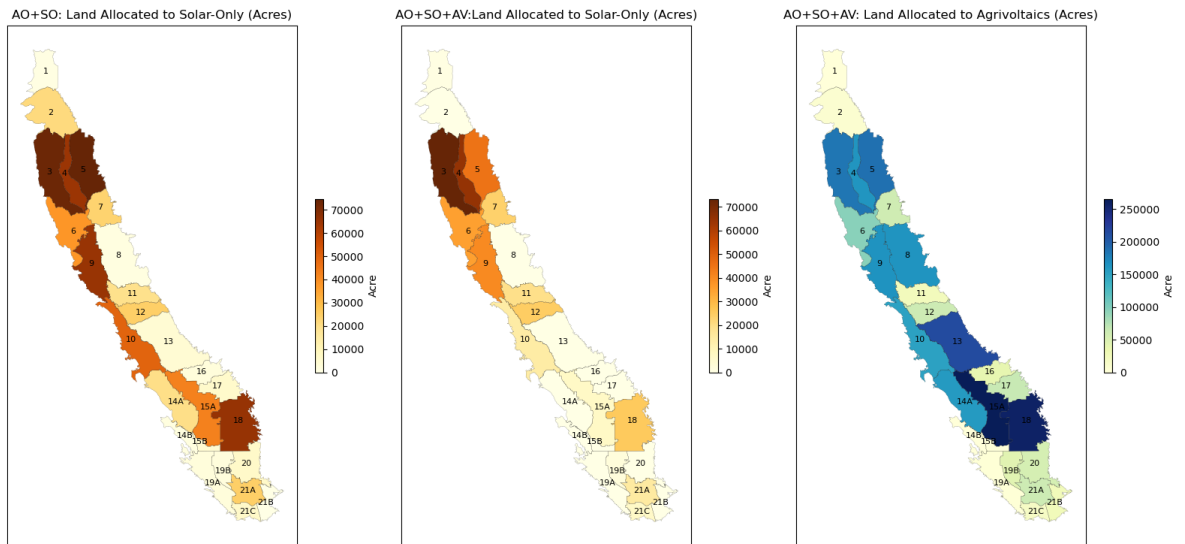


Figure 3.5: Regional allocation of land to solar-only (SO) and agrivoltaics (AV)

Impact on Water Use

Figure 3.6 illustrates the total groundwater and surface water use over the 30-year simulation for the three land-use scenarios. In the status quo scenario (S1), water use remains

stable, relying more than half on groundwater for agricultural irrigation. On the extensive margin, introducing utility-scale solar (S2) reduces total water use, primarily by decreasing agricultural land area. The reduction in total irrigated area results in a decline in total water use, with the majority coming from reduced surface water withdrawal. On the intensive margin, adding utility-scale solar decreases groundwater withdrawal by 5.4%, and surface water withdrawal by 14.4% on average.

The integration of agrivoltaics (S3) further decreases total water use, reinforcing reductions observed in the extensive margin. On the intensive margin, both groundwater and surface water use decreases, with surface water withdrawals decreasing by 9.6% and groundwater use dropping by 19.5% on average. These results indicate that agrivoltaics can not only maintain crop production but also contribute to greater water conservation compared to solar-only expansion.

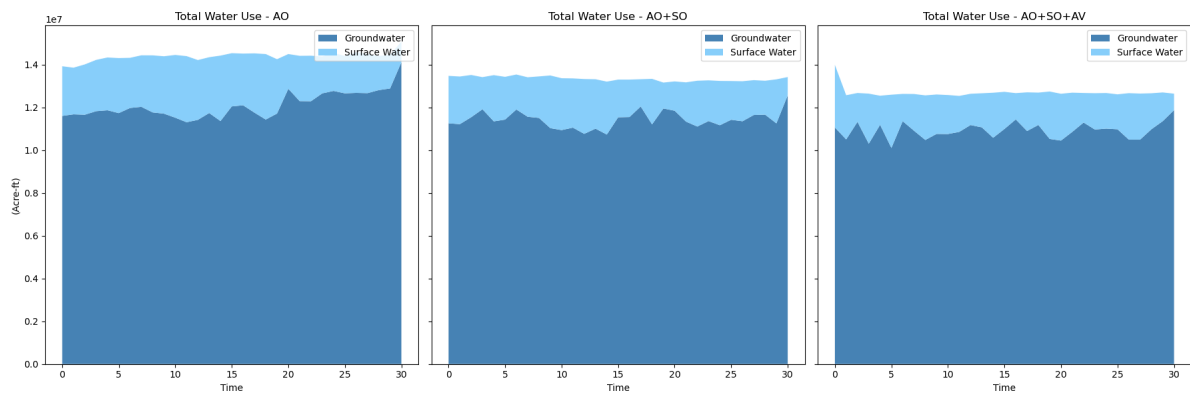


Figure 3.6: Water Use Over Time Under the Three Land-use Scenarios.

In addition to changes in total water use, the different land-use scenarios also influence irrigation strategies in terms of irrigation intensity levels. As discussed in section 3.4, the model drives endogenous decisions in irrigation levels across Low, Medium, High, and Potential. Figure 3.7 shows the distribution of land by irrigation intensity across scenarios.

Among all three scenarios, the largest share of agricultural land remains in the potential irrigation level, reflecting the economic preference for maximizing yields when water availability allows. However, the introduction of utility-scale solar in S2 reduces total irrigated acreage, with a noticeable shift toward medium and low irrigation levels. In contrast, agrivoltaics in S3 increases land allocated to high and potential irrigation intensities compared to S2. This shift occurs because agrivoltaic adoption allows landowners to continue farming while receiving additional solar revenue, making higher irrigation intensities more financially viable. Additionally, the reduction in evapotranspiration under agrivoltaic systems may encourage higher irrigation intensities, as the effective water use per acre is improved relative to traditional agriculture.

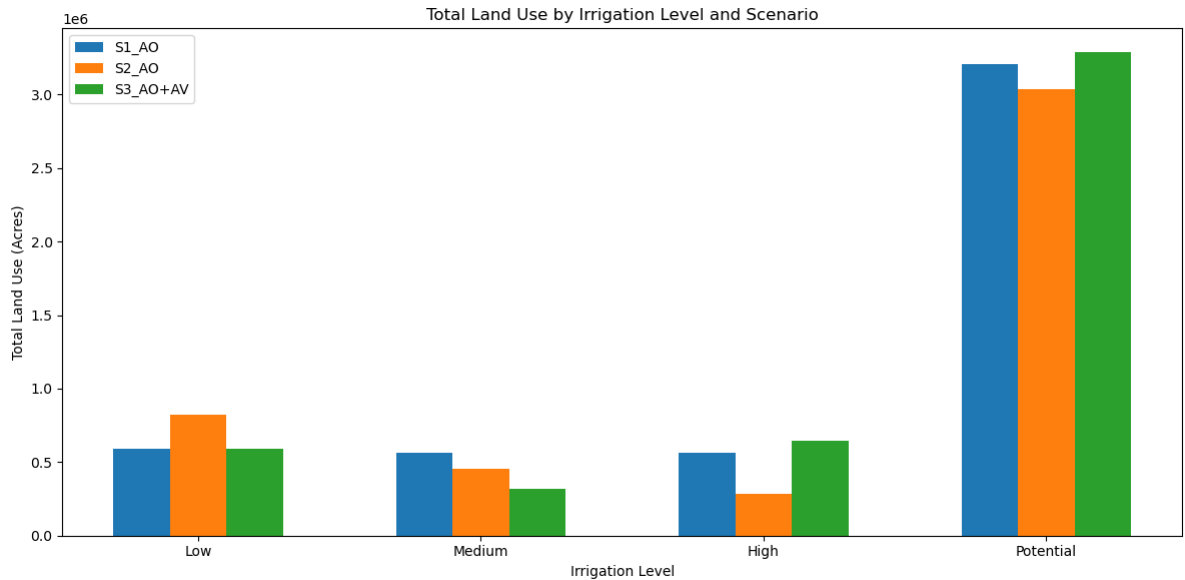


Figure 3.7: Agricultural Land By Irrigation Level.

Figure 3.8 presents the average yearly groundwater usage in each CVPM region under each scenario. In the status quo scenario (S1), regions 4, 5, 13, 15A, and 18 show higher groundwater use compared to others. This can be attributed to differing regional charac-

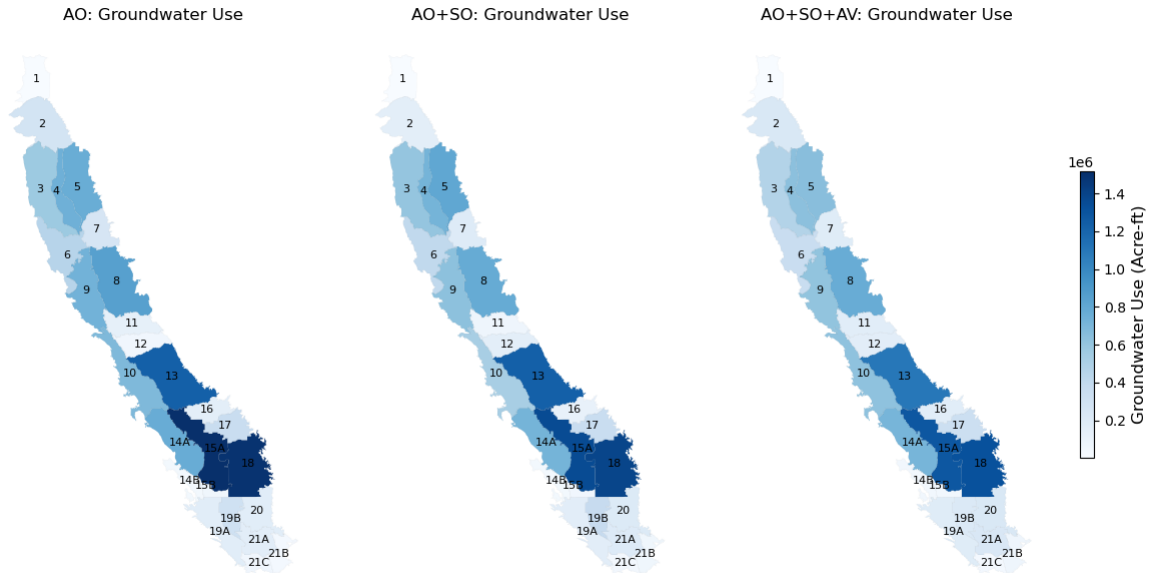


Figure 3.8: Yearly Groundwater Pumping Distribution Under Each Scenario

teristics: regions 4, and 5 allocate significant land to water-intensive crops such as rice and alfalfa. Meanwhile, regions 13 and 18, despite not being dominated by water-intensive crops, extract large amounts of groundwater due to limited surface water availability, as shown in Figure A.2b.

Comparing across land-use scenarios, introducing utility-scale solar (S2) reduces groundwater use in most regions, particularly those that historically rely on groundwater with limited surface water supplies. However, not all regions exhibit the same response. Groundwater pumping actually increases in regions 3, 5, 12, and the southern Delta regions 19B, 20, 21A, and 21B. These areas have higher surface water availability and experience less groundwater table decline in the baseline scenario, meaning that groundwater pumping has remained relatively inexpensive. The expansion of solar developments increases land rents in these regions, which in turn raises the profitability of agricultural production. With higher land values, groundwater pumping costs become a smaller proportion of total farm expenditures, making irrigation more viable despite its increasing intensity. Incorporating

agrivoltaics (S3) displays a similar pattern except for regions 3 and 5, where field crops are both common and compatible with AV adoption, and groundwater use declines as agrivoltaic systems lower irrigation requirements.

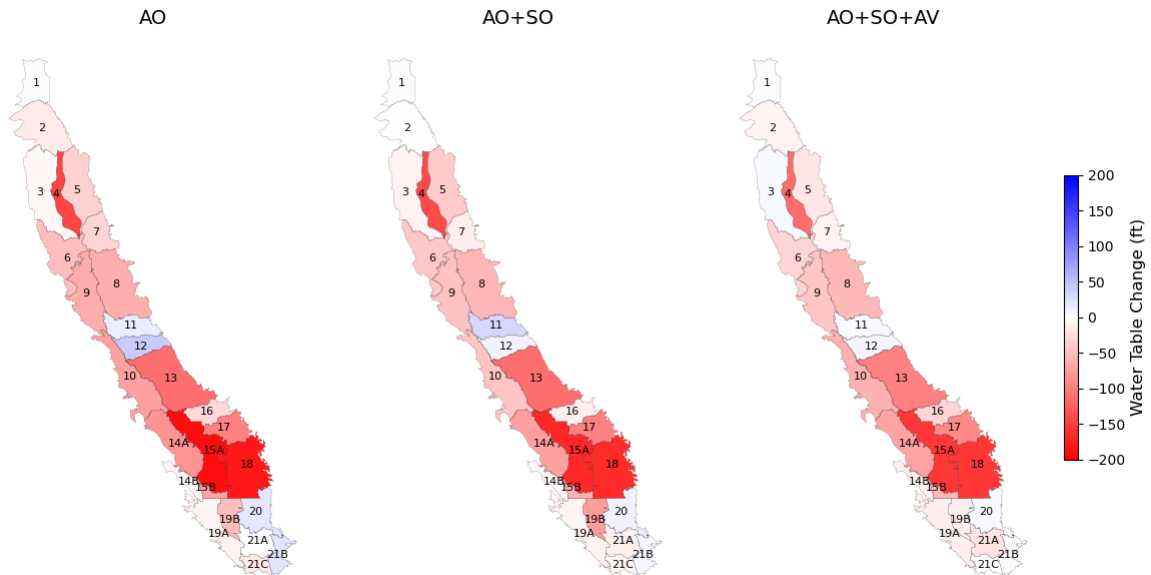


Figure 3.9: Regional Impact of Solar-Only and Agrivoltaics on Groundwater Level

Figure 3.9 compares changes in water table levels between the beginning and the end of the simulation period under each land-use scenario. Across all scenarios, most regions experience varying degrees of groundwater depletion, with regions 4, 15A, and 18 showing the most significant declines. These regions are particularly vulnerable due to their limited surface water resources, which exacerbate reliance on groundwater pumping. However, a few areas, notably regions 11, 12, and the southern Delta, exhibit stable or rising groundwater levels. These regions withdraw less groundwater overall and have greater access to surface water that recharges to the aquifer, allowing for slower rates of depletion or even net recharge over time.

Comparing S1 and S2, the introduction of utility-scale solar slows down groundwater

depletion in most areas, but worsens in regions 3, 5, 12, and the southern Delta. This pattern aligns with the earlier observation that these regions increase groundwater pumping under S2 despite overall reductions in total water use. Their abundant surface water supply that recharges to the aquifer, combined with increased land rents from solar expansion, appears to make groundwater pumping a more economically viable option, contributing to greater depletion despite the general conservation effect of solar adoption.

The introduction of agrivoltaics (S3) further reduces groundwater depletion in many regions, particularly in regions 3 and 5, where field crops are both common and highly compatible with AV adoption, which is consistent with the observation in groundwater withdrawals. We do still observe slightly more groundwater depletion in regions 11, 12, and the southern Delta. While this may initially seem concerning, it is not a major issue since these areas started with relatively low groundwater depletion in S1, meaning that even with higher withdrawals, their overall groundwater sustainability remains intact.

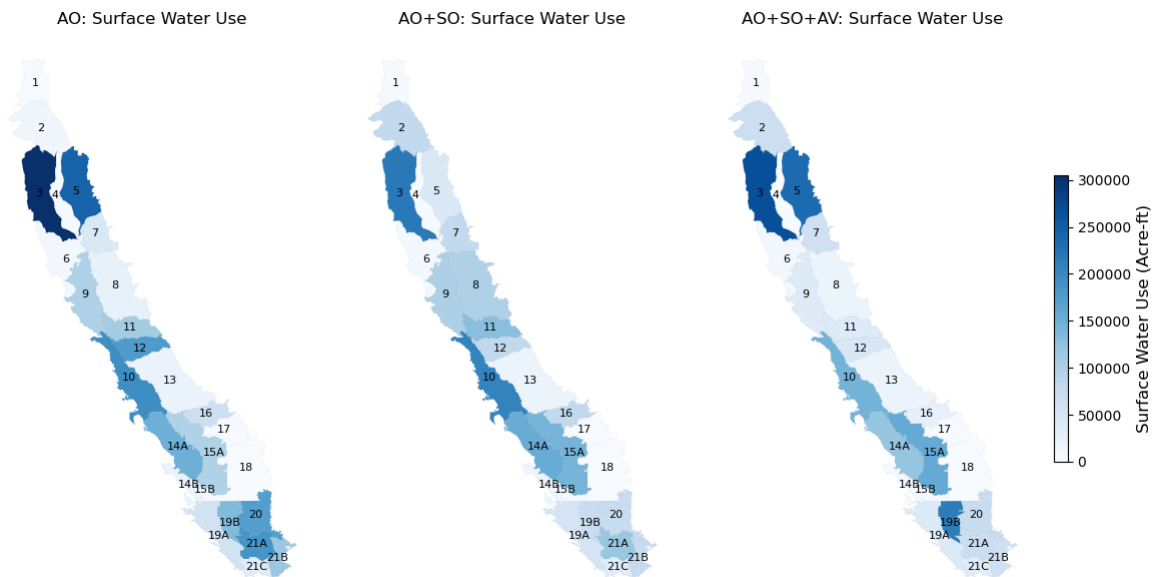


Figure 3.10: Yearly Surface Water Withdrawal Distribution Under Each Scenario

Figure 3.10 illustrates the spatial distribution of surface water use across scenarios. In S1, surface water withdrawals are highest in regions where surface water is abundant and where there are large acreage of water-intensive field crops. The introduction of utility-scale solar in S2 significantly reduces surface water use in these surface-water intensive regions, including 3, 5, 12, and regions in the southern Delta area. This shift mirrors the observed increase in groundwater pumping in these same regions, reinforcing the earlier observation that these regions substitute surface water withdrawals with increased groundwater pumping. Since groundwater pumping remains cost-effective in these areas due to stable groundwater levels, landowners can shift toward greater groundwater dependence. Under agrivoltaics (S3), we observe a more wide-range of decline in surface water withdrawals, as AV adoption lowers total irrigation requirements, particularly in regions where AV-compatible crops are grown.

Comparing the water use changes across CVPM regions, the spatial divergence suggests a regional water leakage effect, where reductions in surface water withdrawals and groundwater use in some regions are partially offset by increased groundwater dependence in others. Rather than achieving uniform water conservation across the Central Valley, reductions in water use in one area redistribute extraction pressures to other regions where groundwater remains a viable and accessible alternative.

NPV

Table 3.1 compares the net present values (NPV) of food, water and energy net benefits across the three land-use scenarios. The agricultural-only scenario (S1) generates the highest food income (\$194.1B), but this comes at a substantial water cost of -\$54.6B. Introducing solar infrastructure (S2) reduces food income by 5.6% (\$183.2B vs. \$194.1B) but generates \$10.0B in energy revenue, more than offsetting the decline in agricultural returns. Water cost in this scenario decreases slightly to -\$52.1B, suggesting the effect of reduced irrigated

land.

The integration of agrivoltaics (S3) further optimizes the balance between economic and resource sustainability. While food income declines compared to status quo (183.5 B), water costs decrease by 11% (-48.8 B vs. -54.6 B), demonstrating improved water efficiency under agrivoltaics. Despite a slight reduction in energy income compared with S2 (\$7.0B vs. \$10.0B), the total NPV under agrivoltaics is higher than that with only utility-scale solar. This suggests that agrivoltaics has the potential to mitigate the trade-offs associated with solar expansion by reducing water expenditures while maintaining agricultural productivity.

	Food Income (B\$)	Water Cost (B\$)	Energy Income (B\$)	Total NPV (B\$)
S1	194.1	-54.6	0	139.5
S2	183.2	-52.1	10.0	141.0
S3	183.5	-48.8	7.0	141.6

Table 3.1: Net Present Value (NPV) breakdown across land-use scenarios

3.5.2 Sensitivity and Policy Analysis

To evaluate how groundwater and energy policies impact land use decisions and groundwater conservation, we conduct sensitivity analysis on two sets of scenarios: 1) SGMA-induced groundwater restrictions, reducing extraction by 10% and 25% relative to baseline; (2) renewable energy policy scenarios that adjust solar lease rates from \$500 to \$2,500 per acre per year, reflecting variations in incentives or market conditions that influence the profitability of solar production for both utility-scale solar and agrivoltaics.

3.5.3 SGMA Restrictions

The Sustainable Groundwater Management Act (SGMA) mandates that each groundwater basin form a Groundwater Sustainability Agency (GSA) and implement a Groundwater Sustainability Plan (GSP) to achieve long-term aquifer stability. A key component of these plans is the imposition of pumping limits, which directly reduce the amount of groundwater available for agricultural use. These restrictions require landowners to adapt their land-use and water-use strategies.

Land Use Changes Under the traditional agriculture scenario (S1, see Figure A.6), due to the absence of alternative income sources, reduction of groundwater availability lead to an increase in fallow land. The more stringent the pumping limit is, the greater the fallowing will be, with the most significant reductions occurring in perennial crops such as grapes and pistachios. These high-value crops require consistent and reliable water supplies, making them particularly vulnerable to groundwater restrictions. As a result, landowners with limited flexibility in crop selection respond by idling land rather than shifting to lower-water-use crops.

However, when solar leasing is available as an alternative (S2, see Figure A.7), the relationship between groundwater restrictions and fallow land weakens significantly. Rather than leaving land fallow, landowners transition to leasing their land to adopt utility-scale solar. Under the most ambitious SGMA restriction, fallow land is nearly eliminated, suggesting that solar development provides a viable economic alternative when agricultural profitability declines due to groundwater constraints.

In S3 (see Figure A.8), where agrivoltaics is an option alongside traditional ground-mounted solar, the response to groundwater restrictions differs. As SGMA stringency increases, both agrivoltaics and SO expand, suggesting that landowners are more likely to integrate solar with continued agricultural production when faced with water constraints.

Nevertheless, under the highest SGMA restriction, fallow land still increases slightly, though to a much smaller extent than in S1. This residual increase suggests that while agrivoltaics can serve as a partial substitute for traditional farming, it is not universally viable, depending on the compatibility of the crop.

Groundwater Conservation In addition to SGMA's impact on land-use changes, we also evaluate how SGMA impacts groundwater sustainability. Figure A.9 to A.11 illustrate the effects of SGMA on groundwater depletion, where positive values indicate a reduction in depletion (shown in blue). These results highlight how groundwater policies impact different regions differently under each land use scenario.

In S1 (Figure A.9), SGMA policies alleviate groundwater depletion in regions where baseline depletion is most severe. The more ambitious SGMA policy improves groundwater levels across all regions, suggesting that stricter pumping limits are effective in slowing depletion. However, the degree of improvement varies, with some areas benefiting more than others depending on their initial groundwater stress.

In S2, where utility-scale solar is an option, the effects of SGMA on groundwater are more spatially differentiated. In areas where surface water is scarce, both the 10% and 25% groundwater reduction policies successfully mitigate depletion. However, in regions where surface water is abundant, groundwater depletion intensifies compared to baseline. This pattern aligns with the water leakage effect observed in the baseline scenario, where groundwater withdrawal increases as solar income increases land rent, and as land set-asides for SO and AV shift regional crop mix strategies and groundwater use intensity in some models.

In S3, where SGMA restrictions are combined with agrivoltaics, the improvement in groundwater depletion is most significant. The combined effect of reduced pumping and agrivoltaic-driven water savings leads to a more widespread and sustained groundwater

conservation.

3.5.4 Solar Lease Rate

To assess the sensitivity of land use and groundwater responses to the solar lease rate, we examine scenarios with lower (\$500/acre) and higher (\$2500/acre) solar rents. Since S1 does not include solar leasing as an option, the analysis focuses on S2 and S3 (See Figures A.12 to A.15). The goal is to determine how variations in solar lease rates influence land allocation and groundwater depletion differently under these scenarios.

Unlike SGMA restrictions, which directly limit groundwater use, changes in the solar lease rate introduce different economic incentives for different regions. In S2, a lower solar lease rate leads to an increase in fallow land, as landowners are less willing to transition away from agriculture at a lower leasing price and would rather fallow their land. Conversely, a higher solar lease rate reduces fallow land as more land is allocated to solar. However, while solar adoption is lower under the low-rent scenario, it does not increase proportionally under the high-rent scenario due to our solar expansion constraint, which assumes diminishing lease rates as solar adoption expands. Despite this limitation, compared to the low-rent scenario, the high-rent scenario still shifts more agricultural land into solar under the baseline.

These land-use changes also translate into different groundwater outcomes. The low solar lease rate scenario results in higher groundwater depletion, as fewer landowners opt for solar, and more land remains in water-intensive agriculture. In contrast, when solar lease rates are higher (baseline), groundwater depletion improves as a greater share of land shifts from agriculture to solar leasing, reducing irrigation demand. This suggests that increasing financial incentives for solar leasing can complement groundwater conservation efforts, particularly in water-scarce regions.

In S3, where SGMA restrictions interact with agrivoltaics, the effects of a low solar lease rate are similar to those observed in S2. As the solar lease rate increases, more land transitions into solar leasing and agrivoltaics. However, due to the solar expansion constraint, we do not compare the high solar lease rate scenario, as the model already imposes diminishing solar rents when adoption expands beyond a certain threshold. Nonetheless, the results indicate that agrivoltaics and solar leasing respond similarly to variations in lease rates, reinforcing the role of economic incentives in shaping land use transitions.

3.5.5 Economic Impact

While the previous sections examine how SGMA restrictions and solar lease rates impact land use and groundwater withdrawals, an important economic question is whether the inclusion of solar and agrivoltaics reduces the overall compliance costs associated with groundwater conservation. Table 3.2 reports the percentage changes in total NPV relative to the baseline AO scenario (S1), comparing the economic outcomes (producer surplus) across policy and market conditions. The results indicate that under SGMA policies alone

	baseline	sgma10	sgma25	solarlow	solarhigh
S1 (AO)	0.0%	-1.1%	-20.3%	-	-
S2 (AO+SO)	+1.0%	-2.8%	-4.9%	+3.2%	+4.5%
S3 (AO+SO+AV)	+1.5%	+1.3%	-6.9%	-3.3%	-0.3%

Table 3.2: Percentage Change in Total NPV Relative to Status-quo

(sgma10 and sgma25), the economic losses are most under the status-quo scenario (S1), with NPV declining by 1.1% under the 10% reduction scenario and 20.3% under a 25% reduction in groundwater use. However, when solar and agrivoltaics are introduced, even under the same groundwater restriction, the losses are moderated. Particularly under the

ambitious SGMA scenario, the NPV loss in S1 is substantially larger than in S2 (-4.9%) and S3 (-6.9%), demonstrating that incorporating solar-based land-use changes reduces the economic burden of groundwater conservation.

This pattern suggests that allowing for solar land-use transitions—whether through utility-scale solar or agrivoltaics— reduces compliance costs for SGMA by providing alternative income sources that offset agricultural losses. Notably, S3 performs better than S2 under mild SGMA restrictions (SGMA-10), actually increasing total NPV by 1.3% relative to S1. However, under more severe groundwater constraints (SGMA-25), agrivoltaic adoption does not fully offset economic losses, though it still performs better than agriculture-only land use.

Under solar price sensitivity scenarios (solarlow and solarhigh), the results indicate that higher solar lease payments increase total NPV, while lower payments reduce its attractiveness. In S2, high solar lease payments (+4.5% NPV) significantly outperform low payments (+3.2%), reinforcing the role of economic incentives in shaping land-use decisions. Interestingly, S3 exhibits a negative NPV change under low solar lease payments (-3.32%), suggesting that agrivoltaic adoption is less viable when solar incentives are weak.

3.6 Discussion

3.6.1 Key Findings

From the simulation results and sensitivity analysis, this study highlights the potential for agrivoltaics to serve as a sustainable land-use strategy that balances food production, water conservation, and renewable energy expansion in California's Central Valley. The model outcomes illustrate how agrivoltaic adoption influences groundwater use, land allocation, and economic returns under different policy and market conditions. By comparing scenar-

ios with and without utility-scale solar and further agrivoltaics, the findings provide insight into the extent to which dual-use solar systems can mitigate groundwater depletion, reduce land retirement, and support agricultural resilience under SGMA-imposed constraints.

First, agrivoltaics demonstrates its potential to mitigate groundwater depletion while maintaining agricultural productivity. By reducing crop evapotranspiration through shading, agrivoltaics lowers overall irrigation demand, easing the pressure on groundwater resources in the Central Valley. The model results indicate that agrivoltaic adoption leads to significant reductions in both groundwater and surface water withdrawals compared to traditional agriculture without forcing large-scale reductions in cultivated land.

Beyond groundwater conservation, agrivoltaics also plays a role in stabilizing food production by moderating land retirement under groundwater constraints. As SGMA regulations limit groundwater withdrawals, many landowners in a traditional agricultural setting are left with few options other than fallowing land, particularly when surface water allocations are insufficient to compensate for reduced pumping. The introduction of agrivoltaics, however, provides an alternative land-use strategy that allows for continued food production while reducing water needs. The model shows that in scenarios with agrivoltaic adoption, landowners are less likely to idle land and instead transition toward dual-use systems that preserve agricultural output while generating additional revenue from solar leasing.

However, the impact of agrivoltaics is not uniform across the Central Valley. By comparing the results across different sub-regions in the Central Valley, we find that water conservation benefits vary significantly across regions, revealing a form of water leakage. In some areas, reductions in groundwater pumping are offset by increases elsewhere, as landowners in regions with relatively stable groundwater levels shift toward higher withdrawal rates. This occurs particularly in regions where solar adoption raises land rents, making intensified agriculture more attractive despite increasing water costs.

SGMA policies themselves introduce further complexity. The model suggests that while SGMA restrictions effectively reduce groundwater withdrawals in critically overdrafted regions, they also create economic pressures that push landowners toward either idling land or transitioning to non-agricultural land uses. When agrivoltaics is included as an option, these pressures are alleviated to some extent, but the extent of adoption depends on economic factors such as solar lease rates and crop compatibility. The results underscore the importance of aligning groundwater regulations with economic incentives to encourage agrivoltaic adoption in a way that balances conservation goals with agricultural sustainability.

3.6.2 Limitation

While this study provides valuable insights into the potential of agrivoltaics for groundwater sustainability, several limitations should be acknowledged. First, the model does not account for inter-regional water trading, horizontal groundwater flow, or water transfers. Groundwater is treated as a confined resource, meaning that withdrawals and recharge within each modeled region affect only that region and do not induce lateral movement of water. In reality, aquifer systems in the Central Valley are interconnected, and changes in one region may have spillover effects on groundwater availability elsewhere. Future work incorporating hydrological linkages between regions would improve the accuracy of projected groundwater conservation outcomes.

Second, the modeled area in this model represents only a subset of the Central Valley, meaning that groundwater depletion may still depend on other activities occurring on the same land but outside the model's coverage. For example, if neighboring regions increase groundwater extraction due to policies favoring agricultural intensification, the benefits of agrivoltaic-induced conservation may be diminished. Expanding the model's geographic

scope to include a more comprehensive representation of regional water use would provide a clearer picture of the aggregate effects of AV adoption.

Third, while the model includes a crop price growth assumption to reflect increasing global food demand, market dynamics are otherwise treated as exogenous. Factors such as fluctuations in crop prices, carbon pricing policies, and shifts in energy market incentives are not explicitly modeled but could significantly influence adoption rates.

Fourth, we do not connect to a regional energy sector model that reflects solar distribution costs and electricity demand in the region, thus yielding an overly-optimistic outlook for SO and AV adoption potential. We do not add additional constraints on solar adoption by design – our results should be interpreted as an overly optimistic outlook for solar area expansion in the region, which allows us to explore regional groundwater implications from extremely ambitious regional solar generation capacity expansion.

Lastly, the study does not include environmental benefits—such as carbon sequestration, biodiversity conservation, or air quality improvements—as a form of externality. While AV adoption likely reduces carbon emissions by displacing fossil-fuel-based electricity generation and may enhance ecosystem services through reduced land conversion, these co-benefits are not monetized in the model. Future research that integrates environmental valuation methods could provide a more comprehensive assessment of agrivoltaics' broader societal impacts.

3.7 Conclusion

This study evaluates the potential for agrivoltaics to balance food, water, and energy objectives in California's Central Valley, addressing key research questions about groundwater sustainability, land-use trade-offs, and policy interventions. The findings suggest that agrivoltaics can serve as a viable strategy for achieving groundwater conservation while

preserving agricultural productivity, particularly under SGMA-imposed constraints. By lowering irrigation demand and providing an additional revenue source, agrivoltaics offers an alternative to land fallowing and mitigates economic disruptions caused by groundwater restrictions.

Compared to traditional agriculture and utility-scale solar, agrivoltaics reduces groundwater withdrawals, slows depletion in overextracted regions, and allows landowners to maintain crop production rather than retiring farmland. Unlike utility-scale solar only, which displaces agriculture, agrivoltaics enables dual land use, preserving food production while expanding renewable energy. The economic diversification it provides makes farming less dependent on water availability, helping landowners adapt to increasing regulatory and environmental pressures.

This study contributes to the literature by incorporating agrivoltaics into a regional dynamic-hydroeconomic model, linking land-use decisions to groundwater sustainability under SGMA. Previous research has focused on farm-level feasibility, but this analysis extends the scope to evaluate large-scale hydrological and economic impacts. By integrating agrivoltaics into a land-use optimization framework, this study highlights its potential role in mitigating groundwater depletion while balancing agricultural and energy needs.

Future research should incorporate inter-regional groundwater transfers and market-driven water allocation mechanisms to assess the broader hydrological effects of agrivoltaics. Modeling endogenous crop price responses and integrating environmental co-benefits, such as carbon sequestration and soil conservation, would provide a more comprehensive evaluation of its sustainability potential. Empirical validation through field studies could refine model assumptions and improve understanding of adoption barriers. Addressing these gaps will strengthen the case for agrivoltaics as a scalable strategy for balancing food security, groundwater sustainability, and renewable energy development in water-scarce regions.

Another important direction is to explore an on-farm agrivoltaics adoption model, where farmers invest in AV systems rather than lease land to external solar developers. Under this assumption, landowners would bear installation costs but gain access to on-site electricity generation, which could be sold back to the grid or used to power groundwater pumps. If electricity costs for pumping decrease significantly, the incentives to conserve groundwater may be weakened, potentially altering land-use and water-use decisions. Future work should evaluate how this alternative investment model influences groundwater extraction behavior, profitability, and adoption dynamics under SGMA constraints.

REFERENCES

- Abadie, A., Diamond, A., Hainmueller, and Jens (2010). Synthetic control methods for comparative case studies: Estimating the effect of California's Tobacco control program. *Journal of the American Statistical Association*, 105(490):493–505.
- Abadie, A., Diamond, A., and Hainmueller, J. (2015). Comparative Politics and the Synthetic Control Method. *American Journal of Political Science*, 59(2):495–510.
- Adelaja, A., Hailu, Y. G., McKeown, C. H., and Tekle, A. T. (2010). Effects of renewable energy policies on wind industry development in the US. *Journal of Natural Resources Policy Research*, 2(3):245–262.
- Al-Agele, H. A., Proctor, K., Murthy, G., and Higgins, C. (2021). A case study of tomato (*Solanum lycopersicon* var. legend) production and water productivity in agrivoltaic systems. *Sustainability (Switzerland)*, 13(5):1–13.
- Alam, H., Alam, M. A., and Butt, N. Z. (2023). Techno Economic Modeling for Agrivoltaics: Can Agrivoltaics Be More Profitable Than Ground Mounted PV? *IEEE Journal of Photovoltaics*, 13(1):174–186.
- Alam, S., Gebremichael, M., Li, R., Dozier, J., and Lettenmaier, D. P. (2019). Climate change impacts on groundwater storage in the Central Valley, California. *Climatic Change*, 157(3-4):387–406.
- Ali Abaker Omer, A., Liu, W., Li, M., Zheng, J., Zhang, F., Zhang, X., Osman Hamid Mohammed, S., Fan, L., Liu, Z., Chen, F., Chen, Y., and Ingenhoff, J. (2022). Water evaporation reduction by the agrivoltaic systems development. *Solar Energy*, 247:13–23.
- Allen, R. G. (2000). *Crop evapotranspiration : guidelines for computing crop water requirements*. FA.O.
- Baker, J. S., Crouch, A., Cai, Y., Latta, G., Ohrel, S., Jones, J., and Latané, A. (2018). Logging Residue Supply and Costs for Electricity Generation: Potential Variability and Policy Considerations. *Energy Policy*, 116:397–409.
- Baker, J. S., Wade, C. M., Sohngen, B. L., Ohrel, S., and Fawcett, A. A. (2019). Potential complementarity between forest carbon sequestration incentives and biomass energy expansion. *Energy Policy*, 126:391–401.
- Bangjun, W., Feng, Z., Feng, J., Yu, P., and Cui, L. (2022). Decision making on investments in photovoltaic power generation projects based on renewable portfolio standard: Perspective of real option. *Renewable Energy*, 189:1033–1045.

- Barbose, G., Bird, L., Heeter, J., Flores-Espino, F., and Wiser, R. (2015). Costs and benefits of renewables portfolio standards in the United States.
- Barnes, J. (2012). RPS Update: 2012's Compliance Modifications, Progress and Prognostications. Technical report, Database of State Incentives for Renewables and Efficiency (DSIRE).
- Barnes, R. (2014). Energy Sovereignty in Marine Spaces. *The International Journal of Marine and Coastal Law*, 29(4):573 – 599.
- Barron-Gafford, G. A., Pavao-Zuckerman, M. A., Minor, R. L., Sutter, L. F., Barnett-Moreno, I., Blackett, D. T., Thompson, M., Dimond, K., Gerlak, A. K., Nabhan, G. P., and Macknick, J. E. (2019). Agrivoltaics provide mutual benefits across the food–energy–water nexus in drylands. *Nature Sustainability*, 2(9):848–855.
- Bhandari, S. N., Schlüter, S., Kuckshinrichs, W., Schlör, H., Adamou, R., and Bhandari, R. (2021). Economic feasibility of agrivoltaic systems in food-energy nexus context: Modelling and a case study in niger. *Agronomy*, 11(10).
- Brush, C. F., Dogrul, E. C., and Kadir, T. N. (2013). Development and Calibration of the California Central Valley Groundwater-Surface Water Simulation Model (C2VSim), Version 3.02-CG DWR Technical Memorandum. Technical report.
- Bryant, B. P., Kelsey, T. R., Vogl, A. L., Wolny, S. A., MacEwan, D., Selmants, P. C., Biswas, T., and Butterfield, H. S. (2020). Shaping Land Use Change and Ecosystem Restoration in a Water-Stressed Agricultural Landscape to Achieve Multiple Benefits. *Frontiers in Sustainable Food Systems*, 4(August):1–15.
- Buckley Biggs, N., Shivaram, R., Acuña Lacarieri, E., Varkey, K., Hagan, D., Young, H., and Lambin, E. F. (2022). Landowner decisions regarding utility-scale solar energy on working lands: A qualitative case study in California. *Environmental Research Communications*, 4(5).
- Buckman, G. (2011). The effectiveness of Renewable Portfolio Standard banding and carve-outs in supporting high-cost types of renewable electricity. *Energy Policy*, 39(7):4105–4114.
- Carley, S. (2009). State renewable energy electricity policies: An empirical evaluation of effectiveness. *Energy Policy*, 37(8):3071–3081.
- Carley, S., Davies, L. L., Spence, D. B., and Ziropiannis, N. (2018). Empirical evaluation of the stringency and design of renewable portfolio standards. *Nature Energy*, 3(9):754–763.
- Closas, A. and Rap, E. (2017). Solar-based groundwater pumping for irrigation: Sustainability, policies, and limitations. *Energy Policy*, 104:33–37.

- Das, A. and Datta, B. (2001). Application of optimisation techniques in groundwater quantity and quality management. Technical report.
- Dinesh, H. and Pearce, J. M. (2016). The potential of agrivoltaic systems.
- Dixit, A. and Pindyck, R. (1994). *Investment under Uncertainty*. Princeton University Press, 1 edition.
- Draper, A. J., Jenkins, M. W., Kenneth, ., Kirby, W., Lund, J. R., and Howitt, R. E. (2003). Economic-Engineering Optimization for California Water Management. *Journal of Water Resources Planning and Management*, 129(3):151–244.
- DSIRE (2022). Database of State Incentives for Renewables & Efficiency (DSIRE).
- Dupraz, C., Marrou, H., Talbot, G., Dufour, L., Nogier, A., and Ferard, Y. (2011). Combining solar photovoltaic panels and food crops for optimising land use: Towards new agrivoltaic schemes. *Renewable Energy*, 36(10):2725–2732.
- EIA 923 (2022). EIA-923 Monthly Generation and Fuel Consumption Time Series Data.
- El Mahdi BENTALEB, M., Jalal ADNANI, M. E., and Zahra BENTALEB, F. (2024). Economic and Environmental Implications of Solar Photovoltaic Pumping Systems in Agri-Water Management: A Case Study of Marrakesh Orchards. *Finance, Auditing, Management and Economics*, 5(10):88–109.
- Elamri, Y., Cheviron, B., Lopez, J. M., Dejean, C., and Belaud, G. (2018). Water budget and crop modelling for agrivoltaic systems: Application to irrigated lettuces. *Agricultural Water Management*, 208:440–453.
- EPA (2015). Energy and Environment Guide to Action: State Policies and Best Practices for Advancing Energy Efficiency, Renewable Energy, and Combined Heat and Power. Technical report, Environmental Protection Agency.
- EPA (2017). Green Power Partnership: U.S. Electricity Grid & Markets. Technical report, Environmental Protection Agency.
- Escriva-Bou, A., Hanak, E., Cole, S., and Medellín-Azuara, J. (2023). The Future of Agriculture in the San Joaquin Valley. *Technical Appendix*.
- Faunt, C. C. (2009). *Groundwater availability of the Central Valley Aquifer, California*. U.S. Geological Survey.
- Favero, A., Mendelsohn, R., and Sohngen, B. (2017). Using forests for climate mitigation: sequester carbon or produce woody biomass? *Climatic Change*, 144(2):195–206.

- Fernández-Solas, , Fernández-Ocaña, A. M., Almonacid, F, and Fernández, E. F. (2023). Potential of agrivoltaics systems into olive groves in the Mediterranean region. *Applied Energy*, 352.
- Ferrara, G., Boselli, M., Palasciano, M., and Mazzeo, A. (2023). Effect of shading determined by photovoltaic panels installed above the vines on the performance of cv. Corvina (*Vitis vinifera* L.). *Scientia Horticulturae*, 308:111595.
- Fischlein, M. and Smith, T. M. (2013). Revisiting renewable portfolio standard effectiveness: policy design and outcome specification matter. *Policy Sciences*, 46(3):277–310.
- Fytily, D. and Zabaniotou, A. (2017). Social acceptance of bioenergy in the context of climate change and sustainability—A review. *Current opinion in green and sustainable chemistry*, 8:5–9.
- Galik, C. S. (2020). A continuing need to revisit BECCS and its potential. *Nature Climate Change*, 10(1):2–3.
- Gonocruz, R. A., Nakamura, R., Yoshino, K., Homma, M., Doi, T., Yoshida, Y., and Tani, A. (2021). Analysis of the rice yield under an agrivoltaic system: A case study in Japan. *Environments - MDPI*, 8(7).
- Gupta, V., Gruss, S. M., Cammarano, D., Brouder, S. M., Bermel, P. A., Tuinstra, M. R., Gitau, M. W., and Agrawal, R. (2024). Optimizing corn agrivoltaic farming through farm-scale experimentation and modeling. *Cell Reports Sustainability*, 1(7):100148.
- Hanak, E., Escriva-Bou, A., Gray, B., Green, S., Harter, T., Jezdimirovic, J., Lund, J., Medellín-Azuara, J., Moyle, P., and Seavy, N. (2019). Water and the Future of the San Joaquin Valley. Technical report.
- Hays, A. and Baker, J. S. (2023). Water management and agricultural land use change could exacerbate food insecurity in California's Central Valley.
- Hillard, M. (2021). Industrial shredding: The rise and fall of Maine's mighty paper industry. *LERA For Libraries*.
- Horowitz, K., Ramasamy, V., Macknick, J., and Margolis, R. (2020). Capital Costs for Dual-Use Photovoltaic Installations : 2020 Benchmark for Ground-Mounted PV Systems with Pollinator-Friendly Vegetation, Grazing, and Crops. Technical report.
- Howitt, R. E., Macewan, D., Medellín-Azuara, J., and Lund, J. R. (2009). ECONOMIC MODELING OF AGRICULTURE AND WATER IN CALIFORNIA USING THE STATEWIDE AGRICULTURAL PRODUCTION MODEL A Report for the California Department of Water Resources Topic: Data and Analytic Tools Economic Modeling of Agriculture and Water in California Using the Statewide Agricultural Production Model. Technical report.

- Insley, M. (2002). A Real Options Approach to the Valuation of a Forestry Investment. *Journal of Environmental Economics and Management*, 44.
- IPCC (2014). *Climate Change 2014: Synthesis Report. Contribution of Working Groups I, II and III to the Fifth Assessment Report of the Intergovernmental Panel on Climate Change*. IPCC, Geneva, Switzerland.
- Irie, N., Kawahara, N., and Esteves, A. M. (2019). Sector-wide social impact scoping of agrivoltaic systems: A case study in Japan. *Renewable Energy*, 139:1463–1476.
- Jones-Albertus, R., Cole, W., Denholm, P., Feldman, D., Woodhouse, M., and Margolis, R. (2018). Solar on the rise: How cost declines and grid integration shape solar's growth potential in the United States. *MRS Energy & Sustainability*, 5:E4.
- Joshi, J. (2021). Do renewable portfolio standards increase renewable energy capacity? Evidence from the United States. *Journal of Environmental Management*, 287:112261.
- Ketzer, D., Schlyter, P., Weinberger, N., and Rösch, C. (2020). Driving and restraining forces for the implementation of the Agrophotovoltaics system technology – A system dynamics analysis. *Journal of Environmental Management*, 270(May).
- Khanna, M. and Zilberman, D. (2017). Bioenergy Economics and Policy in US and Brazil: Effects on Land Use and Greenhouse Gas Emissions. *Handbook of Bioenergy Economics and Policy: Volume II: Modeling Land Use and Greenhouse Gas Implications*, pages 1–11.
- Kikstra, J. S., Nicholls, Z. R. J., Smith, C. J., Lewis, J., Lamboll, R. D., Byers, E., Sandstad, M., Meinshausen, M., Gidden, M. J., and Rogelj, J. (2022). The IPCC Sixth Assessment Report WGIII climate assessment of mitigation pathways: from emissions to global temperatures. *Geoscientific Model Development*, 15(24):9075–9109.
- Knapp, K. C., Weinberg, M., Howitt, R., and Posnikoff, J. F. (2003). Water transfers, agriculture, and groundwater management: A dynamic economic analysis. *Journal of Environmental Management*, 67(4):291–301.
- Krishnamurthy, C. K. B. (2017). Optimal Management of Groundwater Under Uncertainty: A Unified Approach. *Environmental and Resource Economics*, 67(2):351–377.
- Langholtz, M., Stokes, B., and Eaton, L. (2016). 2016 billion-ton report: Advancing domestic resources for a thriving bioeconomy (Executive Summary). *Industrial Biotechnology*, 12(5):282–289.
- Larson, J., Steller, J., Ohrel, S., Baker, J. S., and Bean, A. (2019). Effects of Renewable Portfolio Standards on Bioenergy: An Econometric Approach.
- Latta, G. S., Baker, J. S., Beach, R. H., Rose, S. K., and McCarl, B. A. (2013). A Multi-Sector Intertemporal Optimization Approach to Assess the GHG Implications of US Forest and Agricultural Biomass Electricity Expansion. *Journal of Forest Economics*, 19(4):361–383.

- Levy, Z. F., Jurgens, B. C., Burow, K. R., Voss, S. A., Faulkner, K. E., Arroyo-Lopez, J. A., and Fram, M. S. (2021). Critical Aquifer Overdraft Accelerates Degradation of Groundwater Quality in California's Central Valley During Drought. *Geophysical Research Letters*, 48(17).
- Li, Z. B., Zhang, Y., and Wang, M. (2023). Solar energy projects put food security at risk. *Science*, 381(6659):740–741.
- Liu, P. W., Famiglietti, J. S., Purdy, A. J., Adams, K. H., McEvoy, A. L., Reager, J. T., Bindlish, R., Wiese, D. N., David, C. H., and Rodell, M. (2022). Groundwater depletion in California's Central Valley accelerates during megadrought. *Nature Communications*, 13(1).
- Macknick, J., Hartmann, H., Barron-Gafford, G., Beatty, B., Burton, R., Choi, C. S., Davis, M., Davis, R., Figueroa, J., Garrett, A., Hain, L., Herbert, S., Janski, J., Kinzer, A., Knapp, A., Lehan, M., Losey, J., Marley, J., Macdonald, J., Mccall, J., Nebert, L., Ravi, S., Schmidt, J., Staie, B., and Walston, L. (2022). The 5 Cs of Agrivoltaic Success Factors in the United States: Lessons From the InSPIRE Research Study. *National Renewable Energy Laboratory Technical Report: NREL/TP-6A20-83566*, (August).
- Magarelli, A., Mazzeo, A., and Ferrara, G. (2024). Fruit Crop Species with Agrivoltaic Systems: A Critical Review.
- Maine Public Utilities Commission (2020). Annual Report on New Renewable Resource Portfolio Requirement. Technical report.
- Mamun, M. A. A., Dargusch, P., Wadley, D., Zulkarnain, N. A., and Aziz, A. A. (2022). A review of research on agrivoltaic systems. *Renewable and Sustainable Energy Reviews*, 161(March):112351.
- Marrou, H., Dufour, L., and Wery, J. (2013). How does a shelter of solar panels influence water flows in a soil-crop system? *European Journal of Agronomy*, 50:38–51.
- Meyer, B. D. (1995). Natural and Quasi-Experiments in Economics. *Journal of Business & Economic Statistics*, 13(2):151–161.
- Mohammed, S., Dragonetti, G., Admane, N., and Fouial, A. (2023). The Impact of Agrivoltaic Systems on Tomato Crop: A Case Study in Southern Italy. *Processes*, 11(12).
- Mupambi, G., Sandler, H. A., and Jeranyama, P. (2021). Installation of an agrivoltaic system influences microclimatic conditions and leaf gas exchange in cranberry. In *IX International Symposium on Light in Horticulture 1337*, pages 117–124.
- Mustaq Shaikh and Farjana Birajdar (2024). GROUNDWATER DEPLETION IN AGRICULTURAL REGIONS: CAUSES, CONSEQUENCES, AND SUSTAINABLE MANAGEMENT: A CASE STUDY OF BASALTIC TERRAIN OF SOLAPUR DISTRICT. *EPRA International Journal of Multidisciplinary Research (IJMR)*, pages 237–242.

- Newsom, G. (2022). CALIFORNIA AGRICULTURAL STATISTICS REVIEW State of California. Technical report.
- Pfeiffer, L. and Lin, C. Y. (2014). Does efficient irrigation technology lead to reduced groundwater extraction? Empirical evidence. *Journal of Environmental Economics and Management*, 67(2):189–208.
- Popp, A., Calvin, K., Fujimori, S., Havlik, P., Humpenöder, F., Stehfest, E., Bodirsky, B. L., Dietrich, J. P., Doelmann, J. C., Gusti, M., Hasegawa, T., Kyle, P., Obersteiner, M., Tabeau, A., Takahashi, K., Valin, H., Waldhoff, S., Weindl, I., Wise, M., Kriegler, E., Lotze-Campen, H., Fricko, O., Riahi, K., and Vuuren, D. P. (2017). Land-use futures in the shared socioeconomic pathways. *Global Environmental Change*, 42:331–345.
- Quarshie, P. K. (2023). Effect of Photovoltaic Panel Shading on the Growth of Ginger and Kale.
- Rabasoma, K., Jenkins, N., and Ekanayake, J. (2024). Economic feasibility of using agrivoltaics for tomato farming. *Food and Energy Security*, 13(3).
- Riahi, K., van Vuuren, D. P., Kriegler, E., Edmonds, J., O'Neill, B. C., Fujimori, S., Bauer, N., Calvin, K., Dellink, R., Fricko, O., Lutz, W., Popp, A., Cuaresma, J. C., KC, S., Leimbach, M., Jiang, L., Kram, T., Rao, S., Emmerling, J., Ebi, K., Hasegawa, T., Havlik, P., Humpenöder, F., Da Silva, L. A., Smith, S., Stehfest, E., Bosetti, V., Eom, J., Gernaat, D., Masui, T., Rogelj, J., Strefler, J., Drouet, L., Krey, V., Luderer, G., Harmsen, M., Takahashi, K., Baumstark, L., Doelman, J. C., Kainuma, M., Klimont, Z., Marangoni, G., Lotze-Campen, H., Obersteiner, M., Tabeau, A., and Tavoni, M. (2017). The Shared Socioeconomic Pathways and their energy, land use, and greenhouse gas emissions implications: An overview. *Global Environmental Change*, 42:153–168.
- Roe, S., Streck, C., Obersteiner, M., Frank, S., Griscom, B., Drouet, L., Fricko, O., Gusti, M., Harris, N., and Hasegawa, T. (2019). Contribution of the land sector to a 1.5 C world. *Nature Climate Change*, 9(11):817–828.
- Sarr, A., Soro, Y. M., Tossa, A. K., and Diop, L. (2024). A new approach for modelling photovoltaic panel configuration maximizing crop yield and photovoltaic array outputs in agrivoltaics systems. *Energy Conversion and Management*, 309.
- Shayegh, S. and Sanchez, D. L. (2021). Impact of market design on cost-effectiveness of renewable portfolio standards. *Renewable and Sustainable Energy Reviews*, 136:110397.
- Sojib Ahmed, M., Rezwani Khan, M., Haque, A., and Ryyan Khan, M. (2022). Agrivoltaics analysis in a techno-economic framework: Understanding why agrivoltaics on rice will always be profitable. *Applied Energy*, 323.
- Tahir, Z. and Butt, N. Z. (2022). Implications of spatial-temporal shading in agrivoltaics under fixed tilt & tracking bifacial photovoltaic panels. *Renewable Energy*, 190:167–176.

- Trommsdorff, M., Kang, J., Reise, C., Schindele, S., Bopp, G., Ehmann, A., Weselek, A., Högy, P., and Obergfell, T. (2021). Combining food and energy production: Design of an agrivoltaic system applied in arable and vegetable farming in Germany. *Renewable and Sustainable Energy Reviews*, 140(December 2020).
- Turnley, J. W., Grant, A., Schull, V. Z., Cammarano, D., Sesmero, J., and Agrawal, R. (2024). The viability of photovoltaics on agricultural land: Can PV solve the food vs fuel debate? *Journal of Cleaner Production*, 469.
- Van Der Horst, R. R. (2019). *Solar Farms on Agricultural Land: a Partial Equilibrium Analysis*. PhD thesis.
- Wang, T., Park, S. C., and Jin, H. (2015). Will farmers save water? A theoretical analysis of groundwater conservation policies. *Water Resources and Economics*, 12:27–39.
- Weselek, A., Bauerle, A., Hartung, J., Zikeli, S., Lewandowski, I., and Högy, P. (2021). Agri-voltaic system impacts on microclimate and yield of different crops within an organic crop rotation in a temperate climate. *Agronomy for Sustainable Development*, 41(5):59.
- White, E. M., Latta, G., Alig, R. J., Skog, K. E., and Adams, D. M. (2013a). Biomass production from the US forest and agriculture sectors in support of a renewable electricity standard. *Energy policy*, 58:64–74.
- White, W., Lunnan, A., Nybakk, E., and Kulisic, B. (2013b). The role of governments in renewable energy: The importance of policy consistency. *Biomass and Bioenergy*, 57:97–105.
- Williamson, A. K., Prudic, D. E., and Swain, L. A. (1989). *Ground-water flow in the Central Valley, California*, volume 1401-D.
- Wiser, R., Mai, T., Millstein, D., Barbose, G., Bird, L., Heeter, J., Keyser, D., Krishnan, V., and Macknick, J. (2017). Assessing the costs and benefits of US renewable portfolio standards. *Environmental Research Letters*, 12(9).
- Worthington, V. E., Burt, O. R., and Brustkern, R. L. (1985). Optimal management of a confined groundwater system. *Journal of Environmental Economics and Management*, 12(3):229–245.
- Wu, G. C., Jones, R. A., Leslie, E. I., Williams ID, J. H., Pascale, A., Brand, E., Parker, S. S., Cohen, B. S., Fargione, J. E., Souder, J., Batres, M., Gleason, M. G., Schindel ID, M. H., Stanley ID Edited by M Granger Morgan, C. K., contributions, A., designed research, M., performed research, A., contributed, J., analyzed data, C., and managed project, M. (2023). Minimizing habitat conflicts in meeting net-zero energy targets in the western United States. *NORTH CAROLINA STATE UNIVERSITY*, 120(4).

- Wu, G. C., Leslie, E., Allen, D., Sawyerr, O., Cameron, D. R., Brand, E., Cohen, B., Ochoa, M., and Olson, A. (2019). Power of Place Land Conservation and Clean Energy Pathways for California.
- Yajima, D., Toyoda, T., Kirimura, M., Araki, K., Ota, Y., and Nishioka, K. (2023). Estimation Model of Agrivoltaic Systems Maximizing for Both Photovoltaic Electricity Generation and Agricultural Production. *Energies*, 16(7).
- Yin, H. and Powers, N. (2010). Do state renewable portfolio standards promote in-state renewable generation{glottal stop}. *Energy Policy*, 38(2):1140–1149.

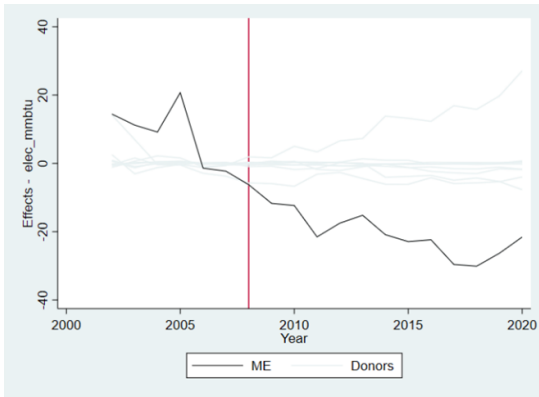
APPENDIX

APPENDIX

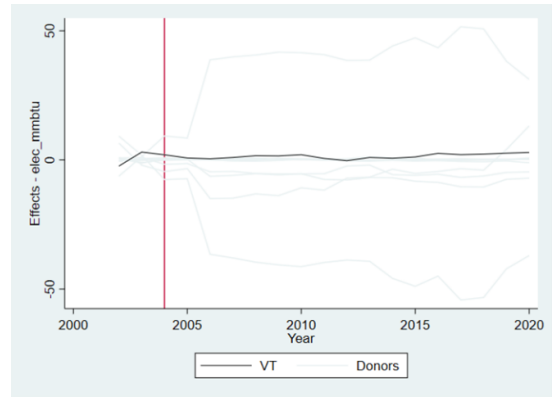
A

SUPPLEMENTARY MATERIALS

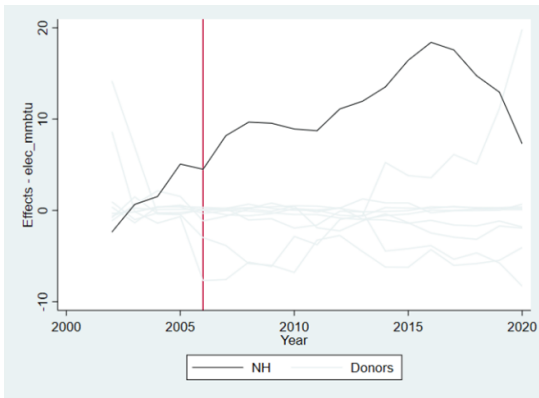
A.1 Synthetic Control Method: Placebo Test Results for Each RPS State



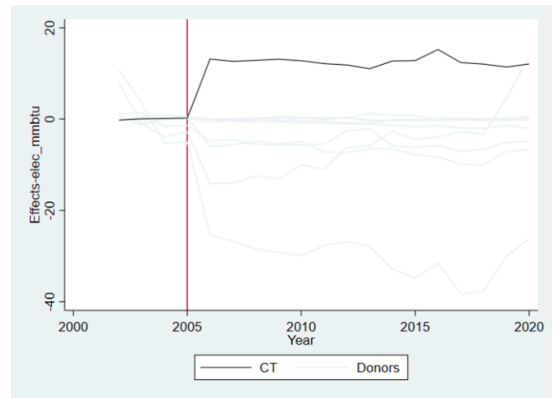
(a) Maine



(b) Vermont



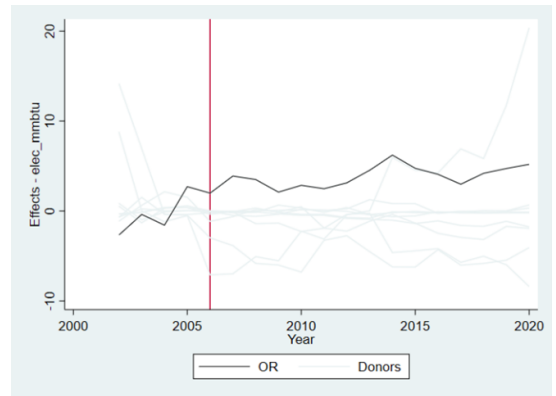
(c) New Hampshire



(d) Connecticut



(e) Massachusetts

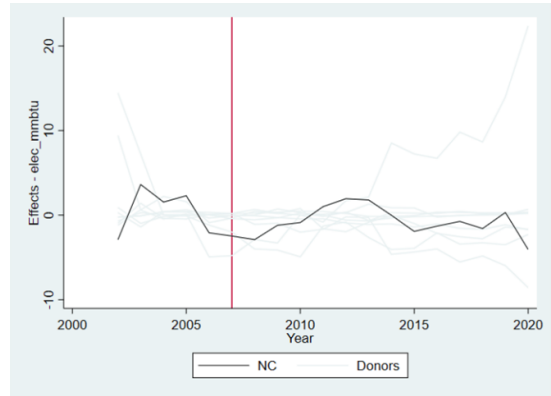


(f) Oregon

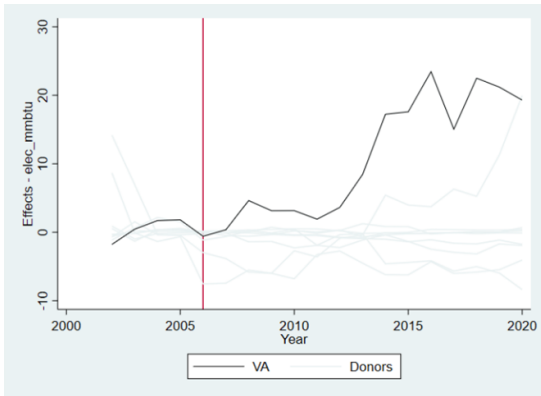
Figure A.1: Placebo Test Results for Each RPS State (I)



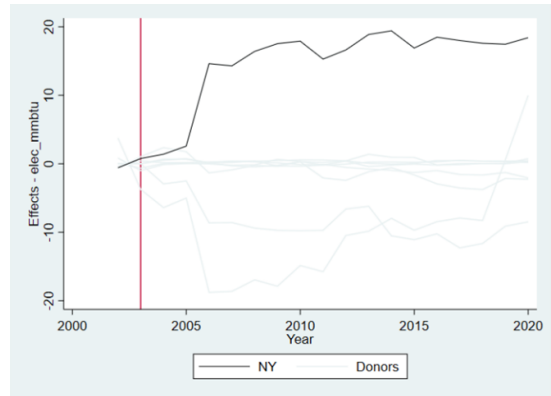
(g) Washington



(h) North Carolina



(i) Virginia



(j) New York

Figure A.1: Placebo Test Results for Each RPS State (II)

A.2 Parameter Values for Chapter 2

Table A.1: Parameters used for Representative Crops

Type	Low AgRev, Low IrrCost	Low AgRev, High IrrCost	High AgRev, Low IrrCost	High AgRev, High IrrCost
Crop	Corn	Alfalfa	Tomatoes	Grapes
μ	[11.779, 3.608]	[10.915, 4.245]	[6.628, 3.737]	[10.886, 3.656]
Φ	$\begin{bmatrix} 0.791 & -2.041 \\ 0.005 & 0.283 \end{bmatrix}$	$\begin{bmatrix} 0.399 & -1.098 \\ 0.062 & 0.222 \end{bmatrix}$	$\begin{bmatrix} 0.83 & -0.96 \\ 0.002 & 0.312 \end{bmatrix}$	$\begin{bmatrix} 0.789 & -1.453 \\ 0.017 & 0.388 \end{bmatrix}$
Σ	$\begin{bmatrix} 0.025 & -0.001 \\ -0.001 & 0. \end{bmatrix}$	$\begin{bmatrix} 0.05 & -0. \\ -0. & 0.001 \end{bmatrix}$	$\begin{bmatrix} 0.015 & 0.001 \\ 0.001 & 0. \end{bmatrix}$	$\begin{bmatrix} 0.01 & 0.001 \\ 0.001 & 0. \end{bmatrix}$
$\log(R^{\text{ag}*})$	6.8	7.2	8.2	8.8
$\log(C^{\text{irr}*})$	5.1	6.0	5.4	6.2
$R^{\text{ag}*}$	860.0	1280.4	3699.9	6834.5
$C^{\text{irr}*}$	160.5	414.3	232.5	500.1
C^{oth}	399.5	566.1	3167.4	6034.4
α	0.2	0.2	0.2	0.2
ρ	0.2	0.2	0.2	0.2
γ	0.6	0.6	0.6	0.6

Table A.2: Parameters used for All Crops (Part I)

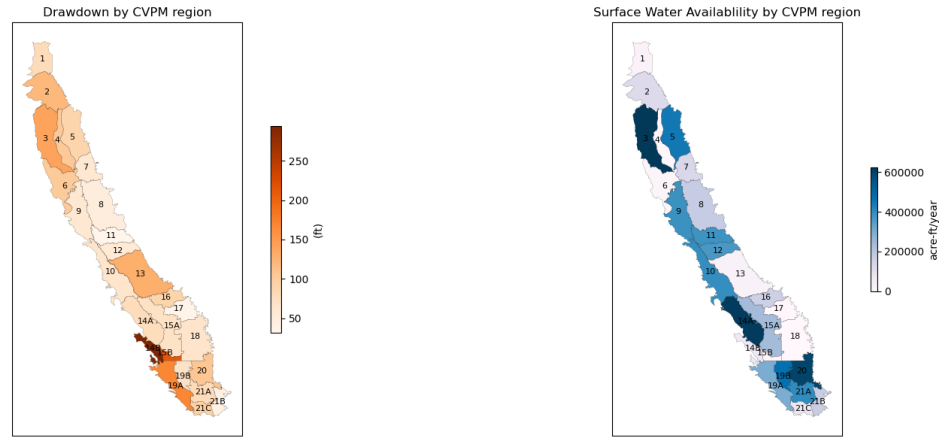
Crop	Alfalfa	Almonds	Corn	Grapes
α	0.1	1.0	0.040	0.12
ρ	0.2	0.0	0.215	0.290
γ	0.5	0.0	0.5	0.750
$R^{\text{ag}*}$	1280.4	5955.2	860.0	6834.5
$C^{\text{irr}*}$	414.3	672.3	160.5	500.1
C^{oth}	716.2	2945.9	1024.7	3168.2
μ	[10.915, 4.245]	[24.33, 3.246]	[11.779, 3.608]	[10.886, 3.656]
Φ	$\begin{bmatrix} 0.399 & -1.098 \\ 0.062 & 0.222 \end{bmatrix}$	$\begin{bmatrix} 0.832 & -3.512 \\ 0.054 & 0.43 \end{bmatrix}$	$\begin{bmatrix} 0.791 & -2.041 \\ 0.005 & 0.283 \end{bmatrix}$	$\begin{bmatrix} 0.789 & -1.453 \\ 0.017 & 0.388 \end{bmatrix}$
Σ	$\begin{bmatrix} 0.05 & -0. \\ -0. & 0.001 \end{bmatrix}$	$\begin{bmatrix} 0.017 & -0.001 \\ -0.001 & 0. \end{bmatrix}$	$\begin{bmatrix} 0.025 & -0.001 \\ -0.001 & 0. \end{bmatrix}$	$\begin{bmatrix} 0.01 & 0.001 \\ 0.001 & 0. \end{bmatrix}$
$\log(R^{\text{ag}*})$	7.2	8.7	6.8	8.8
$\log(C^{\text{irr}*})$	6.0	6.5	5.1	6.2

Table A.3: Parameters used for All Crops (Part II)

Crop	Oranges	Rice	Tomatoes	Wheat
α	1.0	0.11	0.34	0.1
ρ	0.0	0.2	0.365	0.2
γ	0.0	0.325	0.650	0.5
$R^{\text{ag}*}$	3709.3	1518.6	3699.9	499.2
$C^{\text{irr}*}$	913.9	406.6	232.5	194.9
C^{oth}	5660.0	1111.2	3614.6	497.5
μ	[1.766, 4.887]	[-6.825, 4.601]	[6.628, 3.737]	[9.853, 4.017]
Φ	$\begin{bmatrix} 0.606 & 0.216 \\ -0.009 & 0.294 \end{bmatrix}$	$\begin{bmatrix} 0.827 & 1.347 \\ -0.005 & 0.24 \end{bmatrix}$	$\begin{bmatrix} 0.83 & -0.96 \\ 0.002 & 0.312 \end{bmatrix}$	$\begin{bmatrix} 0.798 & -1.631 \\ 0.03 & 0.202 \end{bmatrix}$
Σ	$\begin{bmatrix} 0.059 & 0.002 \\ 0.002 & 0.002 \end{bmatrix}$	$\begin{bmatrix} 0.054 & 0.001 \\ 0.001 & 0. \end{bmatrix}$	$\begin{bmatrix} 0.015 & 0.001 \\ 0.001 & 0. \end{bmatrix}$	$\begin{bmatrix} 0.047 & 0.007 \\ 0.007 & 0.005 \end{bmatrix}$
$\log(R^{\text{ag}*})$	8.2	7.3	8.2	6.2
$\log(C^{\text{irr}*})$	6.8	6.0	5.4	5.3

A.3 Supplementary Materials for Chapter 3

A.3.1 Initial Conditions



(a) Groundwater Drawdown

(b) Surface Water Availability

Figure A.2: Initial Condition of Surface and Groundwater by CVPM

A.3.2 Total Water Use Across Land-use Scenarios

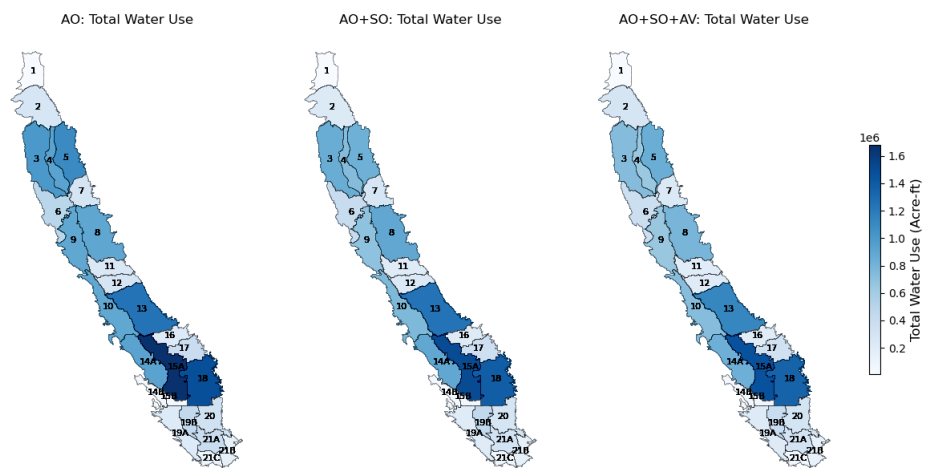


Figure A.3: Total Water Use Across CVPM Regions

A.3.3 Impact of Solar and Agrivoltaics on Water Use

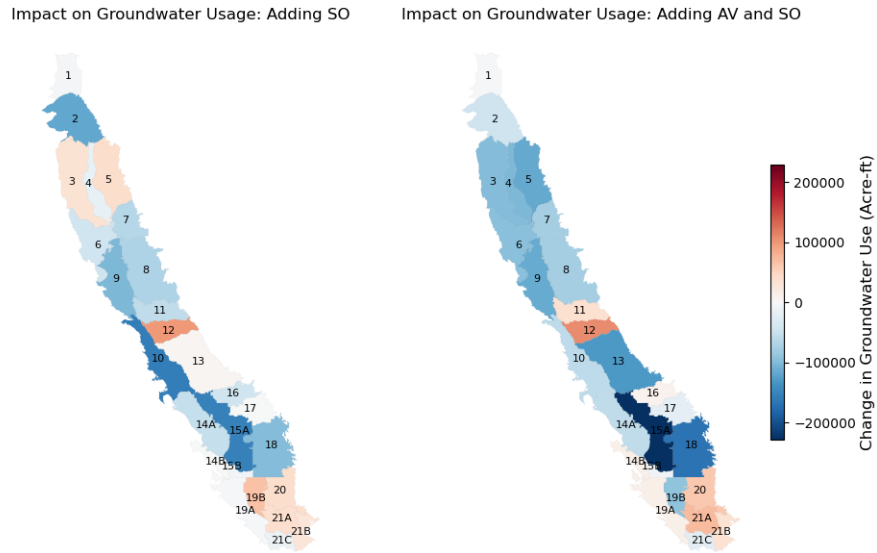


Figure A.4: Impact of Solar and Agrivoltaics on Groundwater Withdrawals

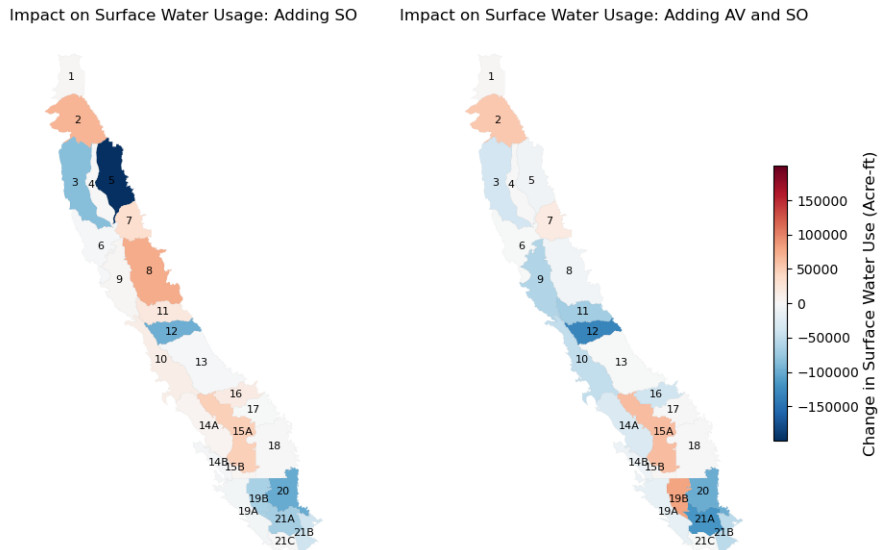


Figure A.5: Impact of Solar and Agrivoltaics on Surface Water Withdrawals

A.3.4 Land Use Allocation Across SGMA Scenarios

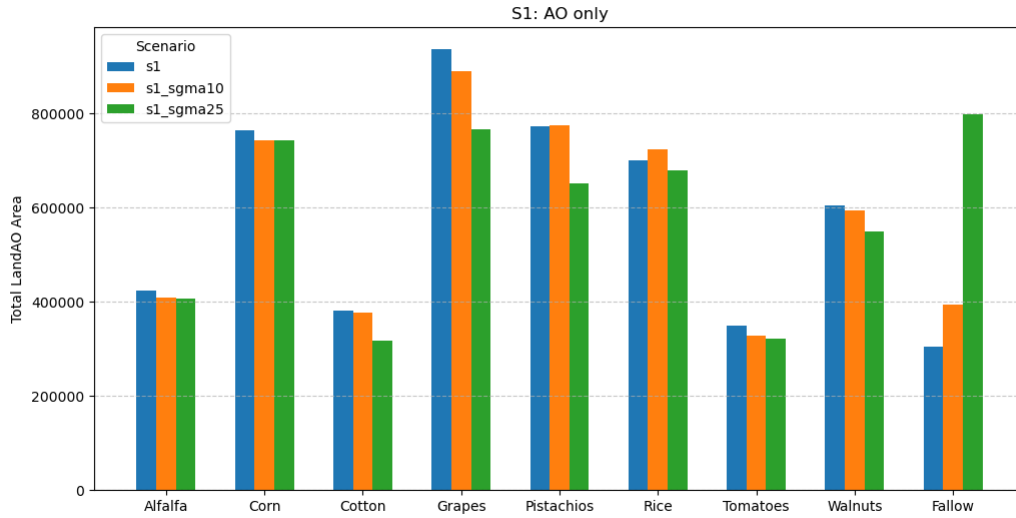


Figure A.6: Land Use Allocation Across SGMA Scenarios (S1)

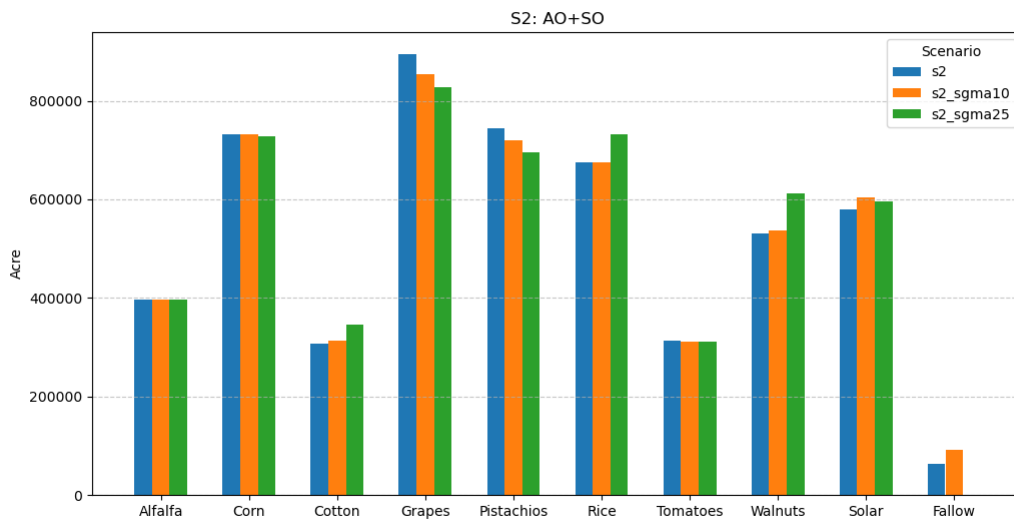


Figure A.7: Land Use Allocation Across SGMA Scenarios (S2)

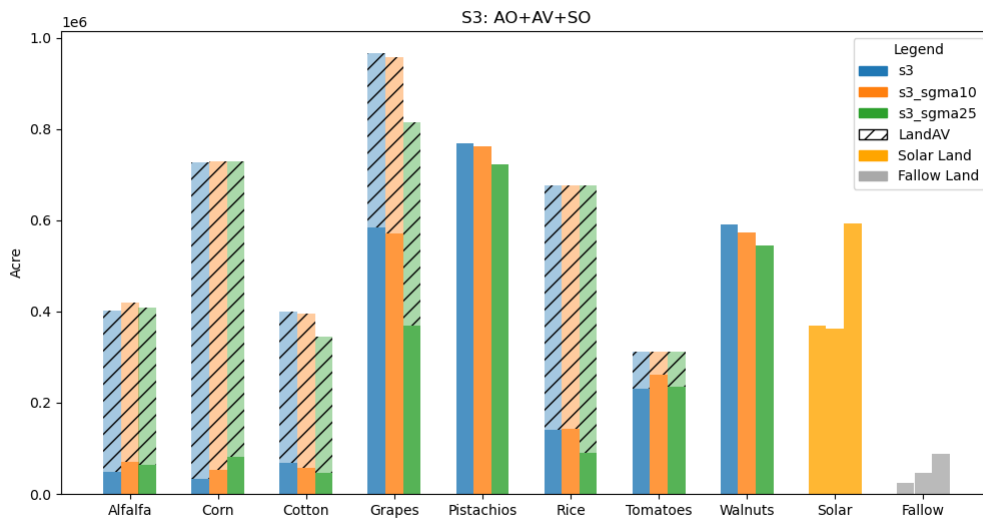


Figure A.8: Land Use Allocation Across SGMA Scenarios (S3)

A.3.5 Impact of SGMA on Groundwater Level

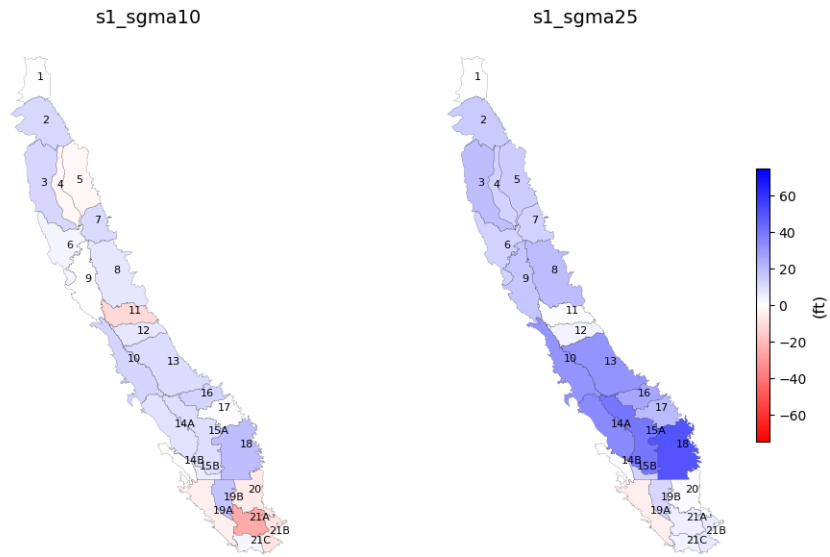


Figure A.9: Impact of SGMA on Groundwater Level (S1)

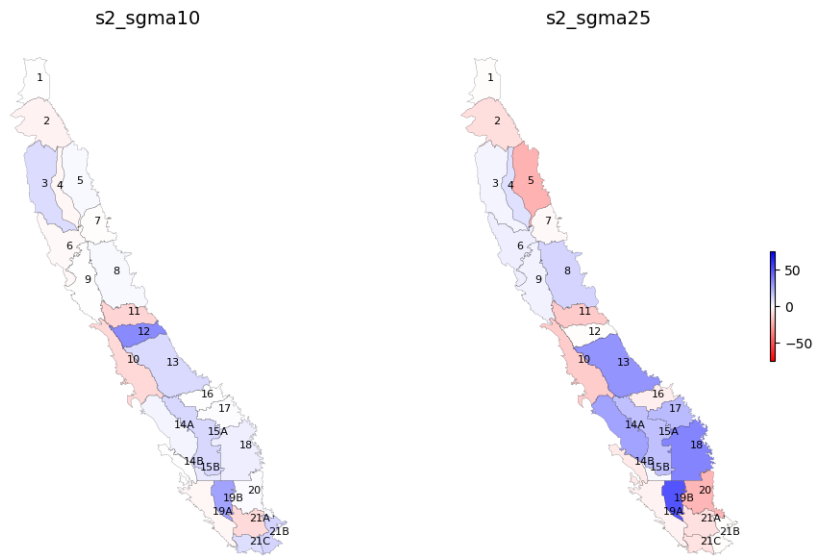


Figure A.10: Impact of SGMA on Groundwater Level (S2)

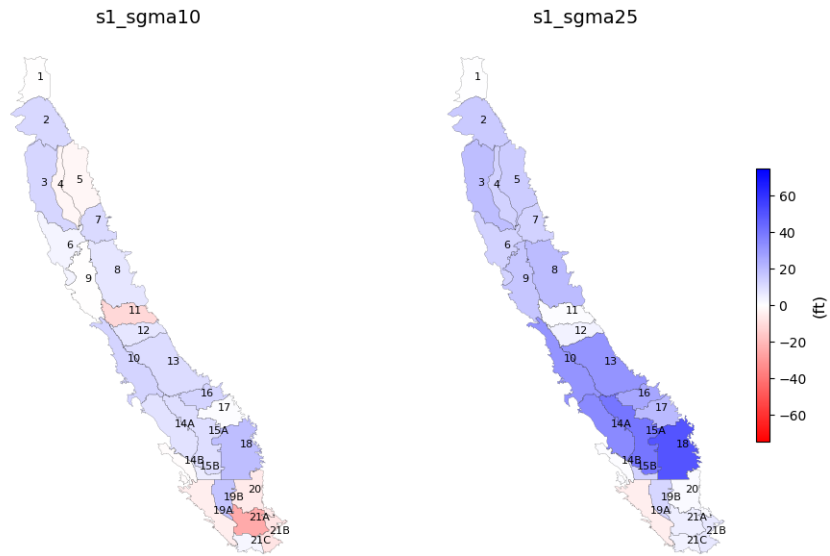


Figure A.11: Impact of SGMA on Groundwater Level (S3)

A.3.6 Land Use Allocation Across Solar Lease Rate Scenarios

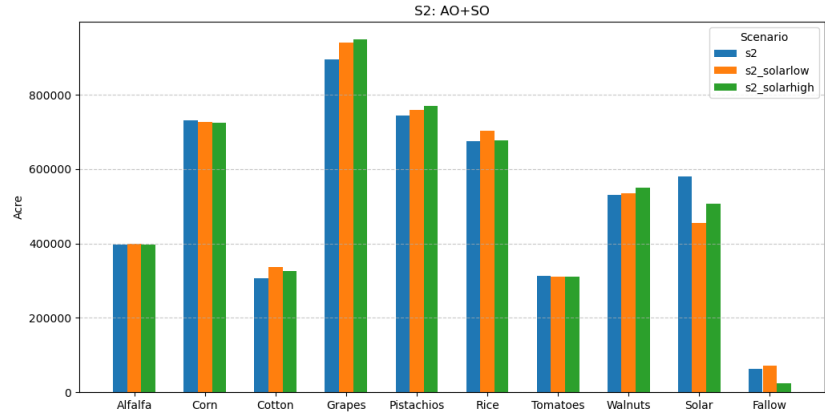


Figure A.12: Land Use Allocation Across Solar Lease Rate Scenarios (S2)

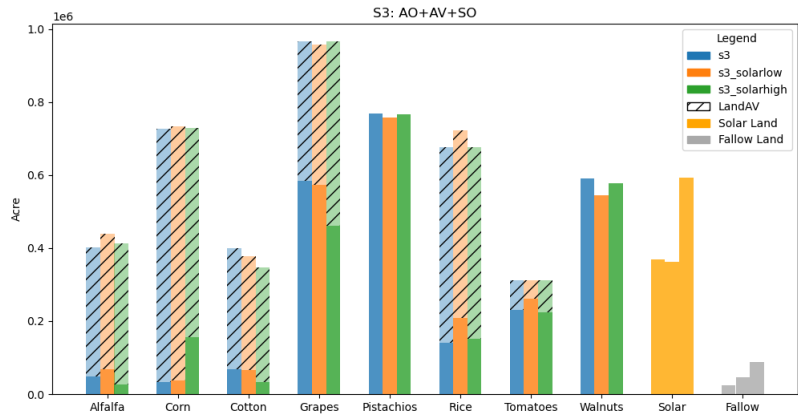


Figure A.13: Land Use Allocation Across Solar Lease Rate Scenarios (S3)

A.3.7 Impact of Varying Solar Lease Rates

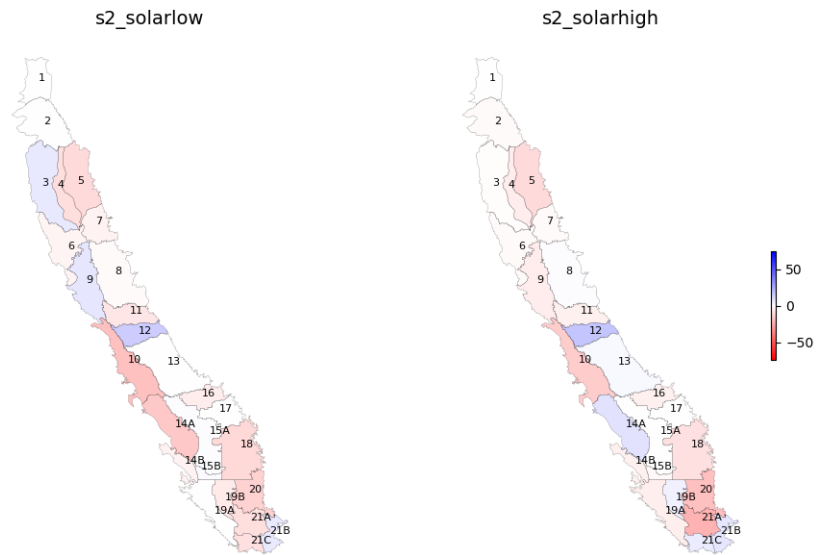


Figure A.14: Impact of Varying Solar Lease Rate on Groundwater Level (S2)

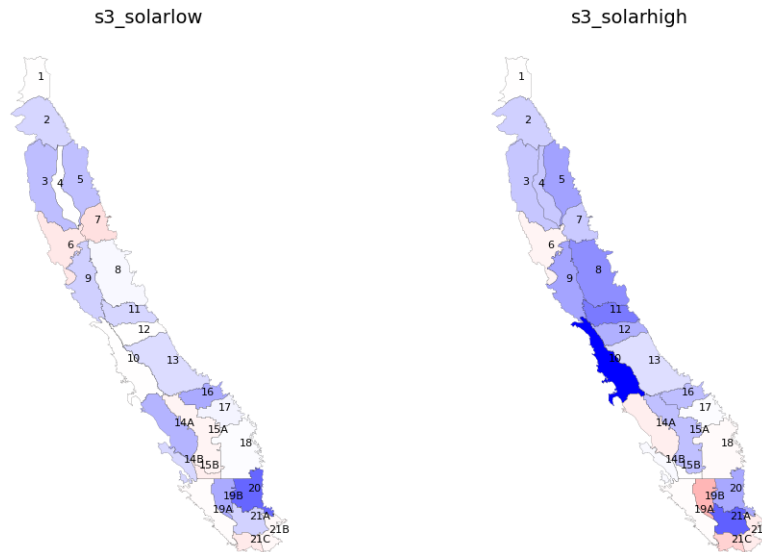


Figure A.15: Impact of Varying Solar Lease Rate on Groundwater Level (S3)